1-1-1995

The chemistry and adhesion of functionalized polymers and surfaces/

Robert J. Fleming
University of Massachusetts Amherst

THE CHEMISTRY AND ADHESION OF FUNCTIONALIZED POLYMERS AND SURFACES

A Dissertation Presented

by

ROBERT J. FLEMING

Submitted to the Graduate School of the
University of Massachusetts Amherst in partial fulfillment
of the requirements for the degree of

DOCTOR OF PHILOSOPHY

February 1995

Polymer Science and Engineering

THE CHEMISTRY AND ADHESION OF FUNCTIONALIZED POLYMERS AND SURFACES

A Dissertation Presented

by

ROBERT J. FLEMING

Approved as to style and content by:

Thomas J. McCarthy, Co-Chair

Richard J. Farris, Co-Chair

John E. Ritter, Member

William J. Macknight, Department Head
Polymer Science and Engineering

ACKNOWLEDGMENTS

My graduate school experience was both a period of adventure and enlightenment, not only as a scientist but as a person. I am very grateful for these experiences.

I would like to thank my advisors Dr. McCarthy and Dr. Farris for their patience and their commendable ability to keep an open mind. Not only have I learned immensely from both, but they taught me the most important skill of learning on my own.

My personal life and scientific life were so intertwined it was impossible to separate the friends from the scientists. Therefore, I would like to thank the following people for their friendship, support, and advice: Jahu, JoAnne, Cormac, Brian, CarolAnne, Vipavee, Wei, Ale Haus, Tak, Anthony, Jim, Scott, Christian, Joan, Erik, Brant, Tim, Damo, Nicole, and Jack. We all ate, drank, worked, and played together, and I thank you all!

Most of all I thank my wife Teresa for her undying patience, support, and love, I really do owe all of my success to her and I can't thank her enough (but I should thank her more often). My daughter Austin was acquired in graduate school; she introduced me to an entirely new element of life, and for that I am very delighted.

ABSTRACT

THE CHEMISTRY AND ADHESION OF FUNCTIONALIZED

POLYMERS AND SURFACES

ROBERT J. FLEMING, B.S., WINTHROP COLLEGE

M.S., UNIVERSITY OF MASSACHUSETTS AMHERST

Ph.D., UNIVERSITY OF MASSACHUSETTS AMHERST

Co-directed by: Professor Thomas J. McCarthy, and Professor Richard J. Farris

Poly(chlorotrifluoroethylene) (PCTFE) films were surface-selectively modified with *n*-butyllithium (PCTFE-Butyl) precisely controlling the extent of modification on the surface with reaction time, temperature, and solvent. The adhesion of PCTFE-Butyl to epoxy was investigated using the 180° peel test, double-cantilever-beam (DCB) test, and tapered double-cantilever-beam (TDCB) test. The DCB and TDCB tests gave adhesion values an order of madnitude less than the peel test. The mechanism of adhesion was also investigated and the data suggested that covalent bonding between allylic chlorides (present on the partially modified PCTFE-Butyl) and the amines present in the epoxy curing agent was the mechanism of adhesion.

PCTFE films were also surface-selectively modified with lithiopropyl ethyl acetal (PCTFE-PEA). PCTFE-PEA was hydrolyzed to the alcohol (PCTFE-OH) then reacted with butyryl chloride, adipoyl chloride, heptadecanoyl chloride, or stearoyl chloride, which gave their corresponding esters. The surface modifications effected their wettability as

measured by water contact angle. Adhesion of the modified surfaces to epoxy and a pressure sensitive adhesive was measured by the 180° peel test. Only a loose correlation between the wettability (as measured by water contact angle) and the measured adhesion was observed. Other factors were found to influence adhesion and were discussed.

Polystyrene (PS), poly(styrene-*b*-1,2-butadiene) (PS-B), and poly(styrene-*b*-4-hyroxybutene) (PS-OH) were synthesized with predetermined molecular weight and narrow molecular weight distribution. Adhesion of the polymers to epoxy was measured by the TDCB test. Adhesion of PS to epoxy was found to be poor but increased with increasing butadiene or hydroxybutene block size.

Alternating layers of poly(sodium 4-styrenesulfonate) and poly(allylamine hydrochloride) were adsorbed onto aminopropyltriethoxysilane treated glass. X-ray photoelectron spectroscopy studies showed that the layers were highly organized and approximately 0.6 nm thick. Water contact angle measurements showed that the wettability was effected by the number of layers. Adhesion studies of the layers to a PSA and epoxy showed that the layers could not be easily removed from the glass substrate.

TABLE OF CONTENTS

LIST OF TABLES

LIST OF FIGURES

LIST OF SCHEMES

CHAPTER I

INTRODUCTION

Overview

A complete understanding of adhesion requires a multi-disciplinary effort taking vantages ranging from chemistry to mechanics. Adhesion, by definition, is the joining together of adhesive and substrate resulting in an adhesive joint that has the capacity to withstand stress. The necessity of a multi-disciplinary approach becomes readily apparent. Formation of the adhesive joint may require the formation of chemical bonds across the interface. Assessing the magnitude of adhesion requires a macroscopic measurement of the stresses or energy required to de-bond the adhesive joint.

The objectives of this thesis are to address several key areas in adhesion science. Surface chemistry (Chapters II and III), adsorption (Chapters IV, V, and VI), and fracture mechanics (Chapters III, V, and VI) will be explored as to their impact on understanding adhesion. The experimental results given in this thesis will be compared to modern theories and their implications on adhesion will be discussed. The primary concern of this thesis is to understand the macroscopic-microscopic structure-property relationship in adhesion.

Adhesion

In order to understand adhesion phenomena we must first consider, as generally as possible, why two materials will adhere when brought together. When adhering two materials together to form an adhesive joint, a two-step process takes place: contact and solidification. Before bonding (or adhesion) can occur, intimate molecular contact must be made between the adhesive and substrate. The adhesive must be able to spread over the solid surface, displacing air and other contaminants that may be present and form intimate molecular contact with the surface.[1,2] Once molecular contact is achieved, the adhesive must solidify so that externally applied stresses can be resisted. This is the solidification process and takes place by physical or chemical interactions. The adhesive can be applied as a monomer (or reactive oligomer), in which case the solidification process is a chemical reaction that forms a covalently bonded network. The adhesive can also be a polymer in solution; in this situation the solvent must be removed before the polymer solidifies.

Some adhesives are viscoelastic solids (polymers with low glass transition temperatures, T_g) and may not require a solidification stage. This is a class of adhesives called pressure sensitive adhesives (PSA). PSA's are low T_g polymers that adhere to substrates when pressure is applied, forcing molecular contact, however, the stresses required to separate a PSA from its substrate is dependent on the rate and temperature of loading[3] (i.e. a lower force is required to peel a PSA at a slower rate than a faster rate).

At the molecular level, adhesive bonding occurs by the formation of primary bonds, donor-acceptor bonds, and/or secondary bonds across the interface between

adhesive and substrate (Table 1.1).[1] From the bond energies given in Table 1.1 it would be predicted that adhesion resulting from primary bonds would give stronger adhesive joints than joints formed by secondary bonds. The measured adhesion does not always correlate with the adhesive energy predicted from molecular bonds because many irreversible processes often occur during debonding. For example when two polymers are adhered together, polymer-polymer adhesion may be significantly increased by chains on either side of the interface bridging together by physical entanglements (due to chain interdiffusion). The lateral interactions may be weak van der Waals bonds but when the chains are entangled debonding can occur by chains being pulled out of the substrate. This increases the measured adhesion because large amounts of energy are required to put the chain being pulled out through all the necessary conformations and to overcome the chain-chain frictional forces.[4] It can be seen that relating molecular bonding to the measured adhesion is a challenge to adhesion scientists.

Relating the microscopic forces to macroscopic properties is no simple task. A complete energy balance must take into account all the bonds supplied (i.e. number of covalent bonds and number of van der Waals bonds per unit area) and all the energy supplied and dissipated during debonding. Adhesion is the bonding of two surfaces, so the molecular forces at these surfaces are the driving force for adhesion. It must also be realized that real surfaces are not 2-dimensional. Some 3-dimensional component must be considered to account for surface roughness (real surfaces are not molecularly smooth) and a microstructure or morphology gradient exists that changes from the outermost surface to the bulk.[2]

Table 1.1 Bond types and typical bond energies.[1]

Type	Bond Energy (kJ/mol)
Primary Bonds	
Ionic	600-1100
Covalent	60-700
Metallic	110-350
Donor-acceptor Bonds	
Bronsted acid-base interactions	Up to 1000
(i.e. up to a primary ionic bond)	
Lewis acid-base interactions	Up to 80
Secondary Bonds	
Hydrogen bonds	
Hydrogen bonds involving fluorine	Up to 40
Hydrogen bonds excluding fluorine	10-25
van der Waals bonds	
Permanent dipole-dipole interactions	4-20
Dipole-induced dipole interactions	Less than 2
Dispersion (London) forces	0.08-40

The work done by the surface attractions is the work of adhesion, W_a (energy per unit area). This work can be thought of as the reversible work required to pull apart a unit area of the interface. After separation (of identical surfaces), each surface has a free energy, γ, equal to half W_a ($W_a=2\gamma$) which can pull the surfaces back into contact. In the case of dissimilar surfaces, Dupre derived the thermodynamic work of adhesion, W_a, where:

$$W_a = \gamma_1 + \gamma_2 - \gamma_{12}$$

γ_1 and γ_2 are the surface free energies of two materials and γ_{12} is the free energy of the two bonded materials. The surface energy is the sum of all the effective molecular interactions given in Table 1.1.[5]

Calculations from the bond energies given in Table 1.1 predict adhesion values on the order of 0.01 to 1 J/m^2 for secondary bonding and 1 to 10 J/m^2 for primary bonding.[6] This is in qualitative agreement with measurements made directly by a surface force apparatus[7] and those made by contact angle measurements[5,7] using the Young-Dupre equation:

$$W_a = \gamma_L(1+\cos\theta)$$

where γ_L is the surface tension of a probe fluid, and θ is the angle the probe fluid makes with the solid surface. These microscopic values of adhesion often significantly differ from the magnitude of adhesion measured from macroscopic tests. Table 1.2 compares the surface energy of a material measured from a macroscopic fracture mechanics test to the surface energy determined by contact angle measurements, a more microscopic test.[8] Table 1.2 shows that some materials have a much greater surface energy measured by the

fracture mechanics test than from contact angle measurements. This forces the investigator to take a closer look at the debonding process in macroscopic tests in order to obtain a more accurate energy balance.

Table 1.2 Comparison between the cohesive fracture energy, G_c, and the surface free energy for some materials.[8]

Material	G_c / 2 (mJ/m^2)	γ (mJ/m^2)
Poly(methyl methacrylate)	2×10^5	41.1
Polystyrene	7×10^5	40.7
Polystyrene oligomer (MW~3000)	40	40.7
Steel	1×10^6	2300
Glass	550	549

The level of adhesion between two polymers depends on the ability of the interface to sustain stress. In order to measure the magnitude of adhesion, the adhesive joint must be stressed until the joint fails. At the macroscopic level, the energy required per unit area to fracture (separate) the interface depends on the ability of the interface and its surrounding volume to dissipate energy by plastic and/or viscoelastic deformation. In the absence of plastic/viscoelastic deformation the fracture energy should be equal to the thermodynamic work of adhesion, W_a, or twice the surface energy of two identical

surfaces. In the absence of covalent bonding, the surface energies can be determined from contact angle measurements or a surface force apparatus.

Materials fail by the initiation and propagation of a crack. The energy criteria arising from fracture mechanics assumes that fracture occurs when sufficient energy is released (from the stress field) by growth of the crack to supply the energy requirements of the new fracture surfaces.[1,9] The energy released comes from stored elastic or potential energy of the loading system and can, in principle, be calculated for any type of test piece. This approach provides a measure of the energy required to extend a crack over a unit area and is termed the fracture energy, G_c.

The energy criterion for fracture describes crack propagation as the conversion of the work done, W_d, by the external force and the available elastic energy stored in the bulk of the specimen, U, into surface energy, γ.[1,9]

$$\partial(W_d\text{-}U)/\partial a \geq \gamma(\partial A/\partial a)$$

Where ∂A is the increase in surface area associated with an increment of crack growth ∂a. For a crack in a material of thickness, b, the criterion becomes:

$$[1/b][\partial(W_d\text{-}U)/\partial a] \geq 2\gamma$$

If it is assumed that energy dissipation around the crack tip is completely elastic, independent of the test geometry, and independent of the way in which the forces are applied to the specimen (the validity of this assumption will be discussed later), then 2γ may be replaced by the symbol, G_c.[1,6] In real systems the value G_c encompasses all the energy losses incurred around the crack tip and the energy required to increase the crack by unit length in a specimen of unit width. Hence, the fracture energy is approximated as:

$$[1/b][\partial(W_b\text{-}U)/\partial a] = G_c$$

Bonded structures exhibiting bulk linear-elastic behavior (away from the crack tip regions) obey Hooke's Law and the above equation may be expressed as:[1,9]

$$G_c = (F_c^2/2b)(\partial C/\partial a)$$

where F_c is the force at the onset of crack propagation, C is the compliance of the specimen, b is the width, and a is the crack length.

In practice G_c is dependent on the mode of stress applied, test rate, and test temperature. Residual stresses and material anisotropy may be important as well.[10] The mode of stress is the geometry in which the body is stressed. There are three types of stress modes, mode I (tensile-opening mode), mode II (in-plane shear mode), and mode III (antiplane shear mode). Taking into consideration these three modes of stress, the fracture energy now becomes:[1]

$$G_c = G_{Ic} + G_{IIc} + G_{IIIc}$$

Chapter III will discuss the affect of the failure mode on the measured adhesion and give some qualitative experimental results.

The rate and temperature effects result from energy dissipated in viscoelastic and plastic deformations at the crack tip. Kinloch[1] proposed a rate/temperature independent parameter called the intrinsic fracture energy, G_o(which should be equal to W_a). From the first law of thermodynamics Kinloch derived:

$$G_c = G_o + \Psi$$

where Ψ is the energy dissipated in viscoelastic and plastic deformations at the crack tip. In almost all cases Ψ is the major contributor to G_c and it is this parameter which

frequently results in the measured value of G_c being highly dependent on the rate and temperature of testing.

In the case of an adhesive joint, it must be considered that two dissimilar materials are being bonded together. The failure may be either in the materials forming the joint, along the interface, or a mixture of both. Thus, an assessment of the fracture energy must also take into account the loci of failure between the adhesive and substrate.

Surface Modification

The chemistry on a material's surface plays an important role in the way it interacts with other materials. Adhesion, friction, wetting, and biocompatability are some examples of physical properties affected by surface chemistry.[11] A material's surface chemistry may be modified by bonding functional groups in the surface region either by covalent, ionic, donor-acceptor, or secondary bonds (van der Waals forces, or hydrogen bonds). Polymer grafting is an example of covalently bonding functional groups (molecules or polymers) to a polymer surface. Polymer adsorption modifies the polymer surface by ionic or secondary bonding.

Altering the chemistry of a polymer or glass surface by the covalent bonding of functional groups has been successfully shown to influence adhesion.[1,2] Some of the methods used to modify surfaces are: polymer grafting,[12,13] flame treatment,[14] plasma treatment,[15,16] corona discharge treatment,[17,18] chemical reduction,[19,20] chemical oxidation,[21,22] and condensation with silane coupling agents.[23] Many of these procedures have been successfully used in industry to modify glass and wide variety of polymers (i.e. polycarbonate, polyethylene, polypropylene, polystyrene, and poly(tetrafluoroethylene).

These modification techniques, however, can be harsh and uncontrolled in nature and often result in a surface which is crosslinked, topographically changed, and/or chemically heterogeneous.[24] It is thus difficult to relate changes in the molecular surface structure resulting from these modifications to changes in macroscopic properties, like wetting, friction, and adhesion. Hence, little advancement has been made in the understanding of surface structure-property relationships.

The surface modification of poly(chlorotrifluoroethylene) can be used as an example on how poorly the surface structure-property relationships in adhesion is understood. Poly(chlorotrifluoroethylene) (PCTFE) is a chemically resistant fluoropolymer that has found uses based on its low permeation, superior thermal stability, and resistance to strong oxidizing agents.[25] These properties also contribute to its poor adhesive properties. In order to circumvent this problem researchers have devised techniques to modify the surface region of PCTFE (and other fluoropolymers), thus improving its adhesive performance.[26] These techniques include: sodium-etching in ammonia,[19.27.28] sodium naphthalide etching in tetrahydrofuran, [29-32] CASING (crosslinking of activated species by inert gas),[33.34] glow discharge,[16.35] microwave plasma,[36] radiation induced grafting,[37] ion beam texturing,[38] abrading beneath reactive adhesives,[39-41] tetra-alkylammonium naphthalide etching in dimethyl-formamide,[42] alkali metal amalgam treatment,[43] inert metal cathode in an aprotic electrolyte treatment[44] and heterogeneous nucleation against high energy surfaces.[33.4546]

Fluoropolymers surface-modified by the above techniques exhibit enhanced adhesive properties but contribute little to a fundamental understanding of how adhesion is

improved. Noble gas and reactive gas treatment of fluoropolymers defluorinate, roughen, cross-link, introduce chemical groups, and even induce morphological changes in the surface region.[47] Detailed studies of fluoropolymers modified with sodium/ammonia,[19] and sodium naphthalide in tetrahydrofuran[48-50] show that these treatments defluorinate the surface producing unsaturation which then reacts with oxygen and moisture to give hydroxyl and/or carboxylic acid groups on the surface. Scanning electron micrographs of the modified surfaces show that they are roughened considerably.

It is clear that these surface modification reactions induce a multitude of changes to the surface making it very difficult to deduce the important variable(s) contributing to their increased adhesive properties. By introducing specific functional groups to the surface of PCTFE in a layer of known thickness and a manner in which the surface structure is not degraded or roughened, we can begin to understand structure-property relationships in adhesion.

Research in the McCarthy group[51-60] has focused on modifying polymer surfaces in a controlled manner. This research program utilizes relatively (compared to the surface modifications mentioned above) nondestructive techniques to introduce a variety of specific functional groups into the surfaces of polymer films. Polymer surfaces that have been successfully modified in a controlled manner are: poly(ether ether ketone) (PEEK),[51] poly(tetrafluoroethylene) (PTFE),[52] poly(vinylidene fluoride) (PVF2),[53] poly(tetra-fluoroethylene-co-hexafluoropropylene) (FEP),[54] and poly(chlorotrifluoroethylene) (PCTFE).[55-60] These surface modifications open the possibility of understanding the relationship between surface structure and macroscopic adhesion.

Polymer Adsorption

The covalent bonding of molecules or polymers to a surface is one approach to surface modification. Surfaces can also be modified by the adsorption of molecules utilizing ionic or secondary bonds. In fact, most commercial adhesives "stick" by the adsorption of the adhesive onto the substrate.[1] For this reason, theoretical treatment of polymer adsorption onto surfaces is a growing area of interest in adhesion. Intensive research efforts have been invested to understand ionic[61] and nonionic homopolymer adsorption,[62] grafted polymer adsorption,[63] random copolymer adsorption,[64] and block copolymer adsorption.[65-67]

Through the combination of experimental and theoretical research it is currently accepted that polymer adsorptions are controlled by a specific set of energies.[61] These energies can be classified into four main areas: (i) secondary bonds, that are always attractive; (ii) ionic bonds, that are repulsive for the same charge sign and attractive for opposite signs; (iii) solvent structure-based short range forces; and (iv) osmotic and entropic interactions that may be attractive or repulsive.

Adsorption theory of nonionic polymers incorporate the energies of (i), (ii), and (iv). The adsorption of polyelectrolytes (ionic polymers) is more complex because electrostatic interactions (ii) must be taken into account, as well as configurational and electrostatic effects, which are strongly interrelated.[61] So, for the sake of clarity the adsorption of nonionic polymers will first be discussed, then the essential components of polyelectrolyte adsorption will be added.

The first set of energies to be considered are the matrix/segment surface interactions, which are a sum of two different interaction energies. These are the matrix/segment interaction energy and the segment/surface interaction energy. The matrix/segment interaction energy is described by the Flory-Huggins interaction parameter, χ. If the matrix is a solvent, then this is a measure of how much the polymer "wants" to stay in solution. If the matrix is another polymer, χ dictates how much the matrix and polymer prefer to remain a homogeneous mixture or phase separate. The segment/surface interaction energy can be described by the surface interaction parameter, χ_s.[68] This is a measure of the free energy difference for each segment when matrix (air, solvent molecule, or another polymer) is displaced from the surface by a polymer chain segment. Polymer adsorption to a surface can result from either a high surface interaction energy (potentially leading to high adhesion), or a low matrix/segment interaction energy such that the polymer segments prefer to remove themselves from the matrix and adsorb to the surface.

The second energetic factor is the loss of entropy associated with a polymer adsorbing to a surface. When a polymer adsorbs to a surface the number of conformations available to the polymer decreases with respect to the polymer in solution (whether solvent or another polymer). The entropy loss is included in the surface interaction parameter χ_s. When the matrix is a solvent the entropy loss is greater than when the matrix is a polymer.

The final energetic factor in polymer adsorption is the osmotic force. The osmotic force, or crowding force, is the repulsive energy associated with the increase in segment

density at the surface when polymers adsorb. The more the polymers adsorb, the greater the osmotic force is acting to dilute the layers, until finally adsorption is halted.[68]

Nonionic polymer adsorption is controlled by the interplay of these three interaction energies. Adsorption usually takes place when the segment/surface interaction energy is high. If a block copolymer is synthesized containing a segment that preferentially adsorbs to the surface, then a polymer "brush" can be formed. When the matrix molecular weight is much lower than the brush molecular weight then there is a high entropic penalty associated with the exclusion of the matrix molecules from the brush. The concentration of matrix molecules within the brush is therefore quite high, and the brush is referred to as a "wet brush". The volume fraction of the matrix polymer in the brush decreases as the matrix molecular weight increases, until a limiting form is reached for which further increases in the molecular weight do not affect the properties of the brush. This limiting form is referred to as a "dry brush" even though the volume fraction of matrix polymer within the brush may still be appreciable.[67]

Much theoretical and experimental research has gone into understanding the adsorption of wet polymer brushes (polymers adsorbed from solution). Homopolymer, copolymer, and block copolymer adsorption from solution have all been extensively investigated, whereas, the study of dry polymer brushes (polymer adsorption from bulk) and its relationship to adhesion is still in its infancy.

In addition to surface modification, the McCarthy group has investigated the adsorption of polymers to surfaces. Recently, Kolb,[69] Stouffer,[70] Kato,[71] Viviano,[72] and Kendall[73] have studied the adsorption of block copolymers from solution. Kato's and

Kendall's experimental results were in qualitative agreement with the scaling law model by Marques and Joanny,[65] and the mean field model by Scheutjens and Fleer.[66] The adsorption of block copolymers is similar to the adsorption of homopolymers and copolymers in the energetic definitions required for adsorption. The main difference lies in the polymer architecture which results in a different conformation for the adsorbed layer. Under proper conditions, block copolymers have one block which has a very high surface/segment interaction energy (χ_s) which adsorbs flat on the surface, while the other block has a low surface/segment interaction energy and remains in solution. The block with the high surface/segment interaction energy is designated the "sticky foot" (SF). Figure 1.1 shows the effect of high surface affinity blocks (SF) on the amount of polymer adsorbed from solution and Figure 1.2 shows a similar effect on polymers adsorbed from the bulk. The effect of SF on adsorption can be observed for both cases. However, the surface excess of adsorbed polymer shows a much higher affinity isotherm for block copolymers adsorbed from solution. This is due to the stronger osmotic forces (stretching the polymer chains) for polymers in solution.

The adsorption of poly(styrene-4-hydroxybutene) block copolymers from solution was extensively studied by Kendall.[73] The copolymer adsorption was studied under conditions where the styrene segments had a low χ_s and the hydroxybutene segments had a high χ_s. The adsorption experiments indicate that the adhesive properties should be increased with the addition of the hydroxybutene group. However, the adsorption approach to adhesion has not been considered experimentally until only recently.

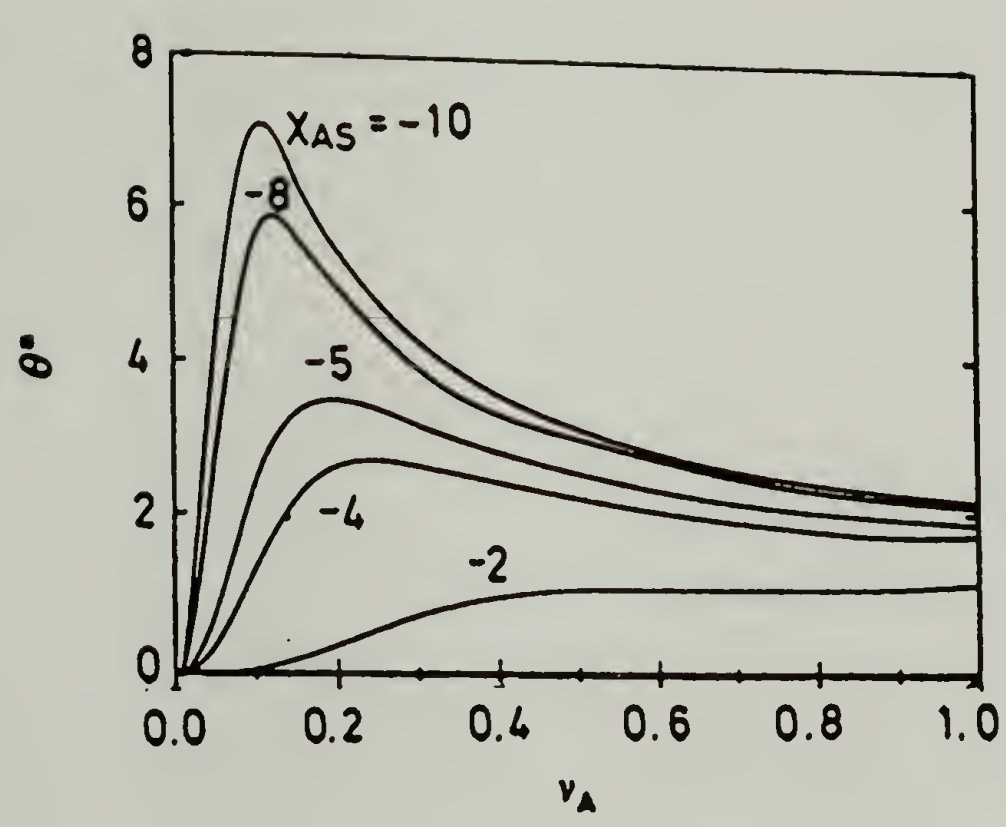

Figure 1.1 The effect of surface affinity of AB block copolymers (A is the high χ_s,"sticky foot" adsorbing segment) on the amount adsorbed. The adsorbed amount θ^a is plotted as a function of the fraction of SF segments per chain and for different adsorption affinities, χ_s, of the SF segments.[65]

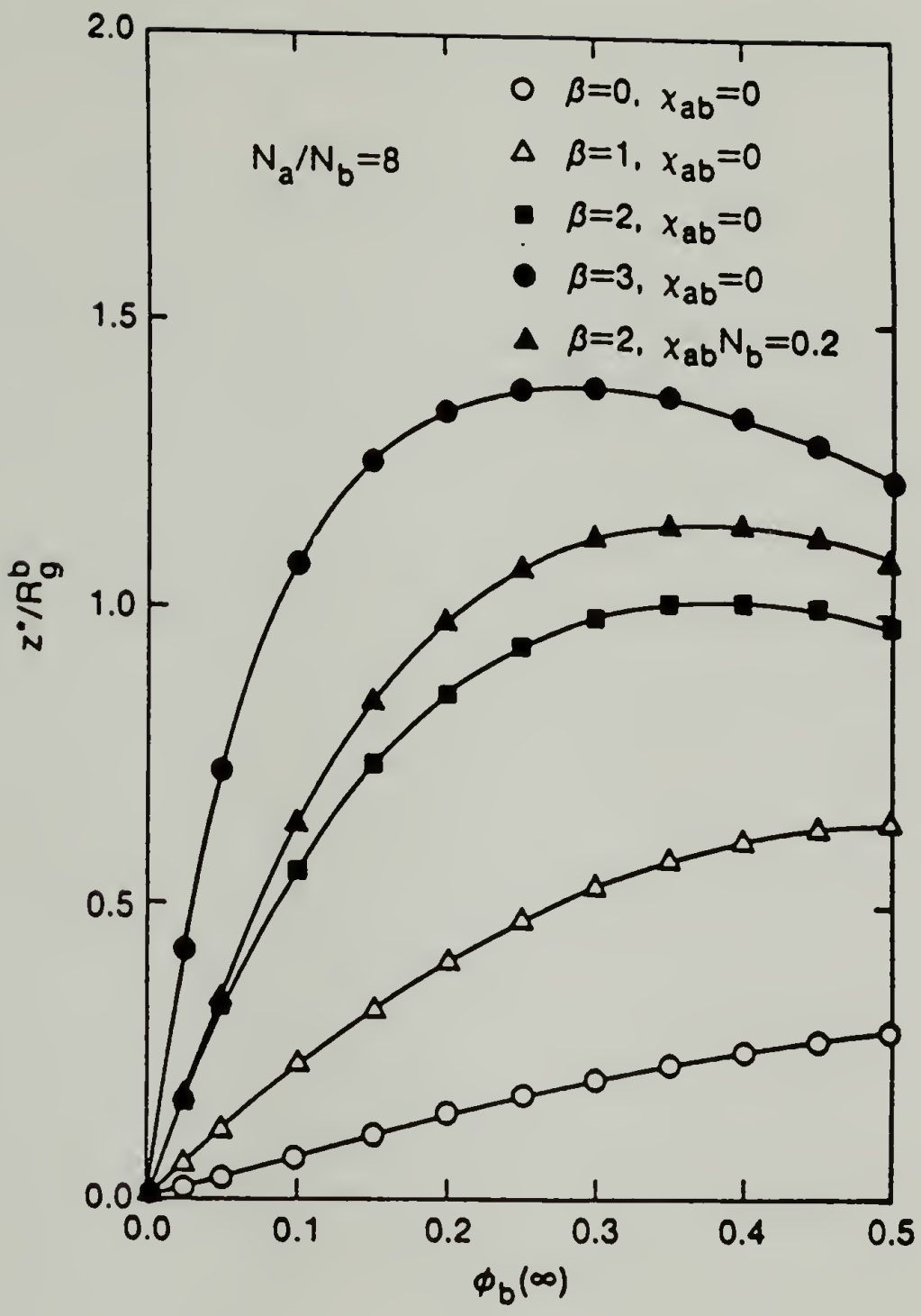

Figure 1.2 Normalized surface excess of adsorbing AB block copolymer as a function of $\phi_b(\infty)$, the equilibrium volume fraction of adsorbing polymer in the bulk matrix phase, for polymers adsorbed from the bulk. Four different values of β are given (β is comparable to χ_s in adsorption from solution).[67]

The formation of dry polymer brushes and their influence on adhesion has been confirmed by Creton et al[4,74,75] and Brown et al.[76,77] Creton measured the effect of poly(styrene-b-methyl methacrylate) (PS-PMMA) on adhesion between poly(methyl methacrylate)(PMMA) and poly(phenyleneoxide)(PPO). The adhesion was determined by measuring a fracture energy using the asymmetric double-cantilever-beam test, this test will be discussed in Chapter VI. Evidence of a polymer brush, which dramatically increased the measured adhesion, was given by secondary ion mass spectrometry (SIMS). In a recent article,[75] Creton investigated poly(styrene-b-isoprene)(PS-I) effects on adhesion between cross-linked polyisoprene and polystyrene grafted onto a silicon wafer. The fracture energy was measured by the JKR method (a method of calculating the fracture energy from the force required to pull the polystyrene from the polyisoprene) at rates from 10^{-10} to 10^{-7} m/s. The influence of the number of PS-I chains and the molecular weight were also investigated. Their results showed that the tether chains across the interface (polymer brushes) had a significant increase on the threshold adhesion. However, the effect of %PI was not thoroughly investigated nor was the effect of χ_s.

From the previous discussion the relevance of polymer adsorption to adhesion seems clear. The adsorption of ionic polymers is known to play important roles in areas such as colloid stabilization, but their use in modifying surfaces for adhesion has gone relatively unnoticed. Recent developments in the layer-by-layer deposition of alternating anionic and cationic polyelectrolytes[78-83] has caused a renewed interest in the adsorption and adhesion of polyelectrolytes.

Polyelectrolyte adsorption theory was developed by Van der Schee and Lyklema[84] and extended to include weakly dissociated polyelectrolytes by Evers et al.[85] Their theories were based on the self consistent field approaches of Sceutjens and Fleer[86] where a lattice model was used to explain the segment-substrate (χ_s) and segment-solvent (χ) interactions. The electrostatic component plays an important role, affecting polymer solution and adsorption conformations.

The theoretical results for polyelectrolyte adsorption are summarized in terms of the strength of the polyelectrolyte (weakly or strongly dissociated), ionic strength of added electrolyte (salts), and charged nature of the substrate (neutral, oppositely, or similarly charged). At low salt concentration, a strong polyelectrolyte adsorbs to an oppositely charged substrate in a flat conformation where segment-segment repulsions inhibit loop and tail formation and promote chain extension in the form of trains on the surface. The amount of polymer that adsorbs is low and increases with increasing surface charge. An increase in salt concentration enhances adsorption by screening lateral electrostatic repulsions in the polymer layer, making the polymer assume a more random conformation, resulting in an increase in the adsorbed amount. Even at high salt concentrations the adsorbed amount increases with increasing surface charge.

The degree of ionization (or pH) is important in the adsorption of weak polyelectrolytes and/or weakly charged surfaces. At a pH where the polyelectrolyte or surface is highly ionized the adsorption behavior follows that of a strong polyelectrolyte. When the solution is at a pH where the polyelectrolyte or surface is neutral, the adsorption follows that of nonionic polymers.

The surface charge also effects polyelectrolyte adsorption in other ways that must be considered. In some cases where the salt concentration is high and the surface charge is high, less polymer adsorbs because the polymer has to compete with the small ions for surface sites to adsorb. In other cases, the surface charge can be overcompensated, resulting in a surface charge reversal.

Experimental evidence of surface charge reversal has been given by Decher.[78,79] He demonstrated that alternating layers of anionic and cationic polyelectrolytes could be adsorbed onto positively charged glass. He investigated the effect of ionic strength and found that as the ionic strength was increased, the layer thickness increased. This is in agreement with theory discussed above for a one-layered system.

Objectives

This thesis explores the relationship between the measured macroscopic adhesion and the molecular interactions. PCTFE films were surface-selectively modified with well characterized chemistries in order to investigate the adhesion resulting from covalent, donor-acceptor, van der Waals, and hydrogen bonding. If the PCTFE film surface is modified to contain functional groups known to interact strongly with a given adhesive, then adhesion can be improved. The objective of this research is to learn how to predict the adhesive properties with knowledge of the surface chemical structure.

Block copolymers have been recently developed as adhesion promoters. Polystyrene, poly(styrene-*b*-1,2-butadiene), and poly(styrene-*b*-4-hydroxybutene) are synthesized with well defined molecular weight, monodispersity, and %SF. Their

measured adhesive properties are correlated with molecular interactions and their known adsorption properties from solution.

The debonding process is also very important in understanding adhesion. This thesis investigates how adhesion test parameters such as the mode of failure and the amount of energy dissipated influences the measured adhesion.

It is also an objective of this thesis to build, characterize, and elucidate the mechanism of the layer-by-layer adsorption of cationic and anionic polyelectrolytes onto glass. Adhesion of the layers to glass, each other, a PSA, and an epoxy are investigated. The effect of surface charge and layer thickness on adhesion and wettability are also studied.

References

1. For a review on adhesion see Kinloch, A.J. *Adhesion and adhesives*, Chapman and Hall: New York, **1987**.

2. Bikerman, J.J. *The Science of Adhesive Joints*, Academic Press: New York, **1961**.

3. Kaelble, D.H. *J. Adhesion*, **1969**, 1, 102.

4. Creton, C.; Brown, H.R.; Deline, V.R. *Macromolecules*, **1994**, 27, 1774.

5. Fowkes, F.M. *Contact Angle, Wettability, and Adhesion*, Advances in Chemistry Series 43, American Chemical Society: Washington, D.C., **1964.**

6. Andrews, E.H. *Developments in Fracture -1*, Applied Science Publishers LTD: London, **1979.**

7. Kendall, K. *Science*, March **1994**, 263, 1720.

8. Wu, S. *Polymer Interface and Adhesion*, Marcel Dekker: New York, **1982**.

9. Williams, J.G. *Fracture Mechanics of Polymers*, Ellis Horwood Limited: Chichester, **1984**.

10. Vrtis, J. Ph.D. Dissertation, University of Massachusetts, **1994**.

11. For a review see Clark, D.T. and Feast, W.J. *Polymer Surfaces*, Wiley-Interscience: New York, **1978**.

12. Oster, G.; Shibata, O. *J. Polym. Sci.*, **1957**, 26, 233.

13. Yamamoto, F.; Yamakawa, S. *J. Polym. Sci.: Polym. Phys. Ed.*, **1979**, 17, 1581.

14. Briggs, D.; Brewis, D.M.; Konieczko, M.B. *J. Mat. Sci.*, **1979**, 14, 1344.

15. Clark, D.T.; Wilson, R. *J. Polym. Sci.: Polym. Chem. Ed.*, **1983**, 21, 837.

16. Collins, G.C.S.; Lowe, A.C.; Nicholas, D. *Eur. Polym. J.*, **1973**, 9, 1173.

17. Rossman, K. *J. Polym. Sci.*, **1956**, 19, 141.

18. Amouroux, J.; Goldman, M.; Revoil, M.F. *J. Polym. Sci.: Polym. Chem. Ed.*, **1982**, 20, 1373.

19. Dwight, D.W.; Riggs, W.M. *J. Colloid Interface Sci.*, **1974**, 47, 650.

20. Barker, D.J.; Brewis, D.M.; Dahm, R.H. *J. Mat. Sci.*, **1979**, 14, 749.

21. Rasmussen, J.R.; Stedronsky, E.R.; Whitesides, G.M. *J. Am. Chem. Soc.*, **1977**, 99, 4736.

22. Baszkin, A.; Ter-Minassian-Saraga, L. *J. Polym. Sci.: Part C*, **1971**, 243.

23. Plueddemann, E.P. *Silane Coupling Agents*, Plenum Press: New York, **1982.**

24. For a review of polymer surface modifications see Ward, W.J.; McCarthy, T.J. *Encyclopedia of Polymer Science and Engineering, 2nd ed.; Supplement*, Wiley: New York, **1989**, 674.

25. Allied-Signal Enc., Aclar Product Bulletin.

26. For a review on fluoropolymer surface modification and adhesion see Siperko, L.M.; Thomas, R.R. *J. Adhesion Sci. Technol.*, **1989**, 3, 157.

27. Purvis, R.J.; Back, W.R. U.S. Patent #2789063, **1957**, 3M Corporation.

28. Brecht, H.; Mayer, F.; Binder, H., *Angew. Makromol. Chem.*, **1973**, 33, 89.

29. Nelso, E.R.; Kilduff, T.J.; Benderly, A.A. *Ind. Eng. Chem.*, **1958**, 50, 329.

30. Benderly, A.A. *J. Appl. Polym. Sci.*, **1962**, 6, 221.

31. ASTM D2093-62T.

32. Cagel, C.V., *Handbook of Adhesive Bonding*, McGraw-Hill Pub.: New York, **1973**, 16.

33. Schonhorn, H.; Ryan, F.W. *J. Adhesion*, **1969**, 1, 43.

34. Schonhorn, H.; Hansen, R.H. *J. Appl. Polym. Sci.*, **1967**, 11, 1461.

35. Gesser, H.D.; Long, R *J. Polym. Sci.: Part B*, **1967**, 5, 469.

36. Kasemura, T.; Ozawa, S.; Hattori, K. *J. Adhesion*, **1990**, 33, 33.

37. Yamakawa, S. *Macromolecules*, **1979**, 12, 1222.

38. Banks, B.A.; Sovey, J.S.; Miller, T.B.; Crandall, K.S. *NASA*, TM-7888 (June **1978**).

39. Lerchenthal, C.H.; Brenman, M.; Yits'Haq, N. *J. Polym. Sci.: Polym. Chem. Ed.*, **1975**, 13, 737.

40. Lerchenthal, C.H.; Brenman, M. *Polym. Eng. Sci.*, **1976**, 16, 747.

41. Lerchenthal, C.H.; Brenman, M. *Polym. Eng. Sci.*, **1976**, 16, 760.

42. Brewis, D.M.; Dahm, R.H.; Konieczko, M.B. *Angew. Makromol. Chem.*, **1975**, 43, 191.

43. Jansta, J.; Dousek, F.P. U.S. Patent #3967018, **1976**.

44. Brewis, D.M.; Barker, J.D.; Dahm, R.H.; Hoy, L.R.J. *Electrochim. Acta.*, **1978**, 23, 1107.

45. Schonhorn, H.; Ryan, F.W. *J. Polym. Sci.*, **1969**, 7(A2), 105.

46. Hara, K.; Schonhorn, H. *J. Adhesion*, **1970**, 2, 100.

47. Kelber, J.A. *Plasma Treatment for Improved Adhesion*, **April 1988**, presented at the Materials Research Society Meeting, Reno, Nevada.

48. Ha, K.; McClain, S.; Suib, S.L.; Garton, A. *J. Adhesion*, **1991**, 33, 169.

49. Marchesi, J.T.; Ha, K.; Garton, A. *J. Adhesion*, **1991**, 36, 55.

50. Marchesi, J.T.; Keith, H.D.; Garton, A. *J. Adhesion*, **1992**, 39, 185.

51. Franchina, N.L.; McCarthy, T.J. *Macromolecules*, **1991**, 24, 3045.

52. Costello, C.A.; McCarthy, T.J. *Macromolecules*, **1987**, 20, 2819.

53. (a) Brennan, J.V.; McCarthy, T.J. *Polym. Prepr. (Am. Chem. Soc., Div. Polym. Chem.)*, **1987**, 29(2), 338. (b) Brennan, J.V.; McCarthy, T.J. *Polym. Prepr. (Am. Chem. Soc., Div. Polym. Chem.)*, **1989**, 30(2), 152.

54. Bening, R.C.; McCarthy, T.J. *Macromolecules*, **1990**, 23, 2648.

55. Huth, J.A.; Danielson, N.D. *Anal. Chem.*, **1982**, 54, 930.

56. Dias, A.J.; McCarthy, T.J. *Macromolecules*, **1985**, 18, 1826.

57. Dias, A.J.; McCarthy, T.J. *Macromolecules*, **1987**, 20, 2068.

58. Lee, K-W.; McCarthy, T.J. *Macromolecules*, **1988**, 21, 2318.

59. Kolb, U.B.; Patton, P.A.; McCarthy, T.J. *Macromolecules*, **1990,** 23, 366.

60. Bee, T.G.; McCarthy, T.J. *Macromolecules*, **1992**, 25, 2093.

61. Cohen Stuart, M.A.; Fleer, G.J.; Lyklema, J.; Norde, W.; Scheutjens, J.M.H.M *Advances in Colloid and Interface Science*, **1991**, 34, 477.

62. Cohen Stuart, M.A.; Cosgrove, T.; Vincent, B. *Advances in Colloid and Interface Science*, **1986**, 24, 143.

63. Iyengar, D.R.; McCarthy, T.J. *Macromolecules*, **1990**, 23, 4344.

64. Cosgrove, T.; Finch, N.A.; Webster, J.R.P. *Macromolecules*, **1990**, 23, 3353.

65. Marques, C.M.; Joanny, J.F. *Macromolecules*, **1989**, 22, 1454.

66. Evers, O.A.; Scheutjens, J.M.H.M.; Fleer, G.J. *J. Chem. Soc. Faraday Trans.*, **1990**, 86, 1333.

67. Shull, K.R. *J. Chem. Phys.* **1991**, 94(8), 5723.

68. Scheutjens, J.M.H.M; Fleer, G.J. *J. Phys. Chem.* **1979**, 83(12), 1619.

69. Kolb, B.U. Ph.D. Dissertation, University of Massachusetts, **1992**.

70. Stouffer, J.; McCarthy, T.J. *Macromolecules*, **1988**, 21, 1204.

71. Kato, T. data to be published

72. Viviano, K. Ph.D. Dissertation, University of Massachusetts, **1994**.

73. Kendall, E.W. Ph.D. Dissertation, University of Massachusetts, **1994**.

74. Creton, C.; Kramer, E.J.; Hui, C-Y.; Brown, H.R. *Macromolecules*, **1992**, 25, 3075.

75. Creton, C.; Brown, H.R.; Shull, K.R. *Macromolecules*, **1994**, 27, 3174.

76. Brown, H.R.; Char, K.; Deline, V.R. *Macromolecules*, **1993**, 26, 4155.

77. Brown, H.R.; Char, K.; Deline, V.R. *Macromolecules*, **1993**, 26, 4164.

78. Decher, G.; Lvov, Y.; Mohwald, H. *Langmuir*, **1993**, 9, 481.

79. Decher, G.; Hong, J-D.; Schmitt, J. *Thin Solid Films*, **1992**, 210/211, 831.

80. Rubner, M.F.; Cheung, J.H.; Fou, A.F.; Ferreira, M. *Polym. Prepr. (Am. Chem. Soc., Div. Polym. Chem.)*, **1993**, 34(2), 757.

81. Rubner, M.F.; Fou, A.C.; Ellis, D.; Ferreira, M. *Polymr. Prepr. (Am. Chem. Soc., Div. Polym. Chem.)*, **1994**, 35(1), 221.

82. Decher, G.; Lvov, Y.; Sukhorukov, G. *Macromolecules*, **1993**, 26, 5396.

83. Decher, G.; Lvov, Y.; Haas, H.; Mohwald, H. *J. Phys. Chem.*, **1993**, 97, 12835.

84. Van der Schee, H.A.; Lyklema, J. *J. Phys. Chem.*, **1984**, 88, 6661.

85. Evers, O.A.; Fleer, G.J.; Scheutjens, J.M.H.M.; Lyklema, J. *J. Colloid Interface Sci.*, **1985**, 111, 446.

86. (a) Scheutjens, J.M.H.M; Fleer, G.J. *J. Chem. Phys.*, **1979**, 83, 1619.
(b) Scheutjens, J.M.H.M.; Fleer, G.J. *J. Chem. Phys.*, **1980**, 84, 178.

CHAPTER II

PREPARATION OF MODIFIED POLY(CHLOROTRIFLUOROETHYLENE) SURFACES FOR ADHESION STUDIES

Introduction

The chemistry on a material's surface plays an important role in the way it interacts with other materials, particularly in adhesion.[1] In order to obtain optimal adhesion, the surface of the substrate must have a strong affinity (χ_s) for the adhesive. The surface must also be mechanically tough, toughness being the area under the stress-strain curve. The surfaces of many substrates do not exibit these properties, and therefore have to be surface-modified to achieve good adhesive performance.

Fluoropolymers are a class of materials that typically exhibit poor adhesive properties.[2] In order to circumvent this adhesion problem, researchers have devised many techniques to modify fluoropolymer surfaces (these techniques were reviewed in Chapter I). These surface modification reactions, however, are corrosive and induce a multitude of changes to the surface making it very difficult to deduce the important variable (s) contributing to their increased adhesive properties.[1-9] Most of the techniques used to surface-modify fluoropolymers defluorinate, roughen, cross-link, introduce chemical groups, and even induce morphological changes in the surface region.[5-9]

Poly(chlorotrifluoroethylene) (PCTFE) is a chemically resistant fluoropolymer that has found specialty uses based on its low permeability, superior thermal stability, and resistance to strong oxidizing agents.[10] These properties also contribute to its poor adhesion to room temperature curing epoxies. By introducing specific functional groups to the surface of PCTFE in a layer of known thickness and in a manner in which the surface structure is not degraded or roughened, we can begin to understand surface structure-property relationships in adhesion.

We have chosen to study adhesion to surface-modified derivatives of PCTFE. Because of its surface-chemical versatility, PCTFE reacts cleanly with lithium reagents to incorporate alkyl and phenyl groups into the surface region.[11-13,17,19] Using lithium reagents containing protected functional groups, a range of chemical functionality can be introduced.[14-16,18,20] Reaction time, temperature, and solvent composition can be manipulated to control the extent (depth) of modification and thus the thickness of the modified layer. This system thus offers unparalleled control of the interface, making it ideal for a fundamental investigation of the role surface structure plays in adhesion.

Changing the chemistry of a polymer surface may affect many surface properties. The effect of the PCTFE surface-modification on some surface properties has been previously investigated. Dias,[13,14] Lee,[15,16] Kolb,[17] Cross,[18] Shoichet,[19,23] and Bee[20,21] investigated the surface structure-property relationship of surface affinity (wettability). Kendall[22] and Shoichet[23] investigated the effect of PCTFE surface functionality on polymer adsorption from solution. Shoichet observed very little adsorption of poly(ethylene oxide) onto unmodified PCTFE but Kendall found that as the surface

affinity (or χ_s, as determined by water contact angle) was increased by suface modification, the amount of poly(styrene-*b*-4-hyroxybutene) adsorbed increased. Bee[21] investigated the influence of PCTFE surface modification on friction properties and the correlation with surface affinity. He concluded that the deformation of the surface region determines the friction behavior which does not always correlate with the surface affinity (as measured by contact angle). To obtain a complete picture of structure-property relationships in adhesion both the surface-chemical and surface-mechanical properties must be considered.

It is also imparative that the adhesion scientist fully understands the 2 to 3 dimensional nature of the surface. The surface is not atomically smooth with a monolayer of interface between the bulk and adjacent medium. Real surfaces are rough with a gradient of properties from the bulk to the surface. When materials are surface-modified, a new gradient in chemistry, and properties exists between the surface and the bulk. Deep surface modifications are more 3-dimensional whereas very shallow modifications are more 2-dimensional in nature. This makes the depth of the surface modification a very important parameter.

It is also very difficult to obtain an accurate picture of the surface structure on a nanometer length scale. The surface chemical functionality can be determined by X-ray photoelectron spectroscopy (XPS) and attenuated total reflectance infrared spectroscopy (ATR IR).[24] These techniques also give a semi-quantitative picture of the modified layer thickness. The change in surface affinity or wettability with surface modification can be measured by contact angle.[25] However, other surface properties such as T_g, modulus, and

toughness are difficult to obtain on the nanometer scale. These properties may contribute significantly to adhesive properties.

While keeping in mind the many factors that contribute to adhesion, we have surface functionalized PCTFE to introduce specific molecular interactions. Table 1.1 gives a list of bond energies for different types of bonds; this table predicts that the adhesive energies should increase or decrease depending on the type of bonding that occurs (i.e. covalent bonds are stronger than van der Waals). PCTFE was surface functionalized with butyl, carboxylic acid, acetal, alcohol, and various ester groups. This chapter discusses the characterization of modified surfaces and the type of bonding that can occur to an adhesive. Contributions to adhesion from secondary bonding can be measured by contact angle (measuring relative surface affinity) and contributions to adhesion from covalent bonding can be determined by studying the chemical reactivity of the surface with model organic compounds (to determine if covalent bonding with an adhesive can occur). Chapter III discusses the relationship between the measured adhesion and the adhesion predicted from the type of bonding that occurs. In addition to chemical interactions, mechanical contributions to the measured adhesion are also discussed.

Experimental

General

PCTFE (Aclar 33c®) was obtained from Allied-Signal as a 125 micron thick film. The film samples were extracted with refluxing dichloromethane for 2 hours and vacuum dried (0.05 mm) for 48 hours. This procedure gives films that are consistently free of any

detectable contaminates. Film samples were stored in Schlenk tubes under nitrogen or vacuum. Tetrahydrofuran was distilled from sodium benzophenone dianion. Heptane was distilled from calcium hydride. 3-bromo-1-propanol (Aldrich) was distilled under vacuum (5 mm, 60-65°C) from potassium carbonate. Ethylvinyl ether (Aldrich) was purified by trap-to-trap distillation. Butyryl chloride (Aldrich) was purified by trap-to-trap distillation. Adipoyl chloride (Aldrich) was purified by vacuum distillation (105°C, 2mm). Heptadecanoyl chloride and stearoyl chloride (Aldrich) were used without further purification. 1-Butyllithium (Aldrich, 1.6M) and *t*-butyllithium (Aldrich, 1.7M) were both purchased as solutions in hexane, the *t*-butyllithium was titrated with biphenylmethanol prior to use.

Air-sensitive reactions were carried out under dry nitrogen. Reactions with films were not stirred. Contact angle measurements were obtained with a Rame-Hart telescopic goniometer and a Gilmont syringe with a 24-gauge flat-tipped needle. Water (doubly distilled) was used as the probe fluid. Dynamic advancing and receding contact angles were determined by measuring the tangent of the drop at the intersection of the air/drop/surface while adding (advancing) and withdrawing (receding) water to and from the drop. The values reported are averages of five measurements made on different areas of the film sample surface. Attenuated total reflectance infrared (ATR IR) spectra were obtained under nitrogen by using a Nicolet IR/44 FTIR spectrometer and a germanium (45°) internal reflection element. X-ray photoelectron spectra (XPS) were recorded using a Perkin Elmer-Physical Electronics 5100 spectrometer with Mg Kα excitation (400 W). The samples charged variably during analysis, and the reported binding energies are not

corrected for charging. Spectra were recorded at two angles, 15° and 75° from the film surface (some surfaces were analyzed at additional angles).

Reaction of PCTFE with *n*-butyllithium (PCTFE-Butyl)

Three (3 cm x 5 cm) PCTFE film samples were placed into a Schlenk tube with glass dividers and purged with nitrogen for 15 minutes. To a nitrogen purged graduated cylinder fitted with a teflon stopcock and septum, 3.5 ml of *n*-butyllithium were added via cannula. Heptane and THF were added to a total volume of 61.5 ml. The solvent compositions investigated (expressed as percent heptane in THF) were 100%, 99.96%, 99.87%, 99.2%, 96.7%, 90%, 50%, and 38.2%. Both the Schlenk tube containing the films and the reagents were equilibrated at the desired reaction temperature before the *n*-butyllithium in solvent was cannulated to the PCTFE films. Reaction temperatures studied were -78°C, -15°C, 0°C, and 25°C. Reaction times investigated were 0.25 hr, 0.5 hr, 3 hr, and 18 hr. After reaction, the *n*-butyllithium solution was removed via cannula. The reaction tube was removed from the temperature bath after the first methanol wash. The methanol used for the first wash was equilibrated at the reaction temperature. The film sample was washed sequentially under nitrogen with methanol (2 x 70 ml), water (2 x 70 ml), methanol (2 x 70 ml), dichloromethane (2 x 70 ml), and dried (72 hr, 0.05 mm, 45°C) before XPS, ATR IR, contact angle, and adhesion data were obtained. (Notebook #1 pp.63-143, #4 pp.7-57)

Oxidation of PCTFE-Butyl (PCTFE-OX)

Concentrated sulfuric acid (100 ml) was added to a beaker containing 2 grams of potassium chlorate.[19] The reaction mixture was stirred 30 minutes with a magnetic stirrer

before adding the PCTFE-Butyl films. After a 2 hour reaction time (at ambient conditions) the films were washed sequentually with water (1 x 100 ml), isopropanol (1 x 100 ml), water (1 x 100 ml), isopropanol (1 x 100 ml), dichloromethane (1 x 100 ml), and dried (3 days, 0.05 mm, 40°C) before XPS, ATR IR, contact angle, and adhesion data were obtained. (Notebook #1 pp.71,75,81,93,97,103)

Reaction of PCTFE-OX with *n*-butyllithium

Three 1 cm x 5 cm strips of PCTFE-OX were added to a Schlenk tube and purged 15 minutes with nitrogen. To a nitrogen purged graduated cylinder fitted with a teflon stopcock and septum, 3.5 ml of *n*-butyllithium were added via cannula. Heptane and THF were added to a total volume of 61.5 ml (38.2% heptane). Both the Schlenk tube containing the films and the reagents were equilibrated at the reaction temperature of 0°C before the *n*-butyllithium in heptane/THF was cannulated to the PCTFE films. The films were reacted for 30 minutes before washing. The films were washed and dried as described for PCTFE-Butyl synthesis. (Notebook #1 pp.81, 99)

Reaction of PCTFE-Butyl with Amines

PCTFE-Butyl was placed into a Schlenk tube and 30 ml of a 40% by weight solution in water of dimethylamine or hexamethylenediamine was added. Reactions were at room temperature for 24, 63, and 96 hours. PCTFE-Butyl surfaces were also reacted with diethylamine (1.0 ml) in THF (35 ml) for 24 hours at 20°C . The films were washed and vacuum dried in the same manner as PCTFE-Butyl. (Notebook #4 pp.131-148)

Acetaldehyde Bromopropyl Ethyl Acetal (BrPEA) Synthesis

BrPEA was prepared from 3-bromo-1-propanol and ethyl vinyl ether using a previously reported procedure.[14] (Notebook #1 p. 21, #4 p. 63, #6 p.18)

Acetaldehyde 3-Lithiopropyl Ethyl Acetal (LiPEA) Synthesis

LiPEA was prepared by a modification of the previously described procedure.[14] BrPEA (1.15 g, 5.5 mmol) was introduced to a nitrogen purged Schlenk tube containing a glass coated magnetic stirring bar, diluted with 18 ml of heptane, and equilibrated at -78°C. To a separate purged Schlenk tube, 4 ml (6.4 mmol) of *t*-butyllithium was introduced, diluted with 14 ml of heptane and equilibrated at -78°C. The *t*-butyllithium was cannulated slowly (10 minutes) to the BrPEA. The suspension was stirred for 30 minutes at -78°C, allowed to warm to -15°C and stirred for 45 minutes then cooled back to -78°C. A white precipitate was present. 32 ml THF equilibrated at -78°C was then cannulated to the reaction mixture, the white precipitate slowly dissolved. If excess *t*-butyllithium was present, the reaction mixture turned yellow. If this occurred, the reaction mixture was allowed to warm until the yellow color disappeared. (Notebook #1 pp.41,50,57, #4 pp.67-79,83-103, #6 pp.5-57)

Reaction of PCTFE with LiPEA (PCTFE-PEA)

PCTFE films were placed in a Schlenk tube and purged with nitrogen (same as *n*-butyllithium modification). The PCTFE films and the reaction mixture were equilibrated at -15°C before the reaction mixture was cannulated to the PCTFE films. The reaction time was 30 minutes. After the reaction, the LiPEA solution was removed via cannula. The reaction tube was not removed from the temperature bath until after the first methanol

wash. The methanol used for the first wash was equilibrated to the reaction temperature. The film samples were washed sequentually under nitrogen with methanol (3 x 70 ml), water (3 x 70 ml), methanol (3 x 70 ml), dichloromethane (3 x 70 ml), and dried (72 hr, 0.05 mm, 45°C) before XPS, ATR IR, contact angle, and adhesion data were obtained. (Notebook #1 pp.41,50,57, #4 pp.67-79,83-103, #6 pp.5-57)

Hydrolysis of PCTFE-PEA (PCTFE-OH)

The PCTFE-PEA films were placed in a 100°C solution of 5 ml concentrated hydrochloric acid and 50 ml of water for 30 minutes.[21] The film samples were removed and washed sequentually with water (2 x 100 ml), methanol (100 ml), water (100 ml), methanol (100 ml), dichloromethane (100 ml), and dried (72 hr, 0.05 mm, 25°C) before XPS, ATR IR, contact angle, and adhesion data were obtained. (Notebook #4 pp.93-107, #6 pp.7-58)

Reaction of PCTFE-OH with Butyryl Chloride (PCTFE-Butyrate)

PCTFE-OH (two 1 cm x 5 cm strips) was added to a Schlenk tube and purged with nitrogen before 50 ml THF and 3.7 ml butyryl chloride were added via cannula. The reaction was run 18 hr at ambient conditions. The film samples were washed under nitrogen with distilled methanol (2 hr soak in 50 ml then 2 x 50 ml), water (1.5 hr in 50 ml, 2 x 50 ml), methanol (3 x 50 ml), dichloromethane (2 x 50 ml), and dried (72 hr, 0.05 mm, 45°C) before XPS, ATR IR, Uv-vis, contact angle and adhesion data were obtained. Reactions were also run as above using pyridine as a catalyst (1.4 ml, distilled over calcium hydride). (Notebook #6 pp.9,31,39,44,51,60)

Reaction of PCTFE-OH with Adipoyl Chloride (PCTFE-Adipate)

The same procedure was used as above except 2.5 ml of adipoyl chloride was used. (Notebook #6 pp.15,29,37,44,51,60)

Reaction of PCTFE-OH with Heptadecanoyl Chloride (PCTFE-Hept)

The same procedure was used as above except 4.7 ml heptadecanoyl chloride was used. (Notebook #6 pp.44)

Reaction of PCTFE-OH with Stearoyl Chloride (PCTFE-Stear)

The same procedure was used as above except 5.9 ml stearoyl chloride was used. (Notebook #6 pp.62)

Results and Discussion

Overview

The reactions utilizing lithium reagents to incorporate functional groups into the surface region of PCTFE are described in Schemes 2.1 and 2.3. The characterization and mechanism of these reactions have been reported elsewhere.[13-21,28] Lithium reagents react by metal-halogen exchange of chlorine for lithium; the lithiated product eliminates lithium fluoride producing a difluoroolefin. A second equivalent of lithium reagent adds to the difluoroolefin and a second lithium fluoride is eliminated, producing the functionalized product.[13] The reduction/functionalization of PCTFE is controlled by reaction temperature, reaction time, solvent, and lithium reagent concentration.

The PCTFE surface modification reactions were characterized by contact angle, XPS, SEM, AFM, ATR IR, Uv-vis, and phase interference microscopy. Water contact angle measurements indicated qualitative changes in surface affinity by the introduction of

surface functional groups. The PCTFE-OX, PCTFE-PEA, PCTFE-OH, PCTFE-Butyrate, PCTFE-Adipate, PCTFE-Hept, PCTFE-Stear surfaces showed changes in water contact angle. The PCTFE-Butyl surfaces showed no change in contact angle when water, glycerol, or hexadecane were used as probe fluids. XPS confirmed the reactions described. XPS spectra were recorded at two takeoff angles (15° and 75° from the film's surface) which analyze the outer 10 and 40 angstroms respectively.[26] Atomic concentrations were determined by integrating the area under the peak of each appropriate region and multiplying by a sensitivity factor. ATR IR was used to probe the surface modification at greater depths, the germanium crystal used had an average penetration depth of 1,000 to 2,000 angstroms depending on the wavenumber.[24] UV-vis showed an absorbance at 270 nm that increased with modification due to unsaturation of the polymer chain.

Phase interference microscopy and scanning electron microscopy exhibited no changes in surface topography, indicating that the reactions were not corrosive on the scale of tenths of microns. Atomic force microscopy (AFM) showed that indeed the unmodified film's surface was very rough on a nano-scale, but no changes in roughness or surface structure were apparent for the PCTFE-Butyl surfaces. However, changes in roughness and surface structure were observed for the PCTFE-PEA and PCTFE-OH surfaces. These AFM results are from only a few preliminary experiments, more quantitative studies are being conducted by the McCarthy group.[27]

PCTFE-Butyl Surface Chemistry (Scheme 2.1)

XPS survey spectra (Figure 2.1) show that the extent of PCTFE surface modification with *n*-butyllithium depends upon reaction time, temperature, and solvent composition. The carbon (C_{1s}) region at 289-296 eV is split into three distinct regions. The CF_2 C_{1s} peak at 296 eV decreases and the CH_2 C_{1s} peak at 289 eV increases with increasing reaction time, temperature or %THF in the solvent system. The center C_{1s} peak at 293 eV is from the carbon-carbon double bonds produced during the reaction and CFCl remaining in the surface region. This peak is very distinct at low levels of surface modification, but at higher modifications only appears as a shoulder on the CH_2 C_{1s} peak. The fluorine (F_{1s}) peak at 700 eV decreases with increasing reaction time, temperature, and %THF; the chlorine (Cl_{2p}) peak at 203 eV quickly decreases and disappears with increasing modification. Table 2.1 summarizes the atomic compositions determined by XPS using a 15° take-off angle.

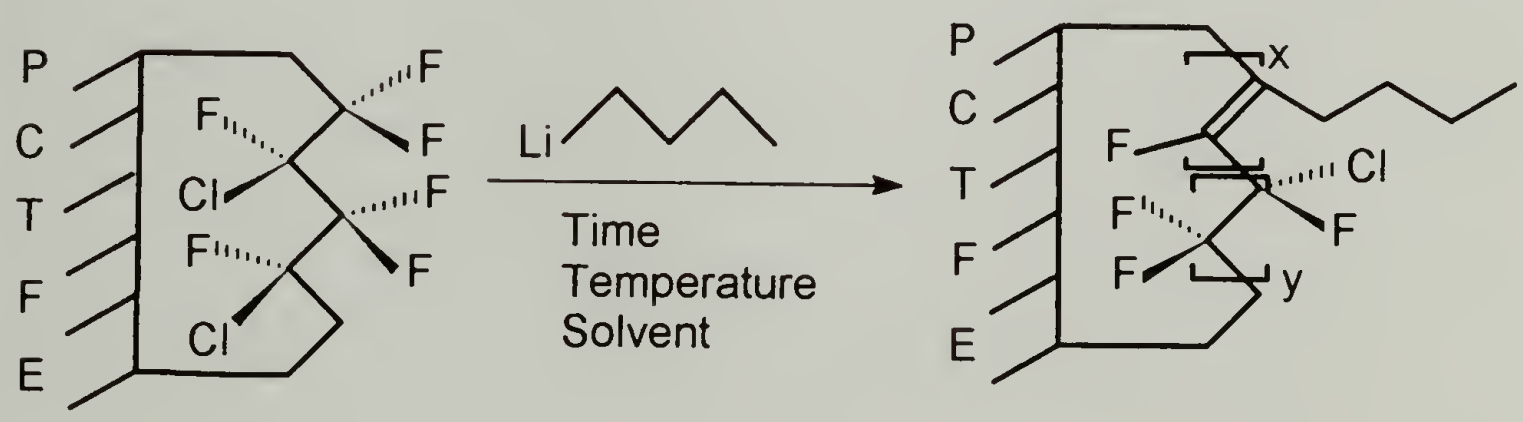

Scheme 2.1. Surface modification reaction of PCTFE with n-butyllithium.

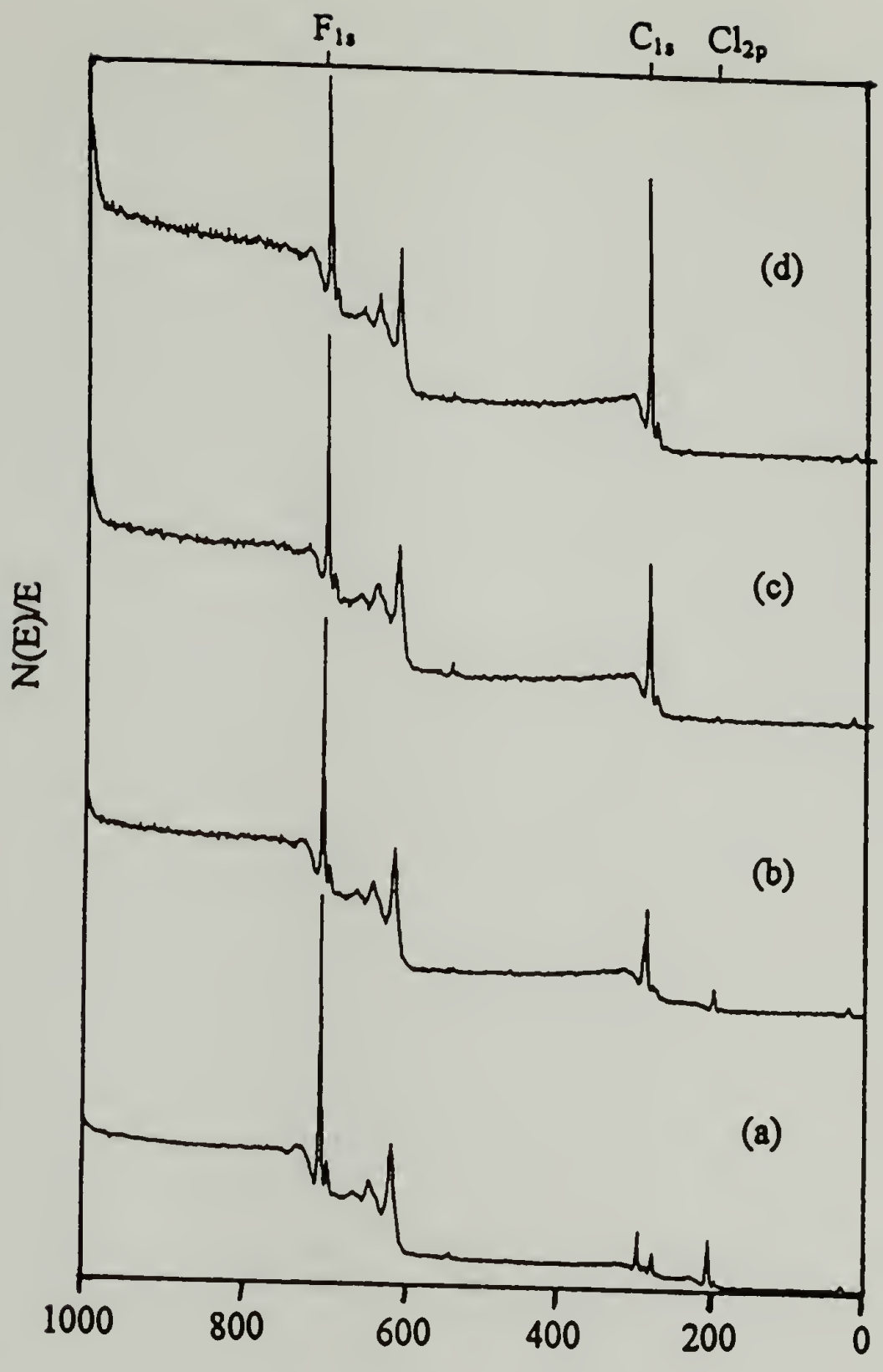

Figure 2.1 XPS survey spectra of (a) PCTFE, (b) PCTFE-Butyl prepared at 0°C for 0.5 hours in heptane, (c) PCTFE-Butyl prepared at 25°C for 0.5 hours in heptane, and (d) PCTFE-Butyl prepared at 25°C for 0.5 hours in 97% heptane/THF.

Table 2.1 Atomic compositions of PCTFE surface modified with *n*-butyllithium under various reaction times, temperatures, and solvent compositions.

Time (hrs.)	Temp.(°C)	Solvent (hept/THF)	Atomic Composition (15° take-off angle)			
			$\%C_{1s}$	$\%F_{1s}$	$\%Cl_{2p}$	$\%O_{1s}$
0.5	-78	100%	38.1	46.4	15.6	
0.5	-15	100%	56.7	35.2	7.6	0.5
0.5	0	100%	67.5	28.2	3.7	0.7
0.5	25	100%	75.1	23.7	0.2	1.1
0.25	25	100%	75.1	24.5	0.4	
3.0	25	100%	78.5	20.2	0	1.4
18	25	100%	79.7	19.1	0	1.3
0.5	0	99.96%	76.0	21.8	0.2	2.1
0.5	0	99.87%	78.0	20.4	0.2	1.6
0.5	0	99.2	81.5	16.8	0.1	1.7
0.5	0	96.7	81.7	16.6	0.4	1.5
0.5	0	90.0	82.0	15.4	0.7	1.9
0.5	0	77.0	81.1	16.7	0.6	1.6
0.5	0	50.0	80.1	15.6	0.6	3.7
0.5	0	37.0	78.2	19.9		1.9
0.5	-78	37.0	81.2	14.9	0.5	1.6
0.5	25	97.0	81.8	17.5	0.1	0.6
0.5	25	37.0	86.3	11.7	0	2.0

The extent of surface modification can be quantified as a carbon to fluorine ratio (C/F) from atomic compositions measured by XPS. A C/F ratio of 0.67 would indicate no reaction has occurred, whereas a C/F ratio of 6.0 would indicate that the surface is fully modified. Figures 2.2-2.4 show the effect of solvent composition (% THF in heptane), reaction time, and reaction temperature on the extent of surface modification, respectively.

From the shape of the C/F ratio versus % THF in heptane curve we can see that the extent of modification in the surface region quickly plateaus with the addition of small amounts of THF (Figure 2.2). Even at a temperature of -78°C, the reactions run in THF/heptane mixtures quickly proceed to completion. The increase in reaction rates and depths with THF addition is from two complementary effects. THF solvates the lithium cation thereby creating a more reactive anion, and the THF "wets" the PCTFE surface aiding in the penetration of the lithium reagent into the surface. However, the plateau value is not the predicted C/F ratio of 6.0; reactions in THF/heptane give a plateau value of 5. It has been proposed that the modified structure is one consisting of ~80% functionalized repeat units and ~20% difluoroolefins.[21,28] This has been rationalized by proposing that the formation of the difluoroolefin proceeds quantitatively, while the introduction of the butyl groups proceeds in 80% yield (in the presence of THF).

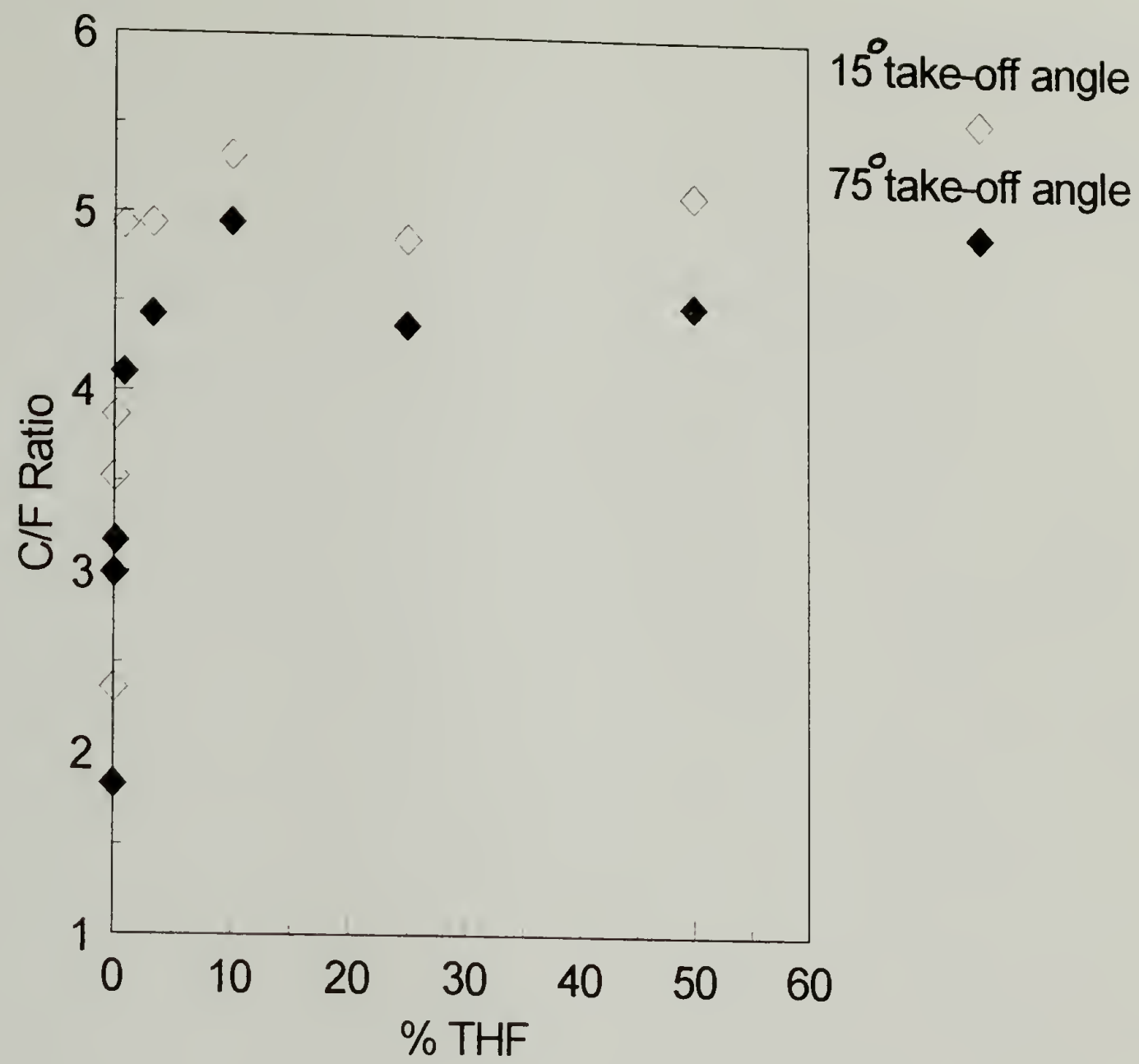

Figure 2.2 Effect of solvent composition (THF/heptane mixtures) on extent of PCTFE-Butyl surface modification, as measured by the C/F ratio. The reactions were run at 0°C for 0.5 hours.

The extent of modification also quickly plateaus with reaction times of greater than 3 hours (reacted in heptane, 25°C). The lower plateau value (C/F ratio of 4) of reactions in heptane is likely due to a greater number of difluoroolefin groups. This is somewhat expected from the proposed mechanism because heptane does not "wet" PCTFE as well as THF, thereby introducing a greater amount of steric constraints during the introduction of the butyl groups and causing a more 2-dimensional or heterogeneous reaction.

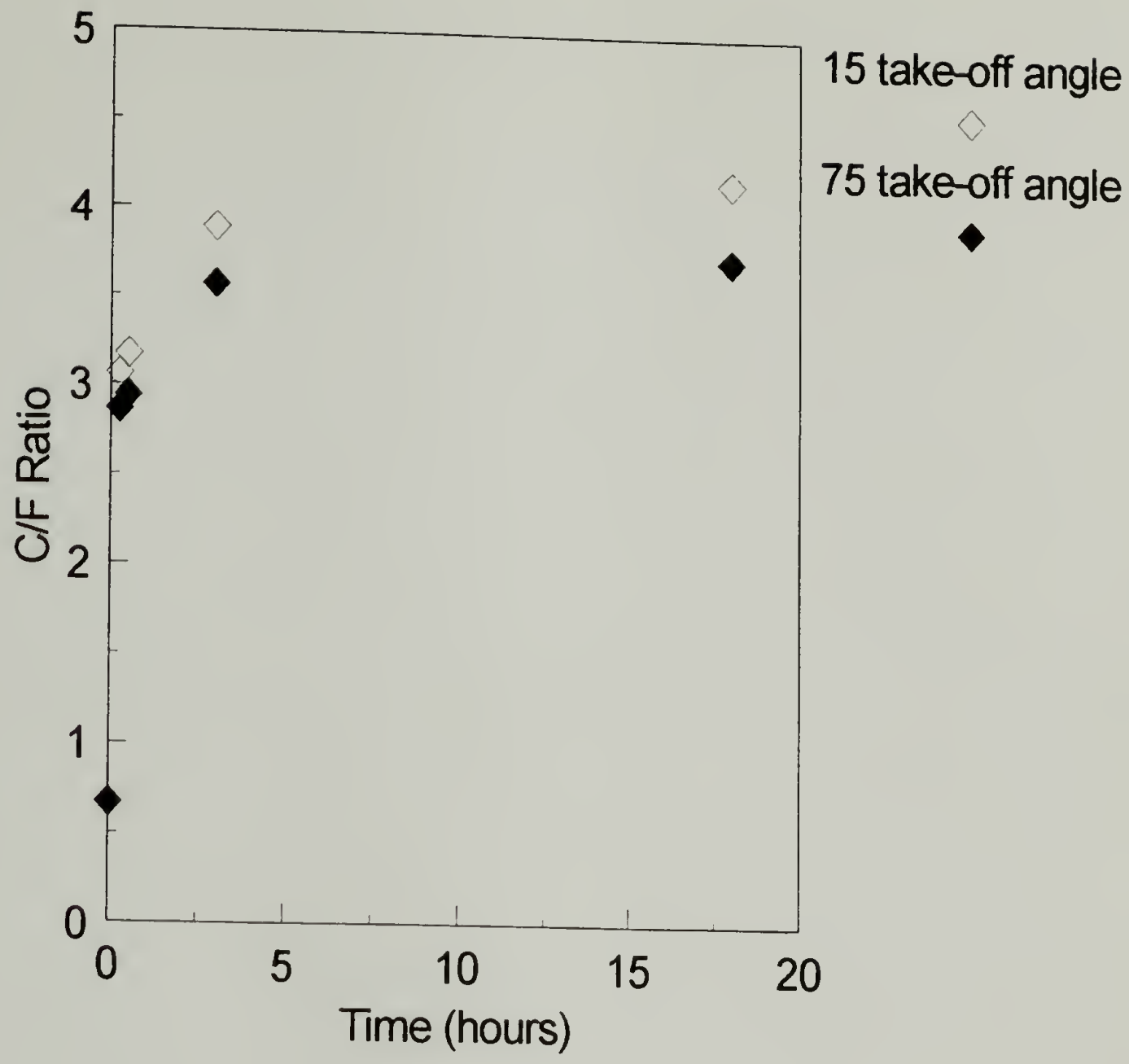

Figure 2.3 Effect of reaction time on the extent of PCTFE-Butyl surface modification, as measured by the C/F ratio. The reactions were run in heptane at 25°C.

The reaction temperature also had a dramatic influence on the extent of modification (Figure 2.4). Reactions run in heptane for 0.5 hours at temperatures ranging from -78°C to 25°C show a strong temperature dependence, but a plateau value was not obtained. This is because the chain mobility and therefore the penetration of the lithium

reagent into the polymer increases with increasing temperature. It is conceivable that at high enough temperatures, reactions would extend through the entire thickness of the film.

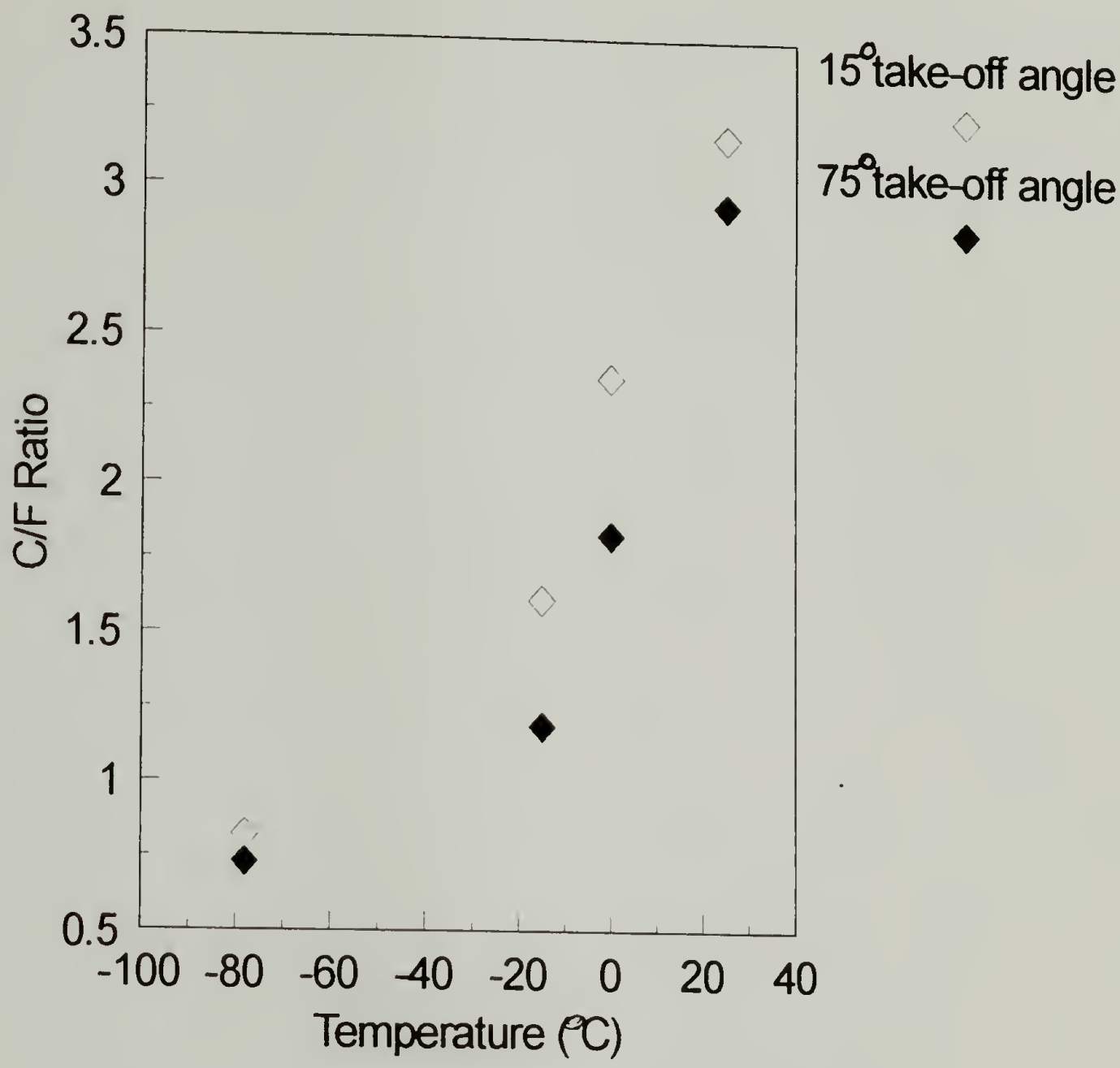

Figure 2.4 Effect of reaction temperature on the extent of PCTFE-Butyl surface modification as measured by the C/F ratio. Reactions were run in heptane for 0.5 hours.

Variable angle XPS studies show a strong angle dependence for reactions run in heptane at -15°C and 0°C for 30 minutes. Under these conditions 3 distinct C_{1s} peaks can be observed. The relative intensity of the C_{1s} peaks vary with XPS take-off angle (Figure

2.5) which shows that the depth of butyl surface modification prepared at -15°C in heptane for 30 minutes is on the order of 10 angstroms, whereas butyl surface modifications prepared at 0°C in heptane for 30 minutes is on the order of 40 angstroms. Precise quantification of the reaction depth is difficult because the escape depth of the electrons ejected from the surface is not know precisely. The depth of surface modification is also likely to be a distribution.

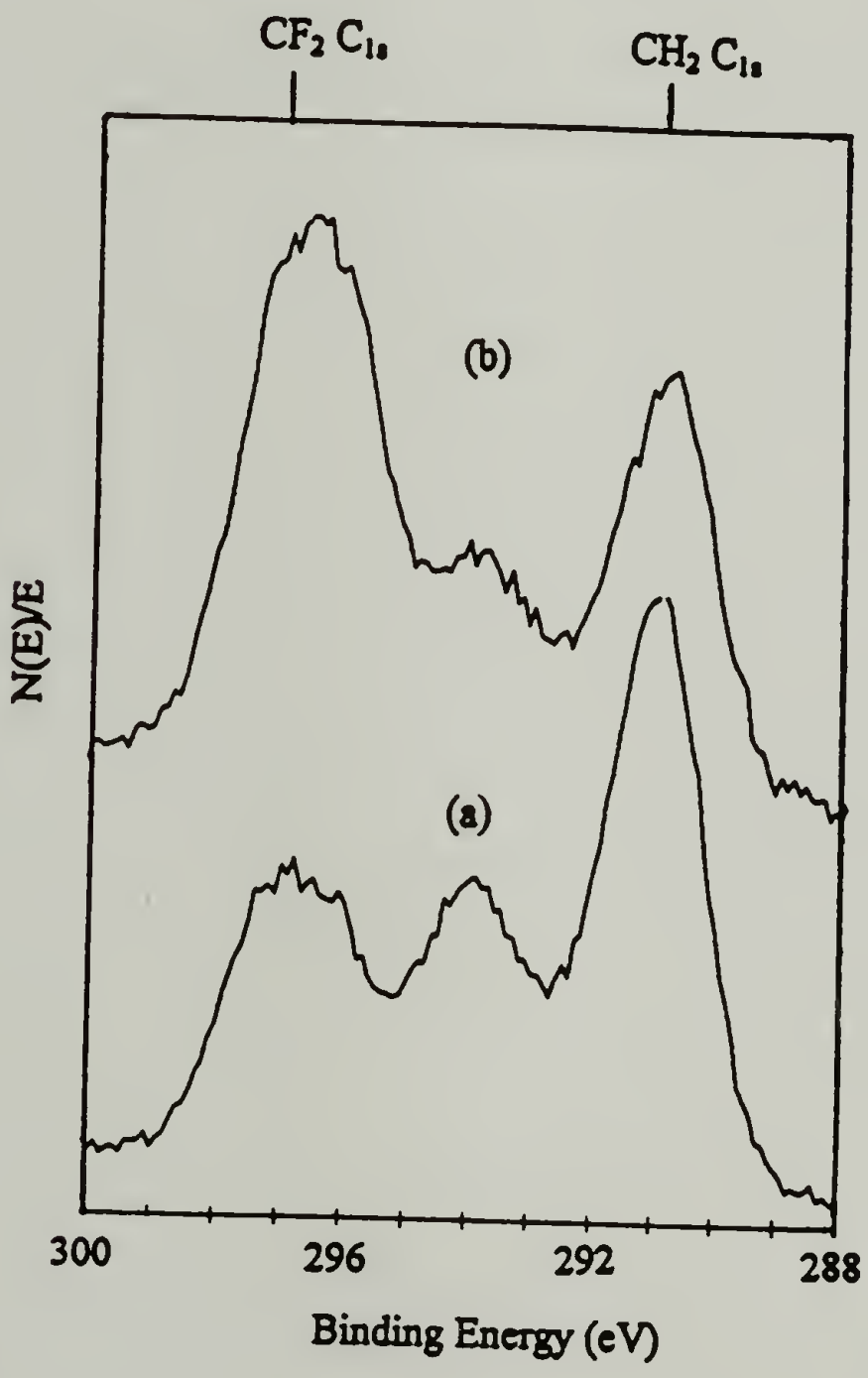

Figure 2.5 XPS multiplex of carbon C_{1s} region at (a) 15° take-off angle and (b) 75° take-off angle for PCTFE-Butyl reacted in heptane at -15°C for 0.5 hours.

ATR IR and UV-vis spectroscopy become useful techniques in characterizing the surface structure and depth of reaction for deeper modifications. ATR IR show the appearance of C-H stretching peaks at 2970, 2940, and 2880 cm^{-1} for reactions run in heptane at 0°C or greater (Figure 2.6). Reactions run in heptane/THF mixtures also show the same C-H stretching peaks. UV-vis transmission spectra look identical to those reported for PCTFE-PEA,[21,28] the UV absorbance arises from the conjugation introduced into the polymer backbone as a result of the modification.[21,28] UV-vis spectra show an increase in absorbance at 270 nm with reaction time and temperature (reactions in heptane only). This increased absorbance can be attributed to an increase in the number of absorbing moieties, which translates into an increase in the thickness of the modified layer. The trends in absorbance with reaction time and temperature complement those found by XPS and ATR IR. Reactions in heptane/THF mixtures show no change in absorbance at %THF≥0.04. This is also in agreement with the XPS and ATR IR data. This data gives evidence that only small amounts of THF are required to accelerate the surface modification, and the addition of more THF in the reaction mixture does not enhance the reaction.

Oxidation of PCTFE-Butyl and Repeat Reaction with *n*-butyllithium

PCTFE-Butyl surfaces were oxidized with a concentrated sulfuric acid/potassium chlorate mixture which oxidatively removed the butyl groups in the surface region. PCTFE-OX surfaces were analyzed by ATR IR, XPS, and contact angle. The oxidized surfaces showed no remaining butyl groups by ATR IR. XPS survey spectra were nearly identical to virgin PCTFE (Figure 2.7). However, 1.5% to 6.0% oxygen was present on

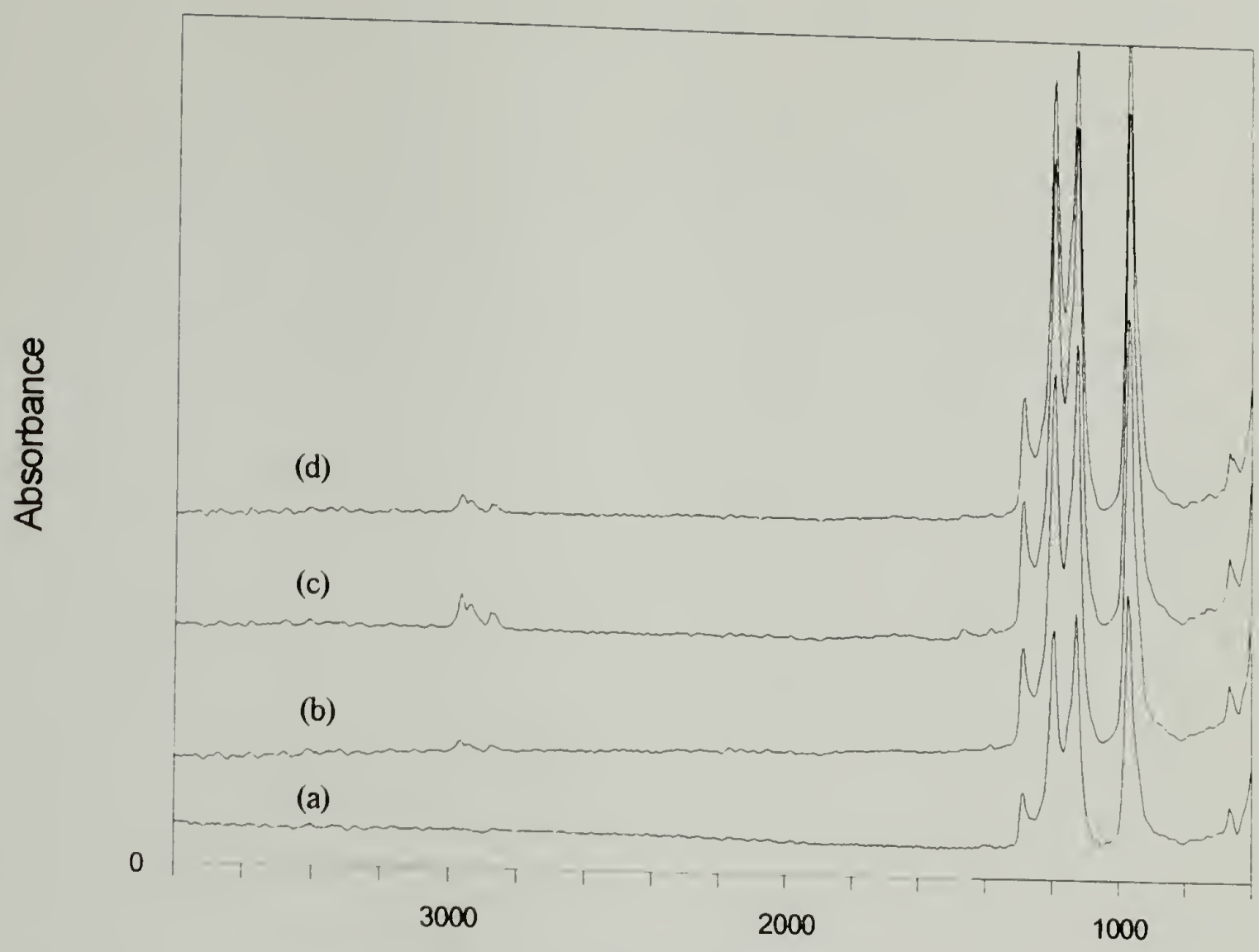

Figure 2.6 ATR IR spectra of (a) PCTFE, (b) PCTFE-Butyl prepared in heptane at 25°C for 0.5 hours, (c) PCTFE-Butyl prepared in heptane at 25°C for 18 hours, and (d) PCTFE-Butyl prepared in 97% heptane/THF at 0°C for 0.5 hours.

the surface by XPS which was likely in the form of carboxylic acid groups because of the low water contact angle (92/28).

The PCTFE-OX surface could also be modified with *n*-butyllithium. This showed a complete reaction by XPS (Figure 2.7) and ATR IR. The water contact angle increased to 107/79 which is identical to virgin PCTFE and PCTFE-Butyl. The atomic composition by XPS at a 15° take-off angle was 13.3% fluorine, 84.1% carbon, 2.1% oxygen, and

0.5% chlorine. To the naked eye of the observer, PCTFE, PCTFE-Butyl, PCTFE-OX, and the PCTFE-OX reacted with *n*-butyllithium all appeared identical. This indicates that excessive corrosion, reduction, or surface roughening are not taking place.

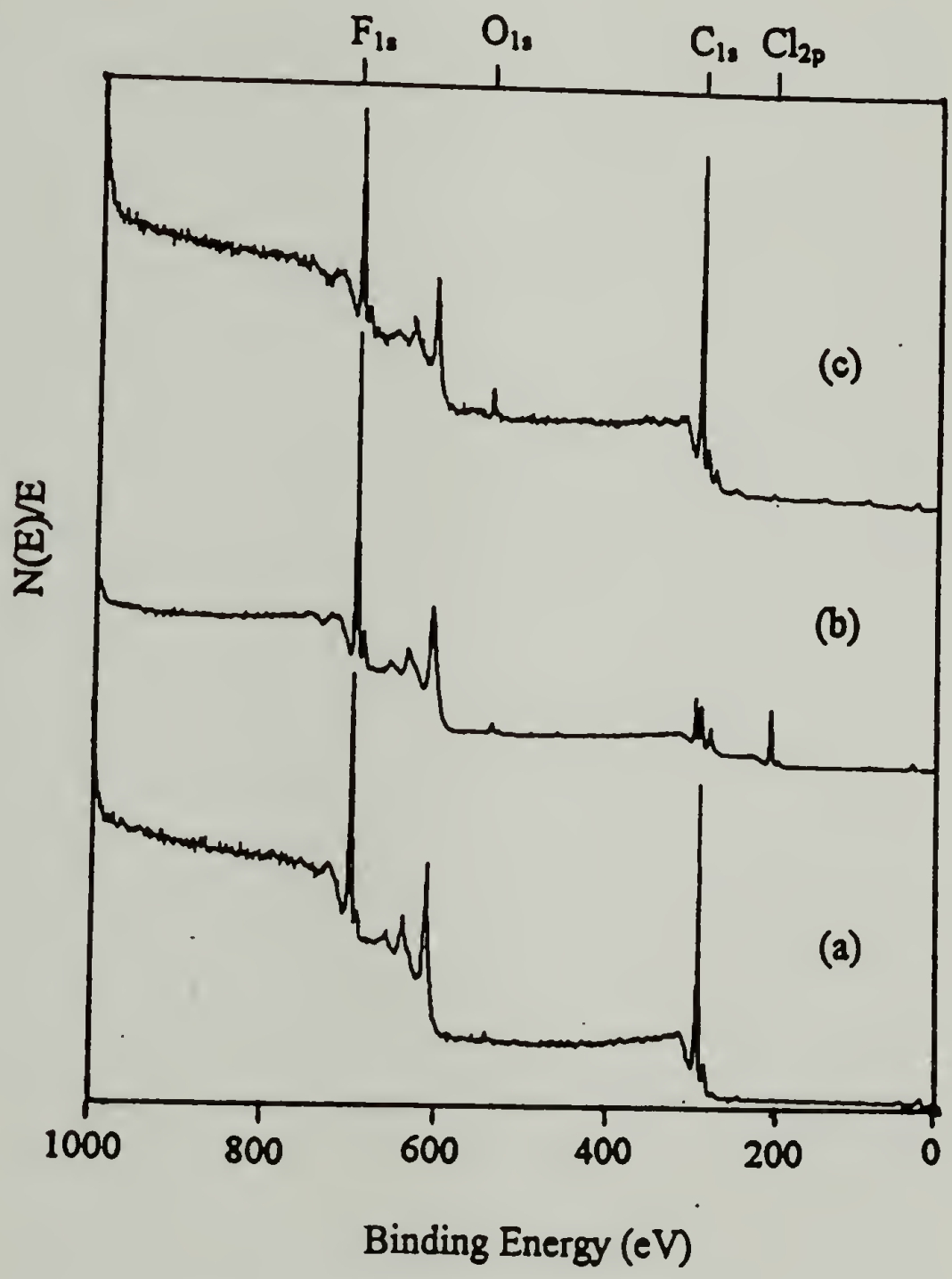

Figure 2.7. XPS survey spectra of (a) PCTFE-Butyl prepared in 97% hept/THF at 25°C for 0.5 hours, (b) PCTFE-OX from previous PCTFE-Butyl, and (c) PCTFE-OX reacted with *n*-butyllithium in 97% hept/THF at 25°C for 0.5 hours.

PCTFE-Butyl-amine Surface Chemistry (Scheme 2.2)

The reactivity of PCTFE-Butyl surfaces was investigated by reacting PCTFE and PCTFE-Butyl (modified to various extents) with dimethylamine, diethylamine, and hexamethylenediamine. The reactivity of PCTFE-Butyl with amines is very important in understanding adhesion mechanisms; chapter III will investigate the adhesion of PCTFE-Butyl to epoxy where an amine curing agent is used to cure the epoxy adhesive.

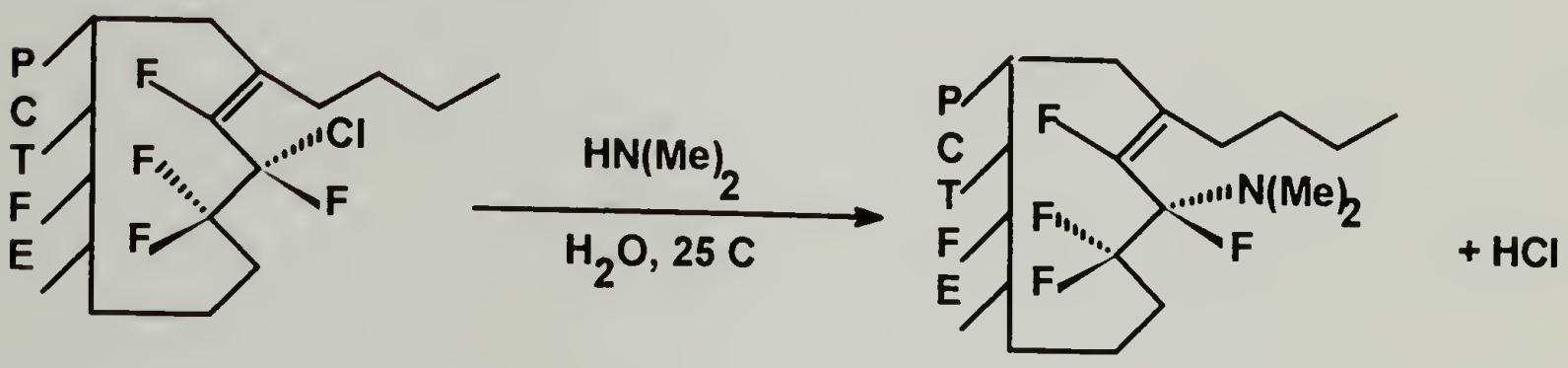

Scheme 2.2. Model reaction of PCTFE-Butyl (butyl modification was in heptane, for 0.5 hr. at 0°C) with dimethylamine.

It is known from the organic chemistry of small molecules that allylic chlorides are reactive towards nucleophiles.[29] It is conceivable that partially modified PCTFE-Butyl surfaces, which contain allylic chlorides, could react with amines. Indirect evidence of reaction was observed by the appearance of a nitrogen N_{1s} peak at 402 eV in the XPS spectrum when PCTFE-Butyl (butyl modifications were in heptane for 0.5 hr. at 0°C) was reacted with either dimethylamine, diethylamine, or hexamethylenediamine. Reactions with dimethylamine were studied extensively. Atomic compositions by XPS showed that the N_{1s} peak (Figure 2.8) and the C/F ratio increased with increasing reaction time. Control reactions of dimethylamine with virgin PCTFE and fully modified PCTFE-Butyl

(reacted in 98.2% heptane in THF at 25°C for 0.5 hr.) for 24 hours showed no nitrogen peaks.

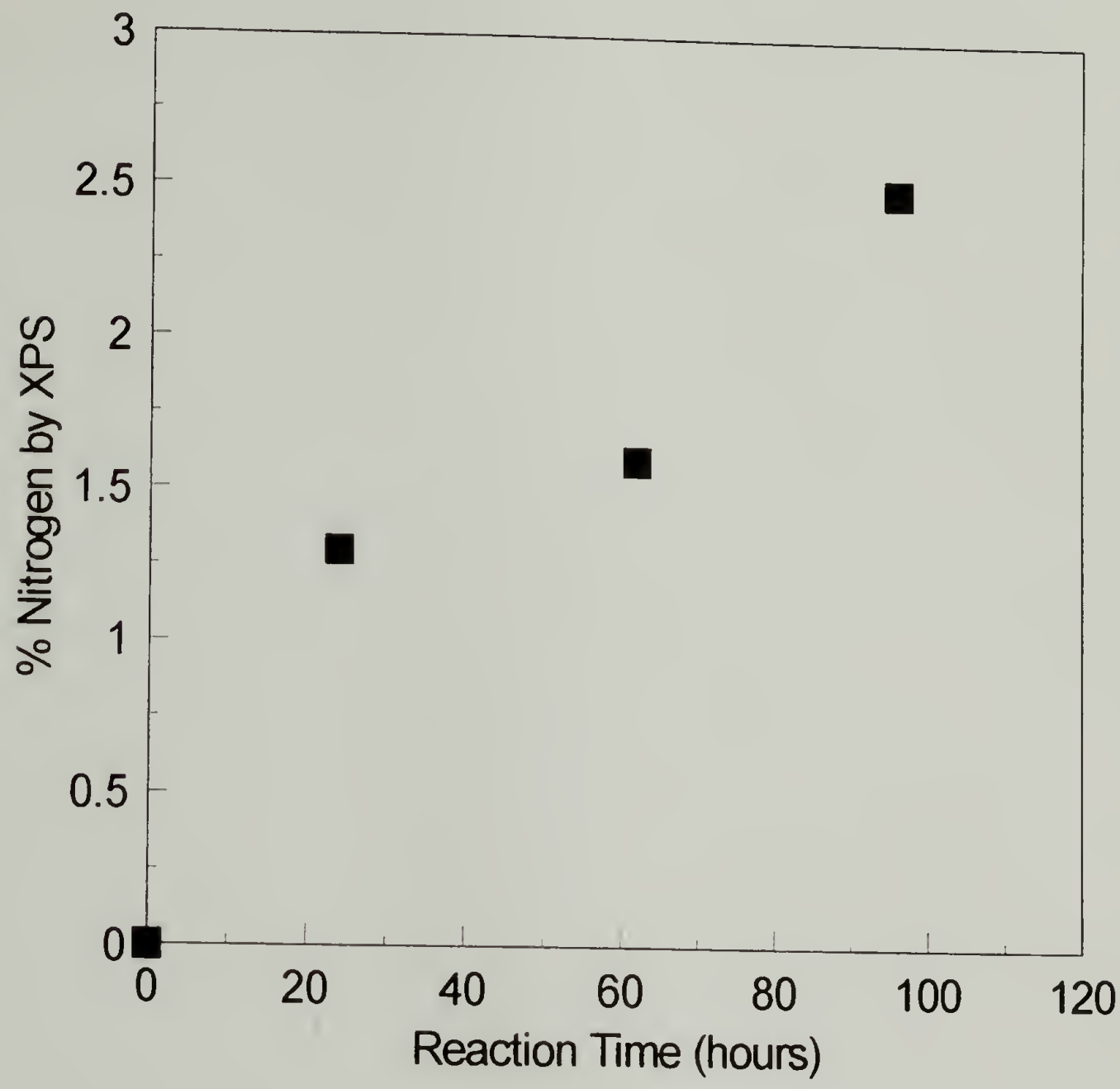

Figure 2.8 Percent nitrogen by XPS using a 15° take-off angle on PCTFE-Butyl reacted with dimethylamine in water at ambient conditions. PCTFE-Butyl was synthesized in heptane at 0°C for 0.5 hours.

PCTFE-PEA and PCTFE-OH Surface Chemistry (Scheme 2.3)

PCTFE was modified with acetaldehyde 3-lithiopropyl ethyl acetal (LiPEA), a lithium reagent containing a protected alcohol, by the same mechanism discussed for the PCTFE-Butyl synthesis. The reaction conditions, mechanism, and depth of modification have been studied in detail by others.[14-16,21,28]

Reactions at -15°C for 0.5 hours gave a complete surface modification by XPS. A carbon C_{1s} peak was observed at 290 eV, and a oxygen O_{1s} peak at 546 eV was also observed. The chlorine Cl_{2p} peak disappeared and the fluorine F_{1s} peak decreased (Figure 2.9). Atomic composition data are reported in Table 2.2. ATR IR showed C-H stretching peaks between 2840 and 3000 cm^{-1}, and a C-O stretching peak at 1050 cm^{-1} (Figure 2.10). UV spectra showed an absorbance at 270 nm, analogous to the PCTFE-Butyl modification, but the absorbance was greater by a factor of 10. The receding water contact angle decreased significantly but the advancing contact angle decreased only slightly (Table 2.2), so the interpretation of whether or not there was an increase in surface affinity is difficult to assess.

The PCTFE-PEA surface was then hydrolyzed to the alcohol. The advancing and receding water contact angles decreased with hydrolysis, giving evidence of an increase in surface affinity (Table 2.2). An O-H stretching peak at 3300 cm^{-1} appeared in the ATR IR spectrum with hydrolysis (Figure 2.10).

The XPS, ATR IR, UV, and contact angle data for the PCTFE-PEA and PCTFE-OH surfaces are in good agreement with the results of Bee.[21] For the above reaction, Bee

calculated a modified layer thickness of approximately 100 nm, which he found to be very sensitive to the reaction temperature. This differs significantly from the PCTFE-Butyl surface modifications in heptane/THF mixtures. Under identical reaction conditions the PCTFE-Butyl modifications do not proceed as deep and are not as temperature-sensitive. This is due to the greater reactivity of the LiPEA and the greater wettability of the PCTFE-PEA in the solvent mixture facilitating the reaction.

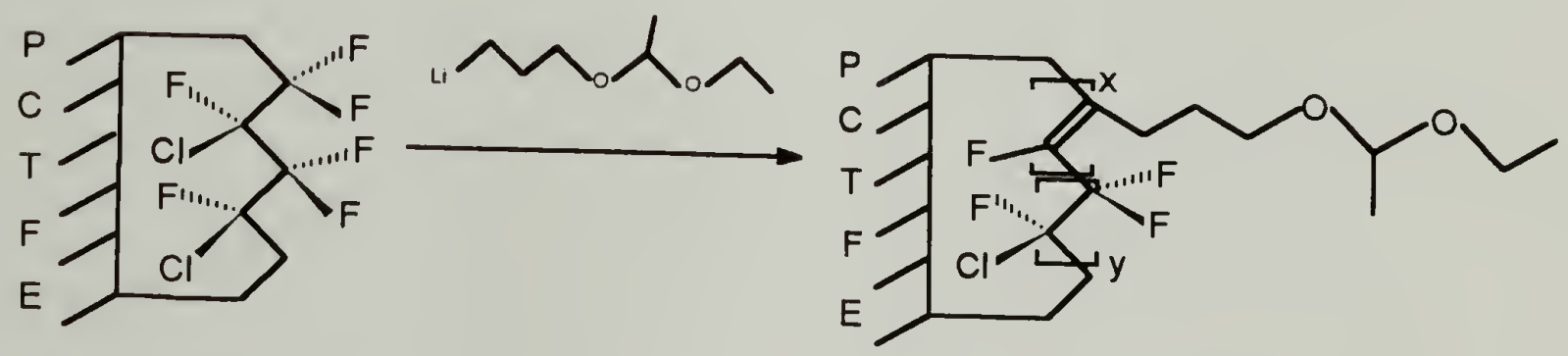

Scheme 2.3. Surface modification reaction of PCTFE with 3-lithiopropyl ethyl acetal and hydrolysis to the alcohol.

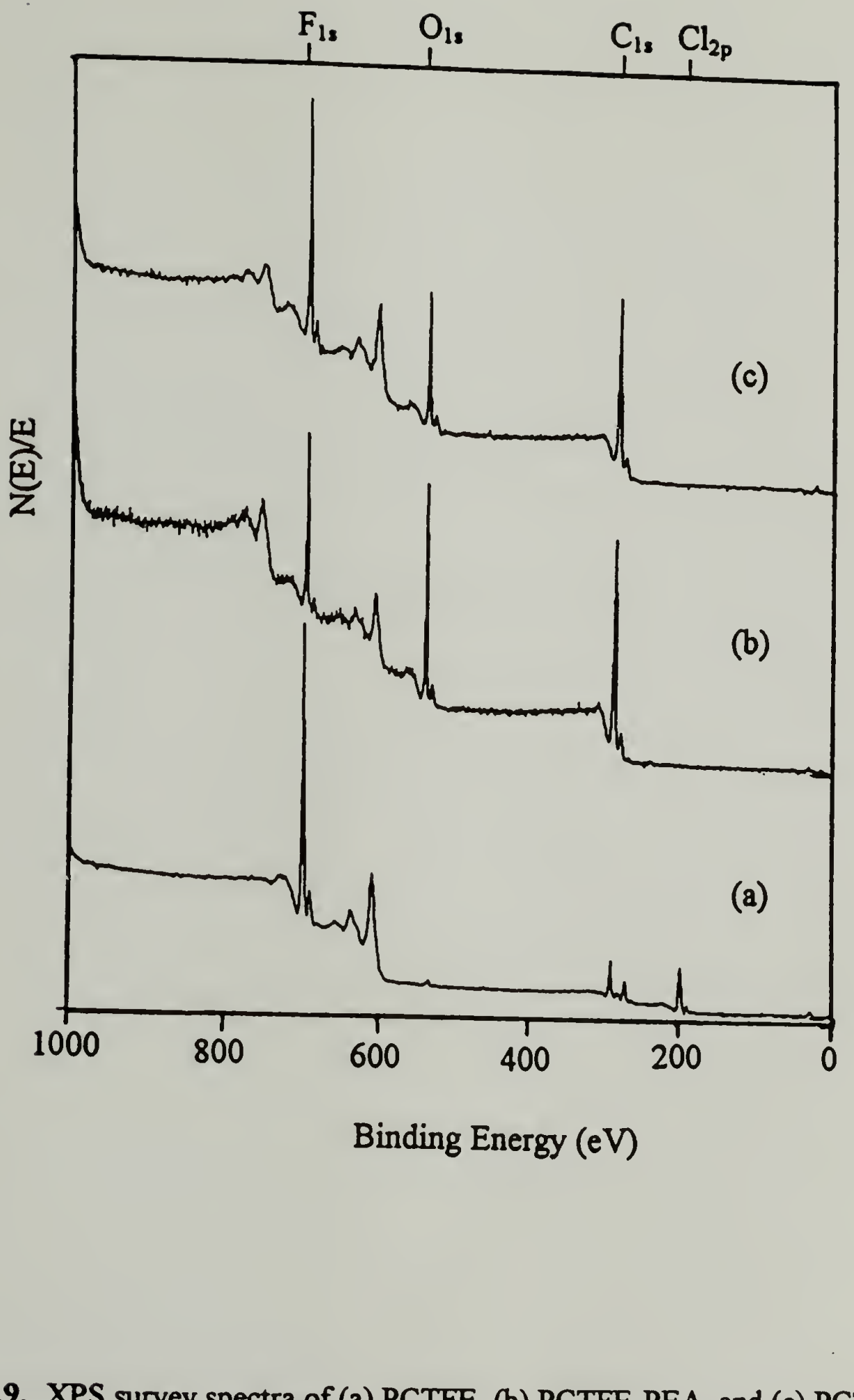

Figure 2.9. XPS survey spectra of (a) PCTFE, (b) PCTFE-PEA, and (c) PCTFE-OH.

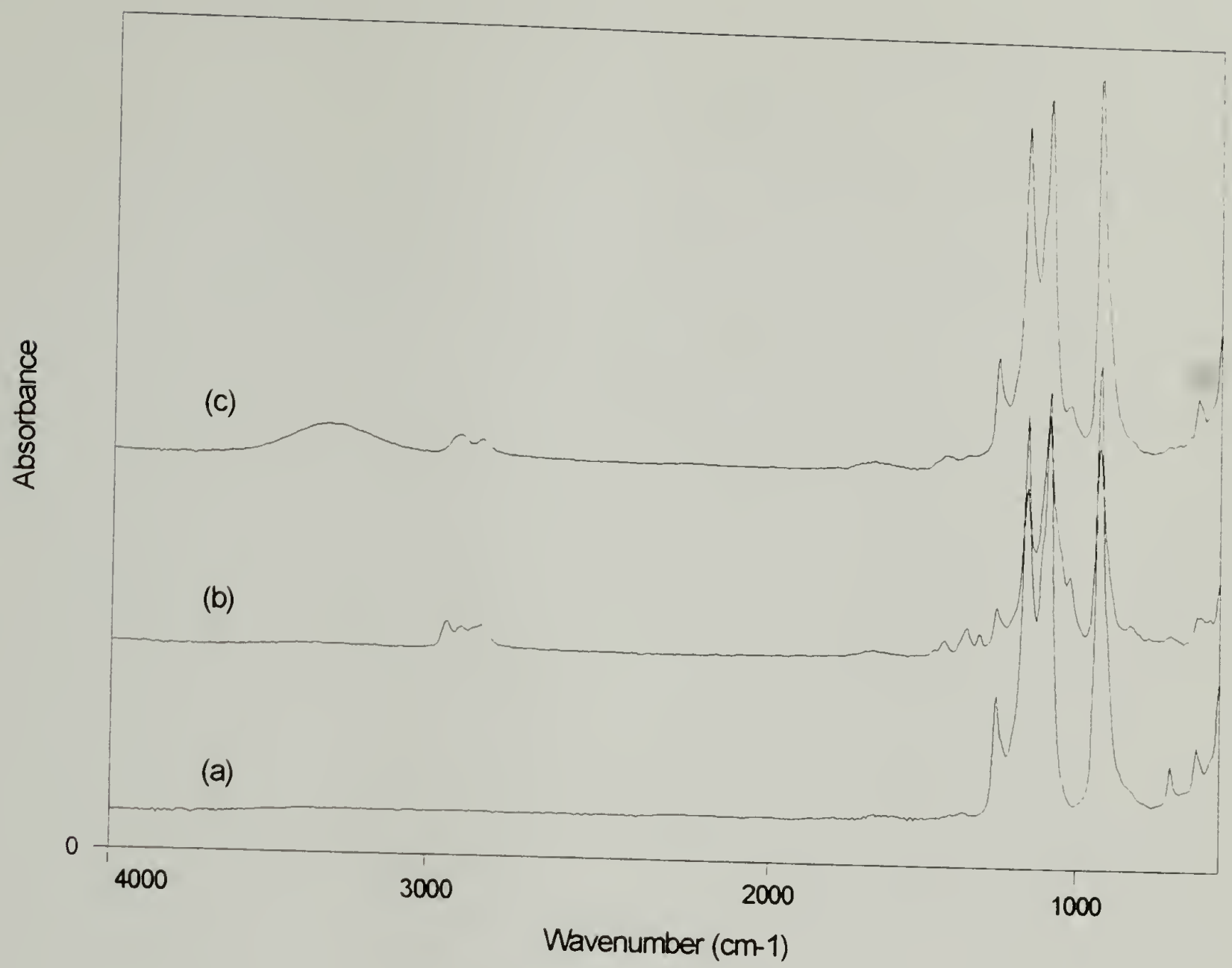

Figure 2.10. ATR IR spectra of (a) PCTFE, (b) PCTFE-PEA, and (c) PCTFE-OH.

PCTFE-Butyrate, -Adipate, -Heptadecanoate, -Stearate Surface Chemistry (Scheme 2.4)

Once the alcohol surface is prepared, a number of ester surfaces can be synthesized. All esterification reactions described were performed using hydrolyzed PCTFE-PEA surfaces that were initially modified at -15°C for 0.5 hours.

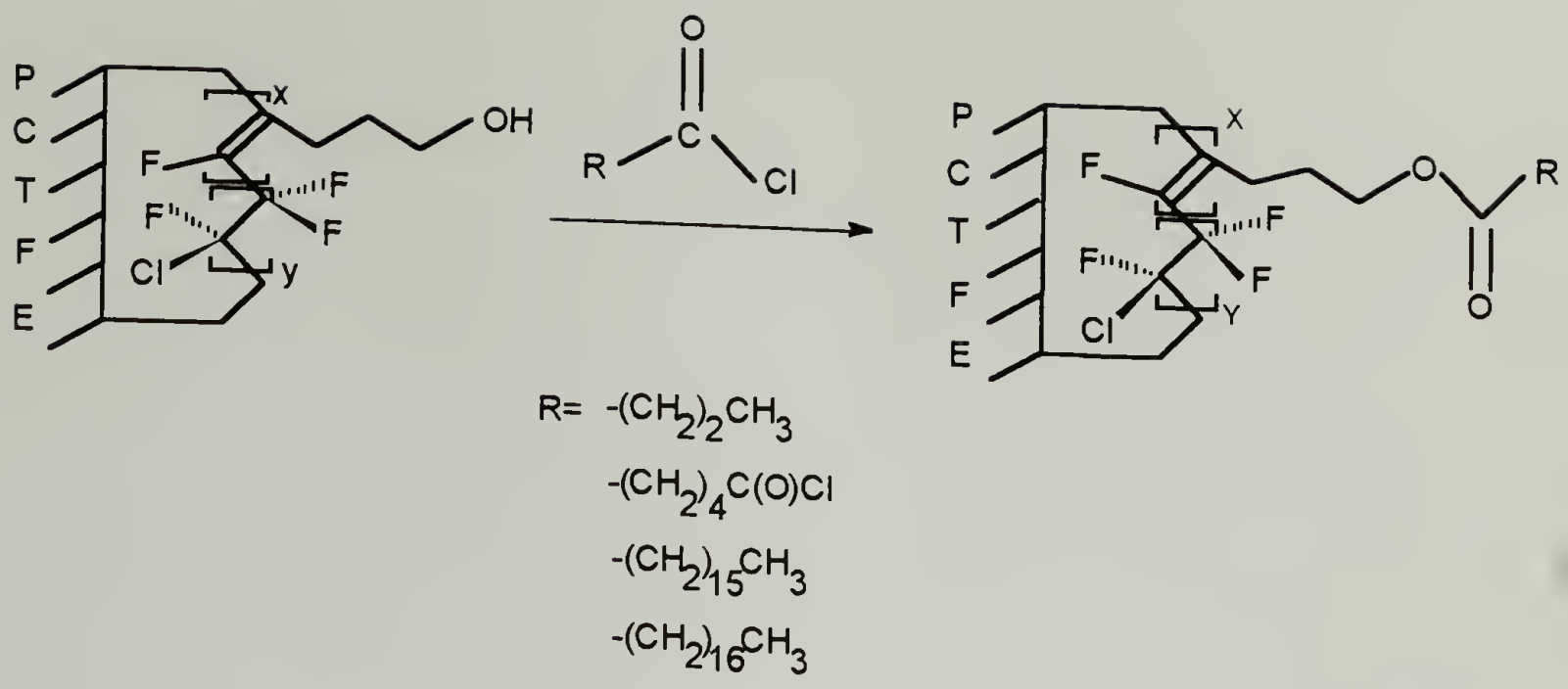

Scheme 2.4. Reaction of PCTFE-OH with butyryl chloride, adipoyl chloride, heptadecanoyl chloride, and stearyl chloride to their corresponding esters.

XPS spectra showed an increase in the C_{1s} peak that increased proportionately with the length of the alkyl chain attached to the ester (Figure 2.11). ATR IR showed a carbonyl peak at 1741 cm^{-1} and C-H stretching peaks at 2840 to 3000 cm^{-1} that also varied in size with the length of the alkyl chain attached to the ester (Figure 2.12). Changes in water contact angle were observed; the ester groups with longer alkyl chains had water contact angles similar to virgin PCTFE (Table 2.2). The PCTFE-Butyrate and PCTFE-Adipate contact angles were slightly higher than PCTFE-OH.

PCTFE-Butyrate was also synthesized using a pyridine catalyst. The catalyzed ester surface was identical to the uncatalyzed surface by XPS, ATR IR, and contact angle, however, by UV-vis a pyridine absorption peak was observed which remained after washing 6 days in THF and water.

Table 2.2 Atomic composition by XPS (15° take-off angle) and water contact angle of surface modified PCTFE.

Surface	Atomic Composition				Water Contact Angle	
	%F	%O	%C	%Cl	advancing	receding
PCTFE	49.4	1.7	31.9	17.0	107	75
PCTFE-PEA	10.9	17.0	72.1	0	100	40
PCTFE-OX	39.7	5.8	39.4	15.2	92	28
PCTFE-OH	16.4	16.0	67.6	0.1	69	28
PCTFE-Butyrate	8.3	16.3	75.3	0.2	90	44
PCTFE-Adipate	9.9	17.2	72.3	0.6	73	41
PCTFE-Heptadecanoate	1.6	9.8	87.9	0.7	118	77
PCTFE-Stearate	1.4	4.1	94.6	0.0	106	81

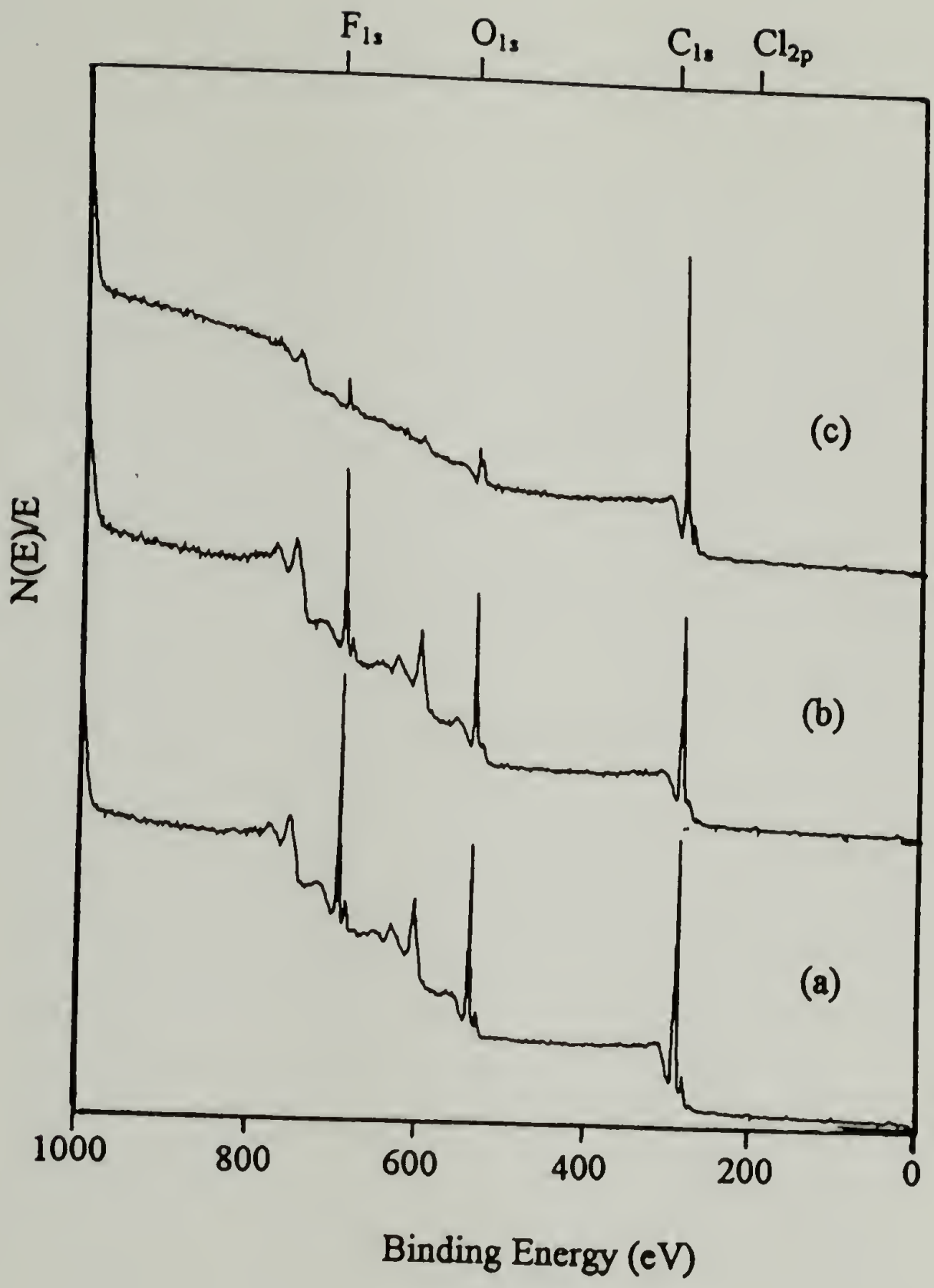

Figure 2.11 XPS survey spectra of (a) PCTFE-Butyrate, (b) PCTFE-Adipate, and (c) PCTFE-Heptadecanoate.

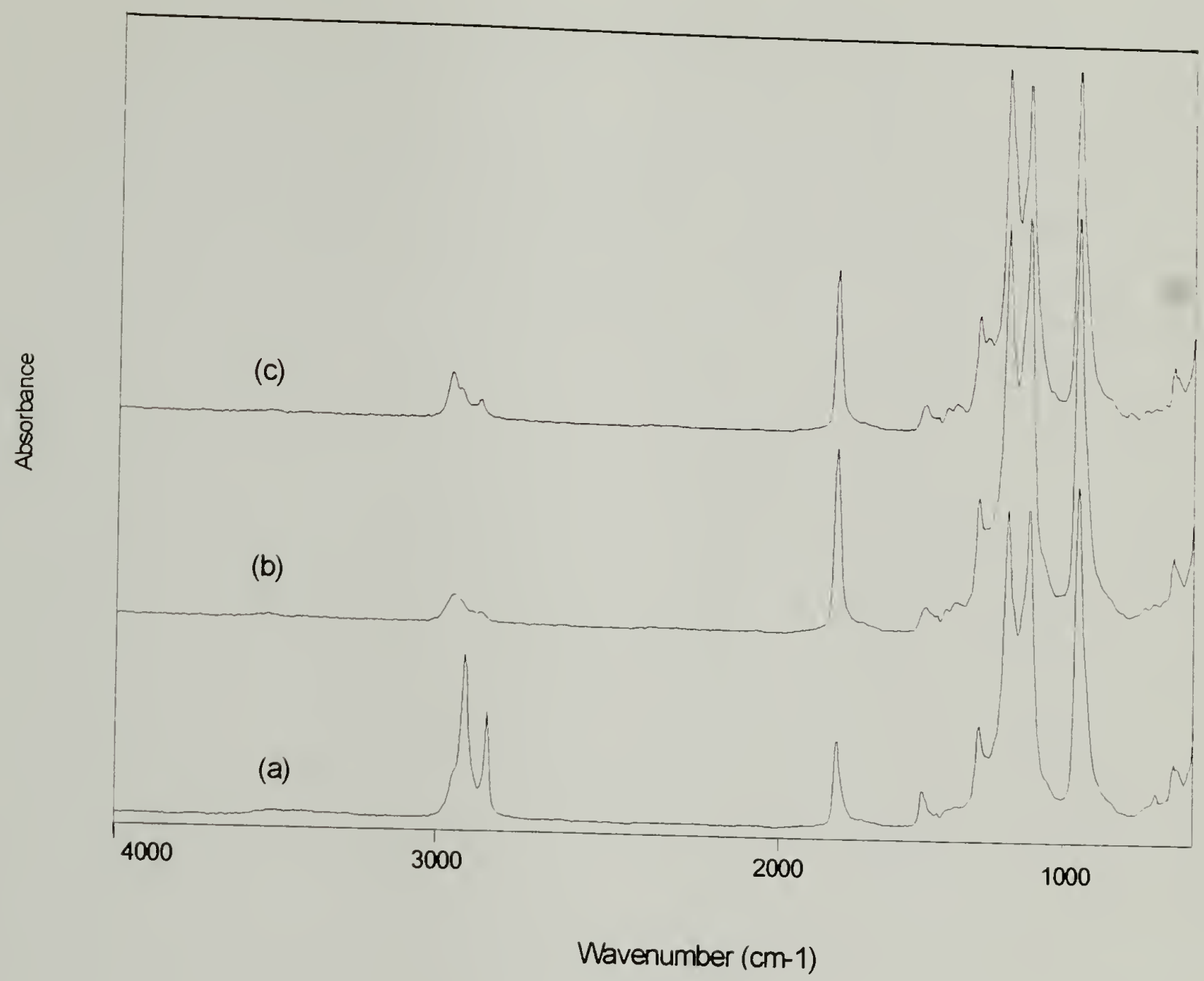

Figure 2.12 ATR IR spectra of (a) PCTFE-Heptadecanoate, (b) PCTFE-Adipate, and (c) PCTFE-Butyrate.

Conclusions

PCTFE was surface-selectively modified with *n*-butyllithium. The depth of modification was controlled by reaction time, temperature, and solvent composition. Under conditions that gave a very shallow modification, a copolymer structure exists as evidenced by the reactivity toward amines. The PCTFE-Butyl surface was oxidized so that the modified layer was completely removed except for a remaining few percent oxygen in the form of carboxylic acid groups. These few percent carboxylic acid groups give a high surface affinity as measured by water contact angle.

PCTFE was also surface selectively modified with acetaldehyde 3-lithiopropyl ethyl acetal. The protected alcohol showed little change in surface affinity but when it was hydrolyzed to the alcohol, an increase in surface affinity was evident by the decrease in water contact angle. The PCTFE-OH was reacted with various acid chlorides giving their corresponding esters. The wettability of these surfaces varied with the surface chemistry, the alcohol surface being the more wettable.

References

1. Ward, W.J.; McCarthy, T.J. *Encyclopedia of Polymer Science and Engineering, 2nd ed.; Supplement*, Wiley: New York, **1989**, 674.

2. Kinloch, A.J. *Adhesion and Adhesives*, Chapman and Hall: New York, **1987**.

3. Siperko, L.M.; Thomas, R.R. *J. Adhesion Sci. Technol.*, **1989**, 3, 157.

4. Brewis, D.M. *J. Adhesion*, **1992**, 37, 97.

5. Dwight, D.W.; Riggs, W.M., *J. Colloid Interf. Sci.*, **1974**, 47, 650.

6. Ha, K.; McClain, S.; Suib, S.L.; Garton, A., *J. Adhesion*, **1991**, 33, 169.

7. Marchesi, J.T.; Ha, K.; Garton, A., *J. Adhesion*, **1991**, 36, 55.

8. Marchesi, J.T.; Keith, H.D.; Garton, A., *J. Adhesion*, **1992**, 39, 185.

9. Kelber, J.A., "Plasma Treatment for Improved Adhesion", presented at Materials Research Society Meeting, Reno, Nevada, April **1988**.

10. Allied-Signal Inc., Aclar Product Bulletin.

11. Huth, J.A.; Danielson, N.D., *Anal. Chem.*, **1982**, 54, 930.

12. Danielson, N.D.; Taylor, R.T.; Huth, J.A.; Siergiej, R.W.; Galloway, J.G.; Paperman, J.B. *Ind. Eng. Chem. Prod. Res. Dev.*, **1983**, 22, 303.

13. Dias, A.J.; McCarthy, T.J., *Macromolecules*, **1985**, 18, 1826.

14. Dias, A.J.; McCarthy, T.J., *Macromolecules*, **1987**, 20, 2068.

15. Lee, K-W.; McCarthy, T.J., *Macromolecules*, **1987**, 20, 1437.

16. Lee, K-W.; McCarthy, T.J., *Macromolecules*, **1988**, 21, 2318.

17. Kolb, B.U.; Patton, P.A.; McCarthy, T.J., *Macromolecules*, **1990**, 23, 366.

18. Cross, E.M.; McCarthy *Macromolecules*, **1990**, 23, 3916.

19. Shoichet, M.S.; McCarthy, T.J. *Macromolecules*, **1991**, 24, 982.

20. Bee, T.G.; McCarthy, T.J., *Macromolecules*, **1992**, 25, 2093.

21. Bee, T.G. Ph.D. Dissertation, University of Massachusetts, **1993**.

22. Kendall, E.W. Ph.D. Dissertation, University of Massachusetts, **1994**

23. Shoichet, M.S. Ph.D. Dissertation, University of Massachusetts, **1992**.

24. Andrade, J.D., *Surface and Interfacial Aspects of Biomedical Polymers*, Volume 1, Plenum Press: New York, **1985**.

25. Fowkes, F.M. Contact Angle, *Wettability, and Adhesion*, Advances in Chemistry Series 43, American Chemical Society: Washington, D.C., **1964**.

26. Clark, D.T.; Thomas, H.R., *J. Polym. Sci., Polym. Chem. Ed.*, **1977**, 15, 2843.

27. Atomic force microscopy experiments on surface modified PCTFE are currently being conducted by Vipavee Phuvanartnuruks.

28. Dias, A.J. Ph.D Dissertation, University of Massachusetts, **1986.**

29. March, J., *Advanced Organic Chemistry*, 3rd edition, John Wiley and Sons: New York, **1985**, p. 287.

CHAPTER III

ADHESION STUDIES OF SURFACE-MODIFIED POLY(CHLOROTRIFLUOROETHYLENE) FILMS

Introduction

PCTFE films have been surface-selectively modified with non-corrosive, well characterized chemistries in order to investigate their influence on adhesion. The surface functional groups were chosen so that the effect of molecular interactions on adhesion could be investigated. The surface affinity was increased by the introduction of alcohol and carboxylic acid groups to the surface region. Then the surface affinity of the PCTFE-OH surface was incrementally decreased by further functionalization with short and long-chain ester groups. Partially modified PCTFE-Butyl surfaces were synthesized and shown to contain reactive sites for covalent bonding, without changing the surface affinity. A study of structure-property relationships in adhesion can now be conducted.

Adhesion, by definition, is the joining together of adhesive and substrate resulting in an adhesive joint that has the capacity to withstand stress.[1] The effect of surface functionality on adhesion cannot be quantified without an adhesion test. Many mechanical tests have been developed to evaluate the stress resisting capacity of adhesive joints. The American Society for Testing Materials (ASTM) outlines methodology for a number of adhesion tests.[1] In practical experimentation the adhesive failure energy is extremely

sensitive to the mechanical properties of the bonded materials and the nature of the stresses at the interface produced by the applied loads. Because of its experimental simplicity, a widely used method for measuring adhesion to films is the peel test. The state of stress during peeling, however, is very complex and depends on the peel angle, the radius of curvature at the crack tip, and the mechanical properties of the film and substrate.[2-6] For many adhesive/adherend combinations including thin films which strongly adhere to rigid substrates, dissipative mechanisms dominate the peel behavior. The peel force is usually sufficient to cause inelastic deformation of the film near the point of detachment where the film is subjected to severe curvature.[4] It has been reported that up to 95-99% of the energy in peeling polyimide and aluminum from each other is given off as heat (as measured by a deformation calorimeter) or stored as latent free energy,[7,8] neither of which are surface/adhesion related. Under these conditions the peel energy will significantly exceed the true adhesion.

The adhesion test method chosen to evaluate the level of adhesion is often predetermined by the use of the adhesive joint in its "real world" application. The peel test may be a useful measure of adhesion in many applications, but in structural applications where the stresses are not in a peeling fashion the peel test may not be suitable. The double-cantilever-beam (DCB) test and the tapered double-cantilever-beam (TDCB) test have proven to be useful methods for measuring the adhesion of epoxy to aluminum.[9-13] We have chosen to investigate the application of the DCB test and the TDCB test to measure adhesion between epoxy and surface modified PCTFE films. The

rigid support of the beams force the deformation to be localized at the crack tip minimizing the amount of viscoelastic/plastic deformation.

The adhesion measured from the peel test, TDCB test, and DCB test are the energies required to extend a crack by unit length in a specimen of unit width and reported as the fracture energy, G_c.[1,14] The dissipative mechanisms between these tests vary, as well as the modes of stress. The peel test used was in a 180° geometry and the stress mode is a mix of mode I and II, but predominantly mode II (shear).[15] The TDCB test and DCB test have also been reported to have a mixed mode of stress but is mostly mode I (tensile).[16]

The objectives of this chapter are two-fold: (a) to measure the effect of surface functionality on adhesion, and (b) to evaluate the TDCB and DCB tests as useful methods to measure adhesion to films. The peel test was used to measure the adhesion of surface modified PCTFE to epoxy and a PSA. Realizing that the magnitude of the measured adhesion by peeling may be greatly inflated, the peel test was assumed to be useful only as a relative measure of adhesion. This assumption was believed to be acceptable because, regardless of the bulk dissipation and mode of failure, the bulk properties of the film were not being altered by the surface-selective modifications.

Experimental

General

The PCTFE (Aclar® 33c) and surface modified PCTFE are those described in Chapter II. The epoxy used for the adhesion tests was Epon 828, a diglycidyl ether of Bisphenol A type epoxy with V-40 curing agent, both products from Shell Chemical Co.

The pressure sensitive adhesive (PSA) used was a 3M Scotch Brand #750. All adhesion tests were run at ambient conditions on an Instron Tensile Tester.

Aclar® 33c is a semi-crystalline polymer (~30%) with a T_g of 58-65°C [17] and a T_m of 202-204°C.[18] It has a tensile strength of 65.5 to 79.3 MPa and a Young's modulus of 1.3 Gpa, both in the maching direction. Aclar® 33c also has the following percent weight gains in the following solvents: 0.02% 1,2-dichloroethane; 5.2% ethyl ether; 3.7% furan; 0% heptane. The Aclar product bulletin also reports that ethyl ether and furan make the films very flexible.[18]

Adhesion of Solvent-Swollen PCTFE to Epoxy Measured by the 180° Peel Test

A 1.5 cm by 6.0 cm PCTFE film was placed into 200 ml of refluxing dichloromethane for 2 hours, then vacuum dried (0.05 mm) for 3 days at 40°C. A 1.5 cm by 6.0 cm PCTFE film was placed into 200 ml of THF for 2 hours at room temperature and then washed with methanol (1 x 100 ml), water (1 x 100 ml), methanol (1 x 100 ml), dichloromethane (1 x 100 ml), and then vacuum dried (0.05 mm) for 3 days at 40°C. A 1.5 cm by 6.0 cm PCTFE film was placed into 200 ml of boiling THF for 2 hours then washed and dried as above. The PCTFE films were placed on a flat surface and a glass mold with a 1.0 cm x 5.0 cm x 0.1 cm hole was placed over the film and taped securely in place. The Epon 828 and V-40 was mixed together 2:1 by weight and poured into the mold. The epoxy was allowed to cure for 7 days at room temperature. The glass mold was then cut away to give a 1.0 cm x 5.0 cm x 0.11 cm epoxy-PCTFE laminate. The epoxy laminate was loaded into an Instron tensile tester and peeled in a 180° geometry at

2.5 cm/minute. The force for peeling was averaged over 1.0 cm length of peeling and divided by the width to give an average peel energy in J/m^2. (Notebook #3 p.95)

Adhesion of Surface-Modified PCTFE to Epoxy Measured by the 180° Peel Test

PCTFE-Butyl (prepared using the conditions given in Table 2.1), PCTFE-OX, PCTFE-PEA, PCTFE-OH, PCTFE-Butyrate, PCTFE-Adipate, PCTFE-Hept., and PCTFE-Stearate films were placed on a flat surface and a glass mold with a 1.0 cm x 5.0 cm x 0.1 cm hole was placed over the film and taped securely in place. The Epon 828 and V-40 was mixed together 2:1 by weight and poured into the mold. The epoxy was allowed to cure for 7 days at room temperature. The glass mold was then cut away to give a 1.0 cm x 5.0 cm x 0.11 cm epoxy-PCTFE laminate. The epoxy laminate was loaded into an Instron tensile tester and peeled in a 180° geometry at 2.5 cm/minute. The force for peeling was averaged over 1.0 cm length of peeling and divided by the width to give an average peel energy in J/m^2.

Using the same procedure as above the adhesion of epoxy to PCTFE-Butyrate pyridine catalyzed was measured. Also the effect of drying conditions were investigated by drying PCTFE-Butyrate for 3 days at 45°C and for 6 days at 95°C. (Notebook #3 p.79)

Adhesion of Surface-Modified PCTFE to a PSA Measured by the 180° Peel Test

Adhesion of PCTFE, PCTFE-Butyl (fully modified, and partially modified), PCTFE-OX, PCTFE-PEA, PCTFE-OH, PCTFE-Butyrate, PCTFE-Adipate, PCTFE-Hept., and PCTFE-Stearate films to a pressure sensitive adhesive was measured. A PSA-PCTFE laminate was prepared by sticking the PSA to the PCTFE and rolling 50 times

with a roller. The PSA laminate was loaded into an Instron tensile tester and peeled in a 180° geometry at 2.5 cm/minute. The force for peeling was averaged over a 1.0 cm length and divided by the width to give an average peel energy in J/m^2. (Notebook #3 p.143)

Adhesion of Surface-Modified PCTFE to Epoxy Measured by the DCB Test

This test was modeled after ASTM D3433 (Figure 3.1). Two aluminum beams (alclad 2024, T3 temper, mill finish) each 2.54 cm wide, 1.27 cm thick, and 35.6 cm long were washed with soap and warm water and air dried with a heat gun. The beams were then blade coated with the epoxy described above. A 2.5 cm x 2.5 cm x 0.0127 cm PCTFE spacer was placed on each end of the beams and each side of the PCTFE film, the spacer acted to maintain constant epoxy thickness and acted as a pre-crack. The PCTFE-Butyl film was then placed over the entire length of the beam and the beams were put together and allowed to cure for 7 days at ambient conditions. After curing, the beams were placed into an Instron Tensile Tester and loaded at 0.2 cm/minute while measuring the displacement, force, and crack length. The displacement was measured using a LVDT fastened to the front of the beams, the force was measured using a 500 lb load cell, and the crack length was measured visually with a ruler. The surfaces investigated were PCTFE modified with *n*-butyllithium in heptane for 30 minutes at -15°C, 0°C, and 25°C.

The equation used to calculate the adhesive fracture energy, G_c, from the DCB test was:[9,10]

$$G_c = (P_c^2/2b)(dC/da)$$

where P_c is the critical load for crack growth. The width is b, and dC/da is the change in compliance with the change in crack length. The compliance was calculated from the inverse slope of the loading lines. The equation used is the general equation for the DCB test and only assumes that force-deflection diagrams are linear; the derivation and application of this equation to the DCB test has been discussed by others.[9,10] (Notebook #5 p.64)

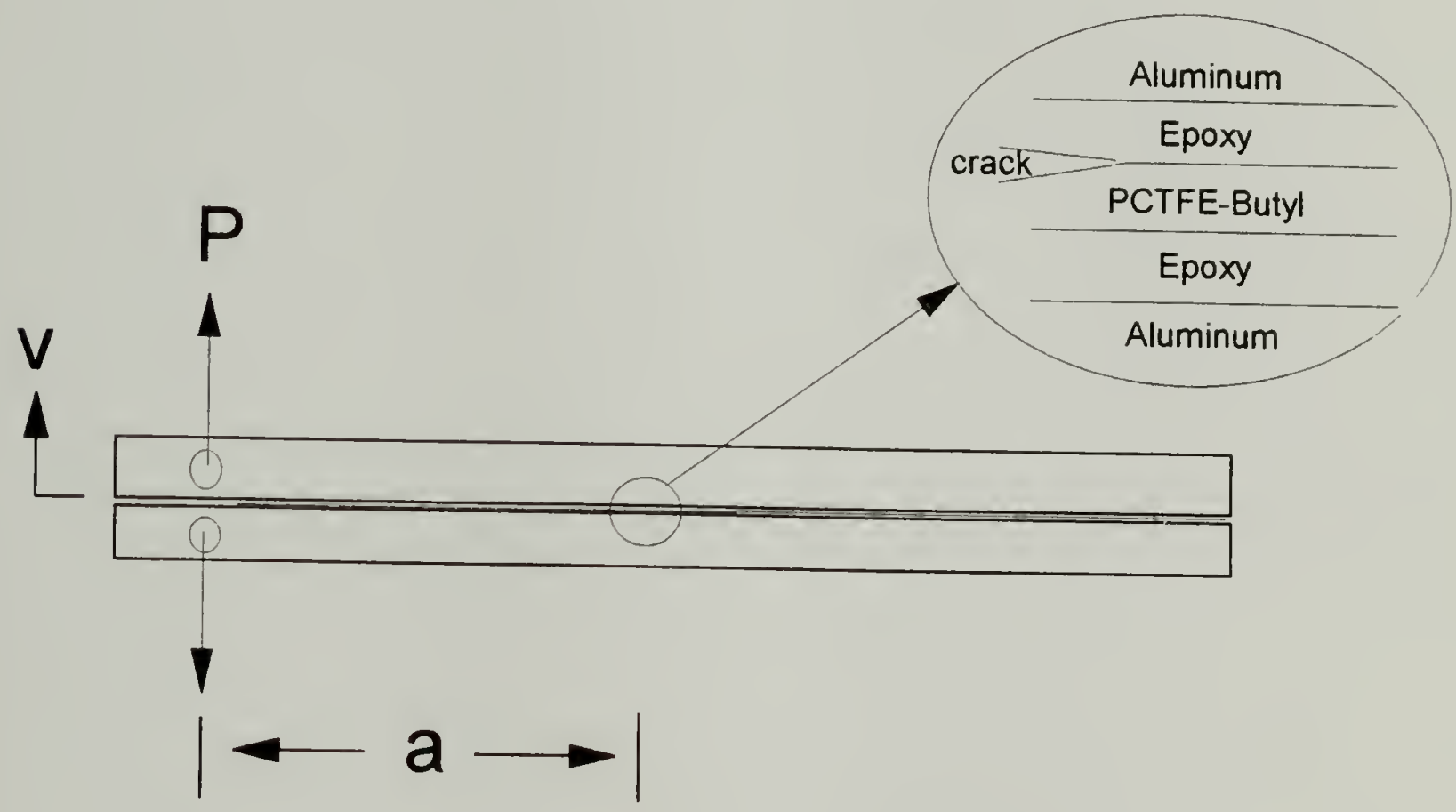

Figure 3.1 Diagram of the double-cantilever-beam test used to measure the adhesion between PCTFE-Butyl and epoxy.

Adhesion of Surface-Modified PCTFE to Epoxy Measured by the Tapered DCB Test

The same procedure was used as above, however, the aluminum beams used were tapered as described in ASTM D3433 (Figure 3.2). The beams were 24.13 cm long, 2.54 cm wide, and the taper was from 1.27 cm to 3.175 cm over a distance of 14.498 cm. The equation used to calculate the adhesive fracture energy, G_c was: [9,10]

$$G_c = (4P_c^2 m)/(Eb^2)$$

where P_c is the critical load for crack growth, m is the taper of the beams (m is a constant and can be calculated from $m=3a^2/h^3 + 1/h=1.165\ m^{-1}$, h is the beam thickness at crack length a), E is the modulus of the aluminum (72.4 GPa), and b is the width of the beams. (Notebook #5 p.63)

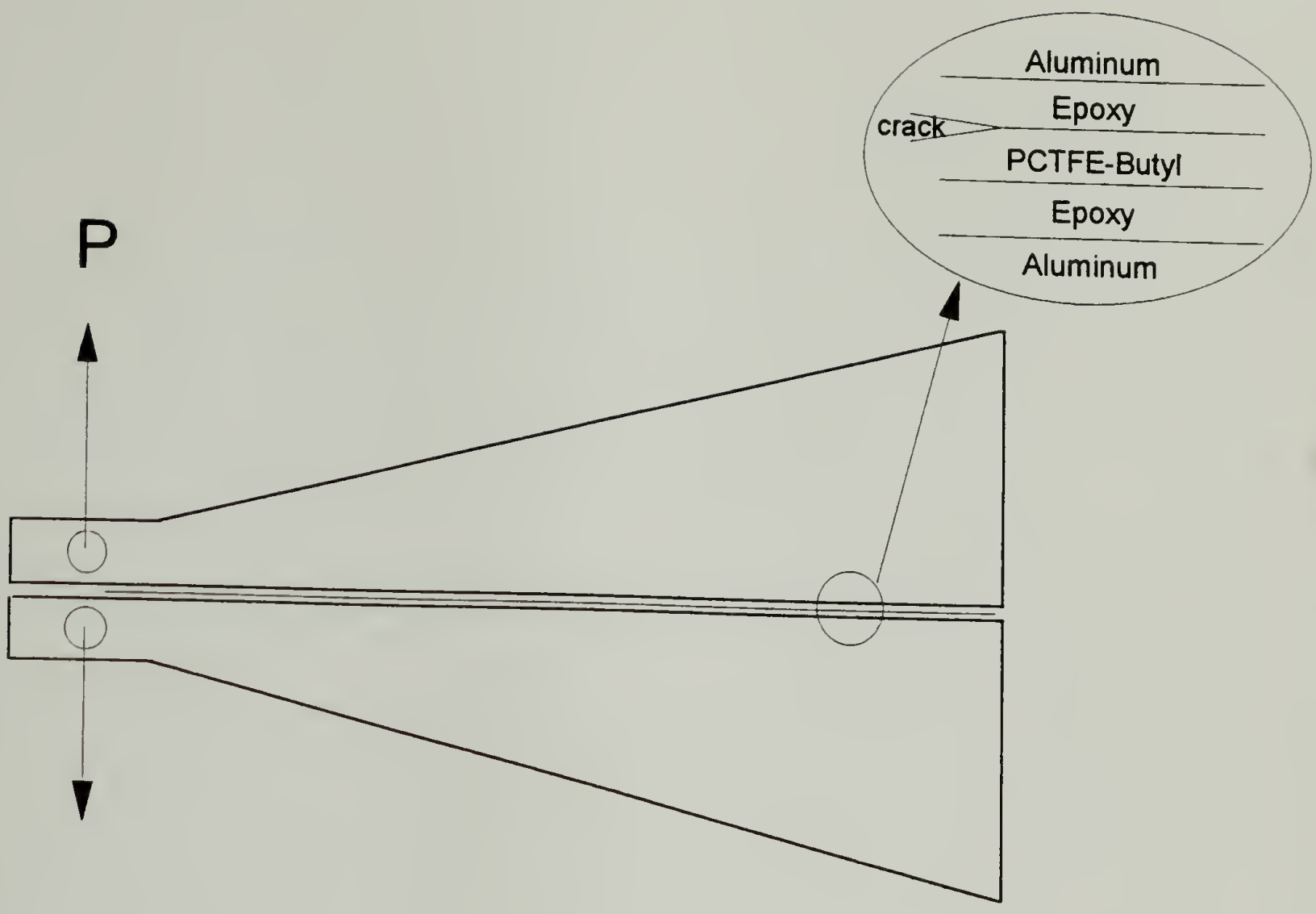

Figure 3.2 Diagram of the Tapered Double-Cantilever-Beam Test used to measure the adhesion between PCTFE-Butyl and epoxy.

Results and Discussion

Adhesion to PCTFE

The PCTFE surface modification reactions described in Chapter II were run in organic solvents; different solvents wet or swell the surface region different amounts. Before the effect of surface-chemical modifications could be evaluated, the surface-swelling effect of the solvents on adhesion were investigated. Adhesion experiments were

conducted on unmodified PCTFE treated with dichloromethane, heptane (both non-swelling solvents), and THF (a swelling solvent).

The treatment of PCTFE with dichloromethane or heptane had no effect on adhesion to epoxy. PCTFE treated in refluxing dichloromethane and vacuum dried 24 hours at room temperature had a peel energy of <4 J/m^2 to epoxy. The loci of failure after peeling from the epoxy was determined by XPS. XPS on the epoxy side after peeling showed both fluorine (from the PCTFE) and nitrogen (from the epoxy), indicating that the failure was both adhesive between the PCTFE and epoxy, and cohesive in the PCTFE (Figure 3.3, and Appendices A and B). XPS on the PCTFE side after peeling showed only PCTFE, no epoxy was transferred to the PCTFE side.

Swelling in THF had a pronounced effect on adhesion to epoxy. PCTFE swollen in THF for 2 hours at room temperature and vacuum dried 3 days at 40°C had a peel energy to epoxy of 57 J/m^2. The failure was also mixed adhesive/cohesive in the PCTFE, identical to PCTFE treated with dichloromethane. PCTFE swollen in refluxing THF greatly enhanced the swelling and the adhesion; the peel energy to epoxy was $>1{,}000$ J/m^2. The film did not peel, it stretched and broke, the failure being cohesive in the bulk of the PCTFE film. These experiments showed that solvents swell the surface region and plasticize the polymer chains on the surface. This solvent-induced plasticization of the surface facilitated interdiffusion of the epoxy and PCTFE, thereby increasing the adhesion. In the remainder of this thesis care was taken to completely remove solvents by drying before adhesion tests were conducted. Interdiffusion of PCTFE and epoxy has also been

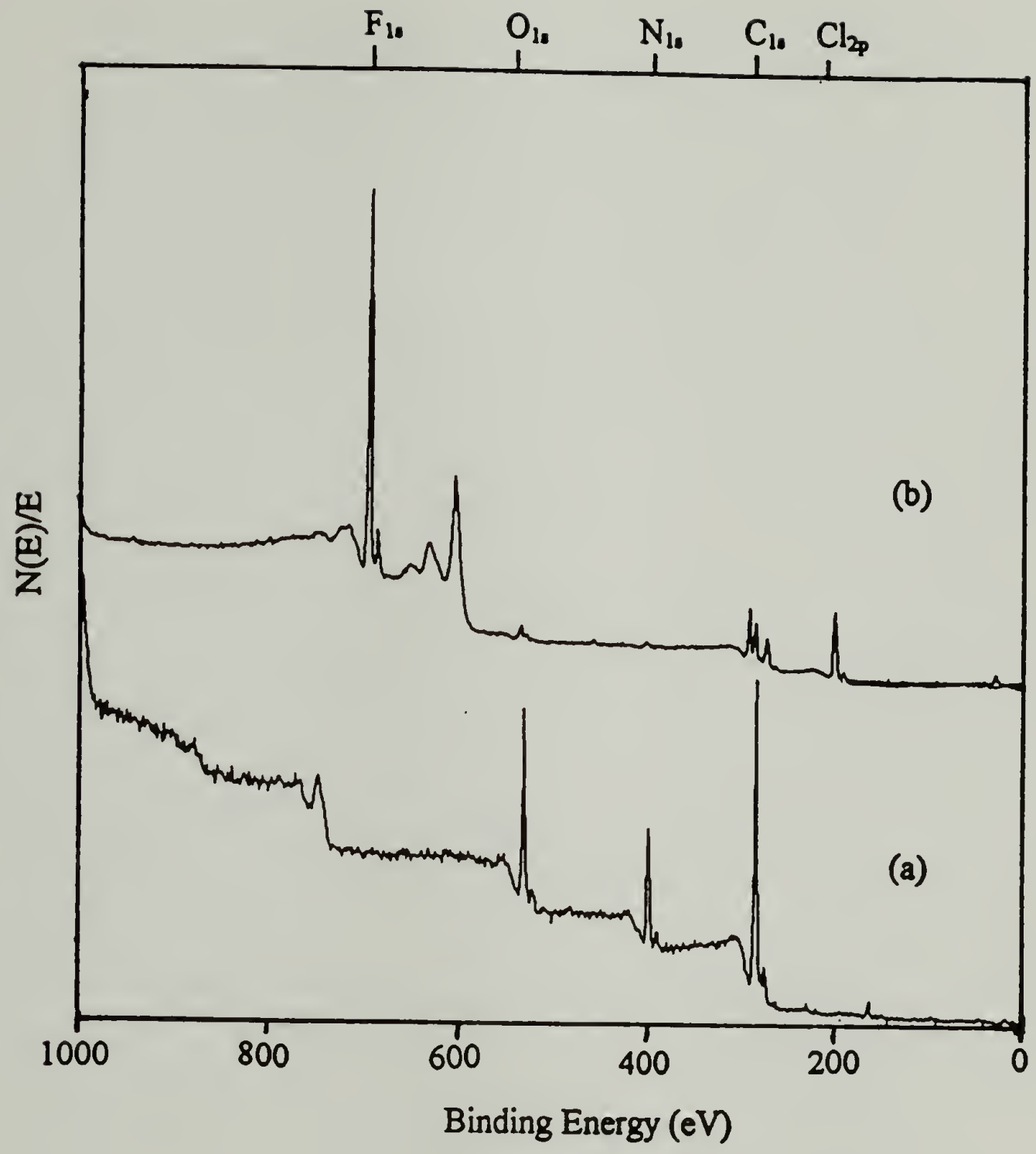

Figure 3.3. XPS survey spectra using a 15° take-off angle of (a) epoxy and (b) epoxy after peeling PCTFE swollen with dichloromethane.

shown to be facilitated by curing at elevated temperatures.[19] To minimize this variable, curing was conducted at room temperature.

The peel energy of PCTFE (refluxed in dichloromethane) to the pressure sensitive adhesive was 173 J/m^2. The loci of failure was adhesive by XPS, no transfer of PCTFE or PSA was observed (Appendix C).

Adhesion to PCTFE-Butyl

The adhesive properties of PCTFE-Butyl to epoxy and a PSA were investigated. The adhesive energy to epoxy was measured by the DCB test, TDCB test, and the 180° peel test. Adhesion to a PSA was measured by the 180° peel test. The extent of PCTFE-Butyl surface modification could be controlled precisely by reaction time, reaction temperature, and the reaction solvent composition (Chapter II). The extent of surface modification affected the adhesion to epoxy but not to the PSA. Care was taken to thoroughly dry films after surface modification reactions. Residual THF from reactions run in THF/heptane mixtures was found to artificially increase adhesion to epoxy.

The extent of PCTFE-Butyl surface modification had a dramatic effect on adhesion to epoxy as measured by the peel test and the DCB tests. Peel energies to epoxy were <4 J/m^2 at high modifications; at partial modifications peel energies were ~1,000 J/m^2 (Figure 3.4). A typical force-displacement diagram for the 180° peel test is given in Figure 3.5. The same trend in adhesion of PCTFE-Butyl to epoxy was found using the DCB test and Tapered DCB test (Table 3.1). The standard deviation of the DCB test was extremely high, a result of the difficulty in measuring the crack length accurately, which is not necessary for the TDCB test. Force-deflection diagrams for the DCB test are shown

in Figures 3.6 and 3.7 for PCTFE-Butyl modified in heptane for 30 minutes at 25°C and 0°C, respectively. The TDCB test proved to be an experimentally simpler test than the DCB test (the compliance and crack length did not need to be measured) with lower standard deviations. Figure 3.8 shows the force-displacement diagrams of the TDCB test for PCTFE-Butyl also modified in heptane for 30 minutes at 25°C and 0°C.

Table 3.1 Effect of measurement system on measured adhesion to PCTFE-Butyl.

Surface	C/F Ratio	DCB Test (J/m^2)		TDCB Test (J/m^2)		180°Peel Test (J/m^2)	
		Avg.	Std	Avg	Std	Avg	Std
-Butyl (-15°C)	1.6	34.4	31.5	20.7	2.5	1244	182
-Butyl (0°C)	2.4	184.4	68.4	119.0	12.2	1246	40
-Butyl (25°C)	3.2	65.2	30.0	29.3	7.0	1344	64

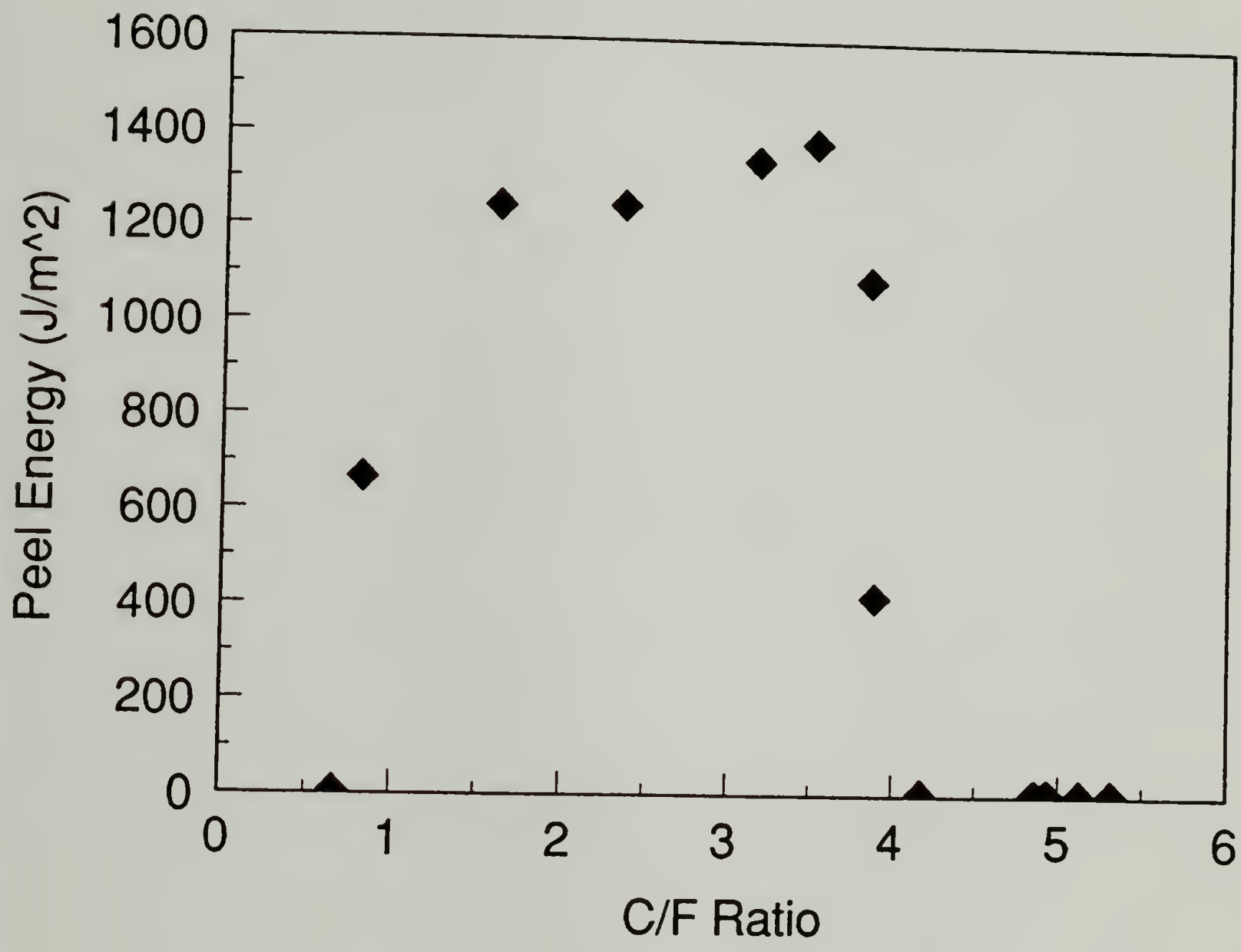

Figure 3.4 Peel energy to epoxy vs. the extent of PCTFE-Butyl surface modification.

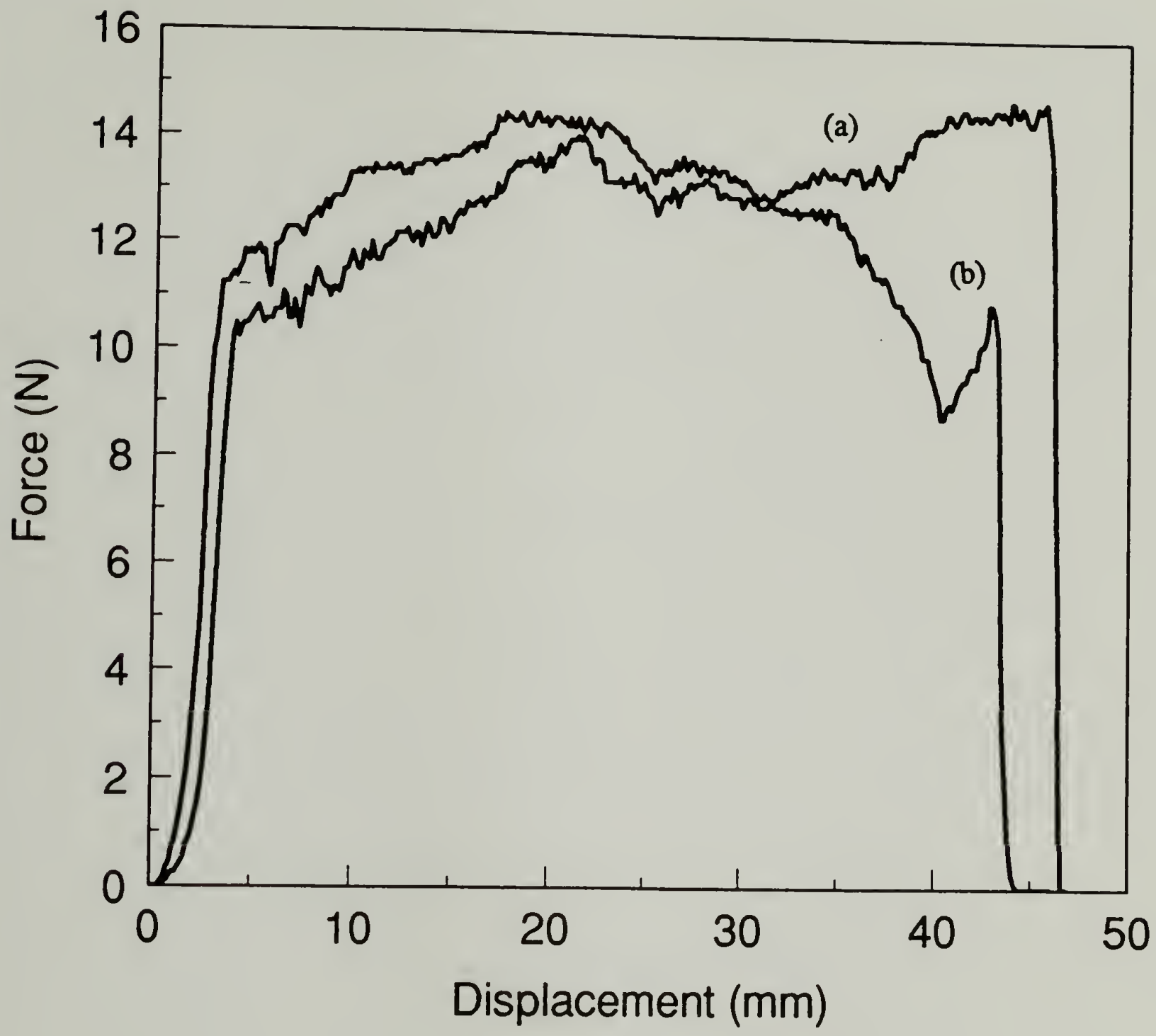

Figure 3.5 180° peel test force-displacement diagram of adhesion between epoxy and PCTFE-Butyl modified in heptane for 30 minutes at (a) 25°C and (b) 0°C.

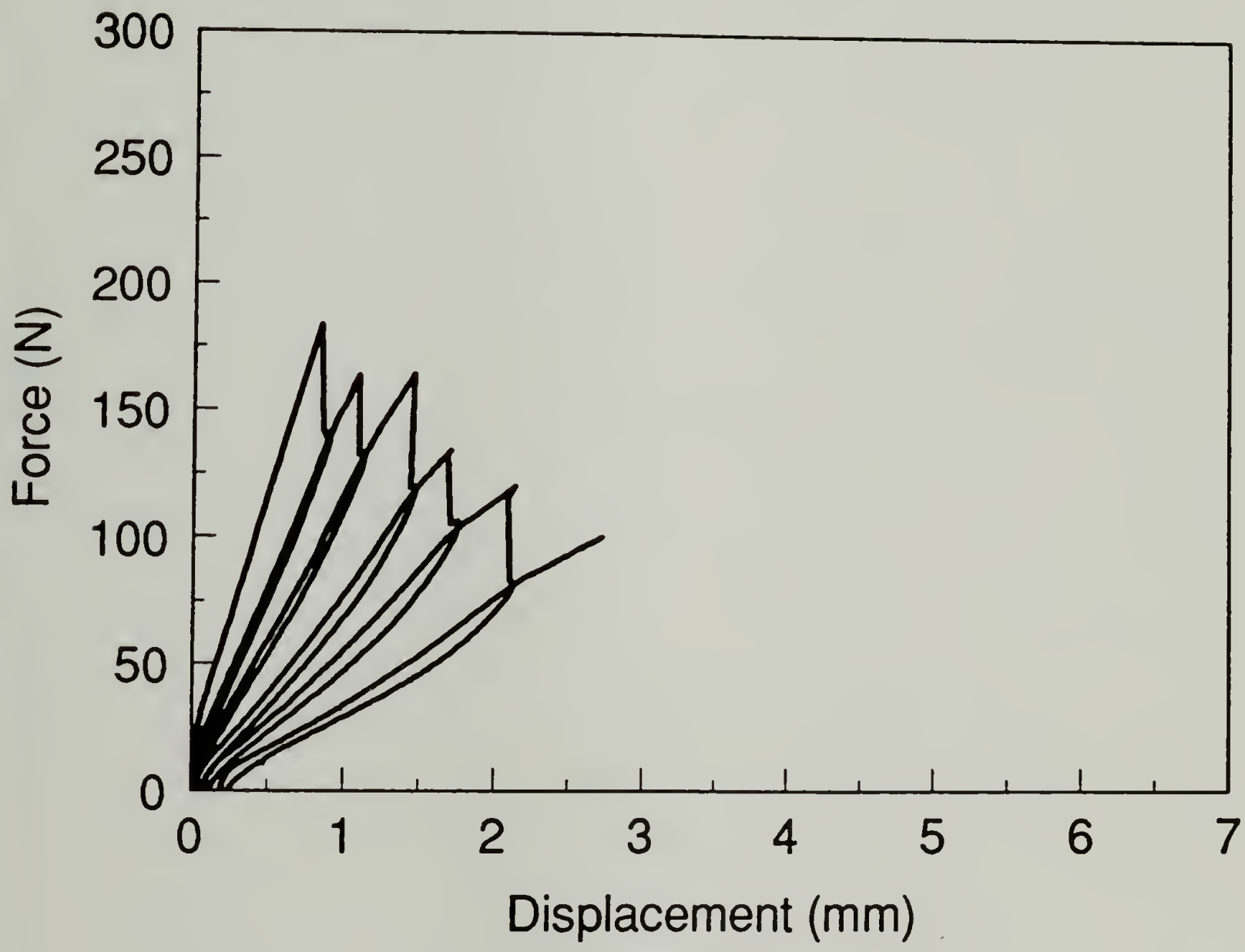

Figure 3.6 DCB test force-displacement diagram of adhesion between epoxy and PCTFE-Butyl modified in heptane for 30 minutes at 25°C.

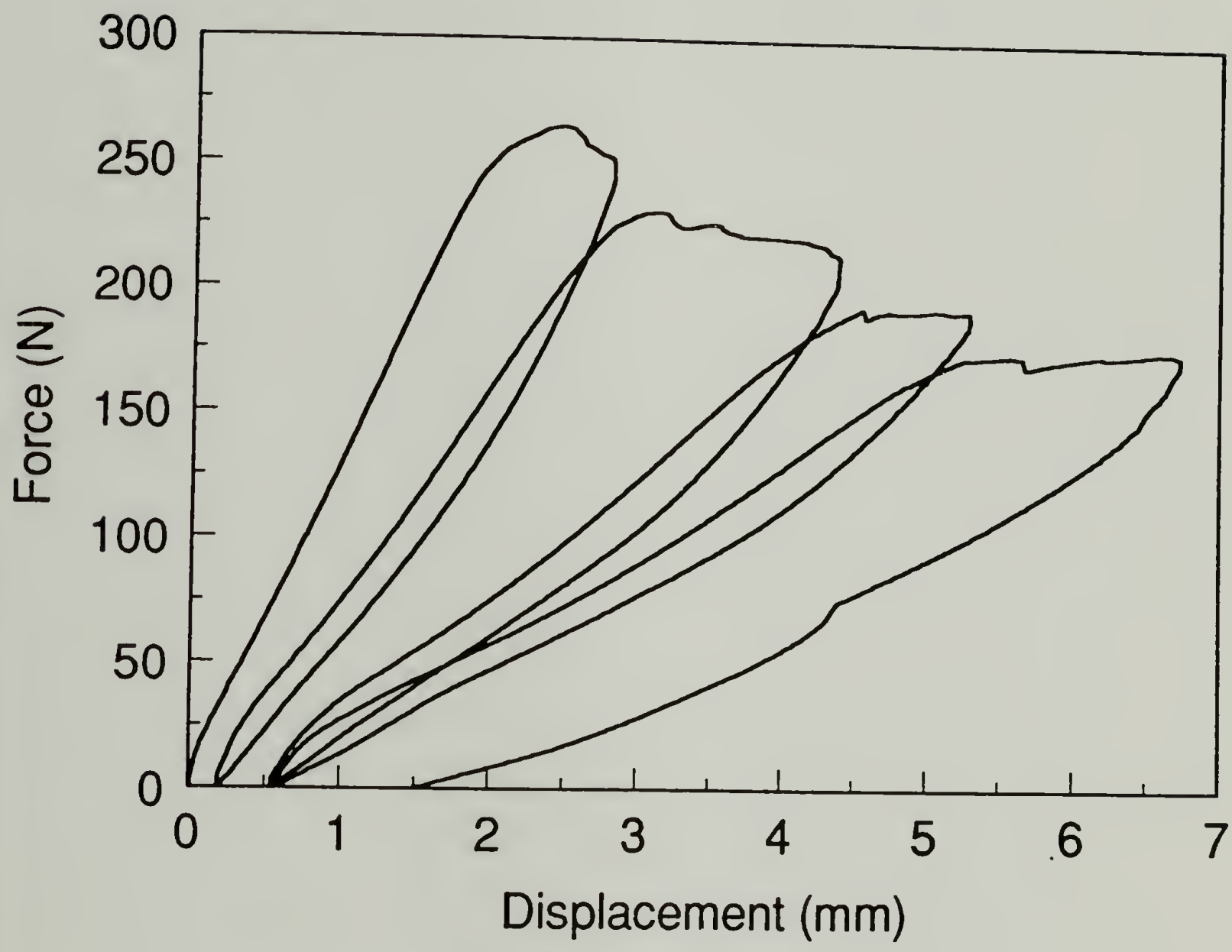

Figure 3.7 DCB test force-displacement diagram of adhesion between epoxy and PCTFE-Butyl modified in heptane for 30 minutes at 0°C.

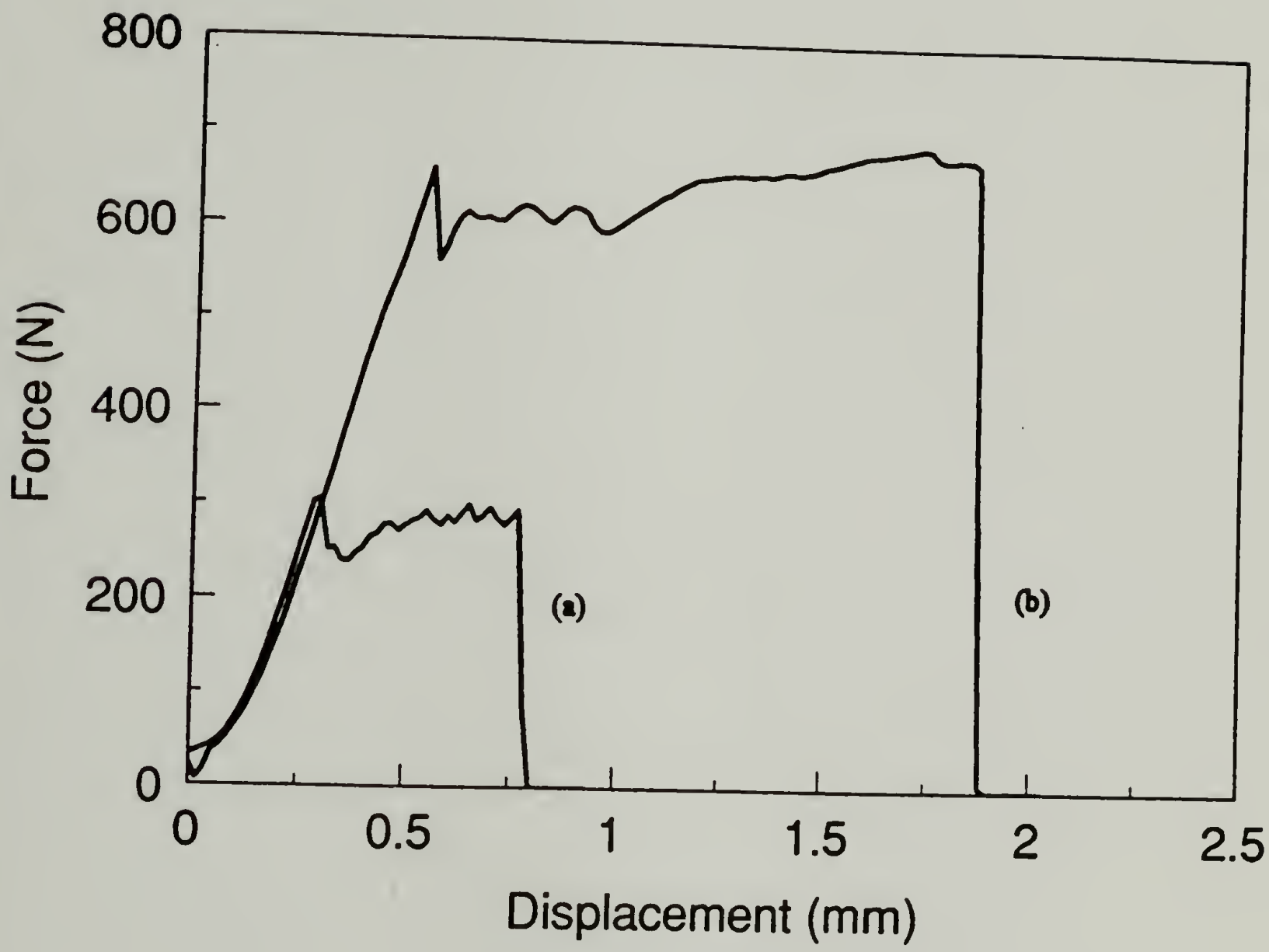

Figure 3.8. TDCB test force-displacement diagram of adhesion between epoxy and PCTFE-Butyl modified in heptane for 30 minutes at (a) 25°C and (b) 0°C.

From the adhesive energies reported in Table 3.1, two dramatic effects of the measurement system can be observed. First, the magnitude of adhesive energy measured by the peel test was greatly inflated compared to the DCB tests; second, the level of adhesion measured by the TDCB test was more sensitive to the extent of surface modification in a regime where the peel test was not. Studies of measured adhesion at different failure modes show that increasing the mode II component of stress can increase the measured adhesion by a factor of 2 or 3.[15,20,21] However, the epoxy PCTFE-Butyl peel energies were inflated by a factor of 10. This can only be accounted for by large amounts of plastic/viscoelastic deformations taking place during peeling as a result of the large bending stresses at the point of detatchment.[4,7]

The mode of stress could not account for the inflated values of the peel test but may account for the sensitivity of the TDCB test to the surface chemistry. Evans[22] has shown that in cases where the mode II stress is not equal to zero, the crack tends to deflect into the lower modulus material, which in this case is the PCTFE. This renders the peel test less sensitive to the surface chemistry than the DCB tests, where the predominantly mode I stress state forces the crack growth along the interface.

If the mode of stress was affecting the crack path then the loci of failure should be different between the peel test and the DCB tests. The loci of failure after peeling PCTFE-Butyl from epoxy depended on the degree of PCTFE-Butyl initial surface modification. When the peel energy was low (high extents of surface modification) the failure was predominately adhesive, meaning only small amounts of fluorine could be detected by XPS on the epoxy surface after peeling (Appendix A). When the peel energy

was high the failure was cohesive in the PCTFE. During peeling the failure appeared to be adhesive by visual inspection, but when the epoxy surface was analyzed by XPS the 15° and 75° survey spectra looked identical to virgin PCTFE film (Figure 3.9 and Appendix A). This data shows that the crack cannot deflect into the PCTFE until a minimum amount of adhesion is achieved. When this critical level of adhesion is reached the crack deflects into the PCTFE and the peel test becomes insensitive to any further surface modifications.

The loci of failure after debonding by the DCB tests were very different than debonding by the peel test. For the PCTFE-Butyl (-15°C), and PCTFE-Butyl (25°C), the failure was mixed adhesive/cohesive as determined by XPS, ATR IR, and optical microscopy. Optical microscopy showed that the crack deflected back and forth between the epoxy/PCTFE-Butyl (25°C) interface and the PCTFE-Butyl film (Figure 3.10). XPS analysis after debonding epoxy from PCTFE-Butyl (25°C) gave: 75.9% carbon, 19.9% fluorine, 3.4% oxygen, on the PCTFE-Butyl side and 75.2% carbon, 13.0% fluorine, 6.9% oxygen, 4.1% nitrogen on the epoxy side. For PCTFE-Butyl (0°C) surfaces, the failure was cohesive in the bulk of the PCTFE. This could be observed visually during the test, by optical microscopy (Figure 3.11), and by the large hysteresis in the force-displacement curve (Figure 3.7), which shows large amounts of plastic/viscoelastic dissipation. Investigations of the loci of failure after debonding correlate with theories describing the tendency of the crack path to deviate from the interface under conditions of mode II stresses, whereas mode I stresses tend to propagate the crack along the interface.[22]

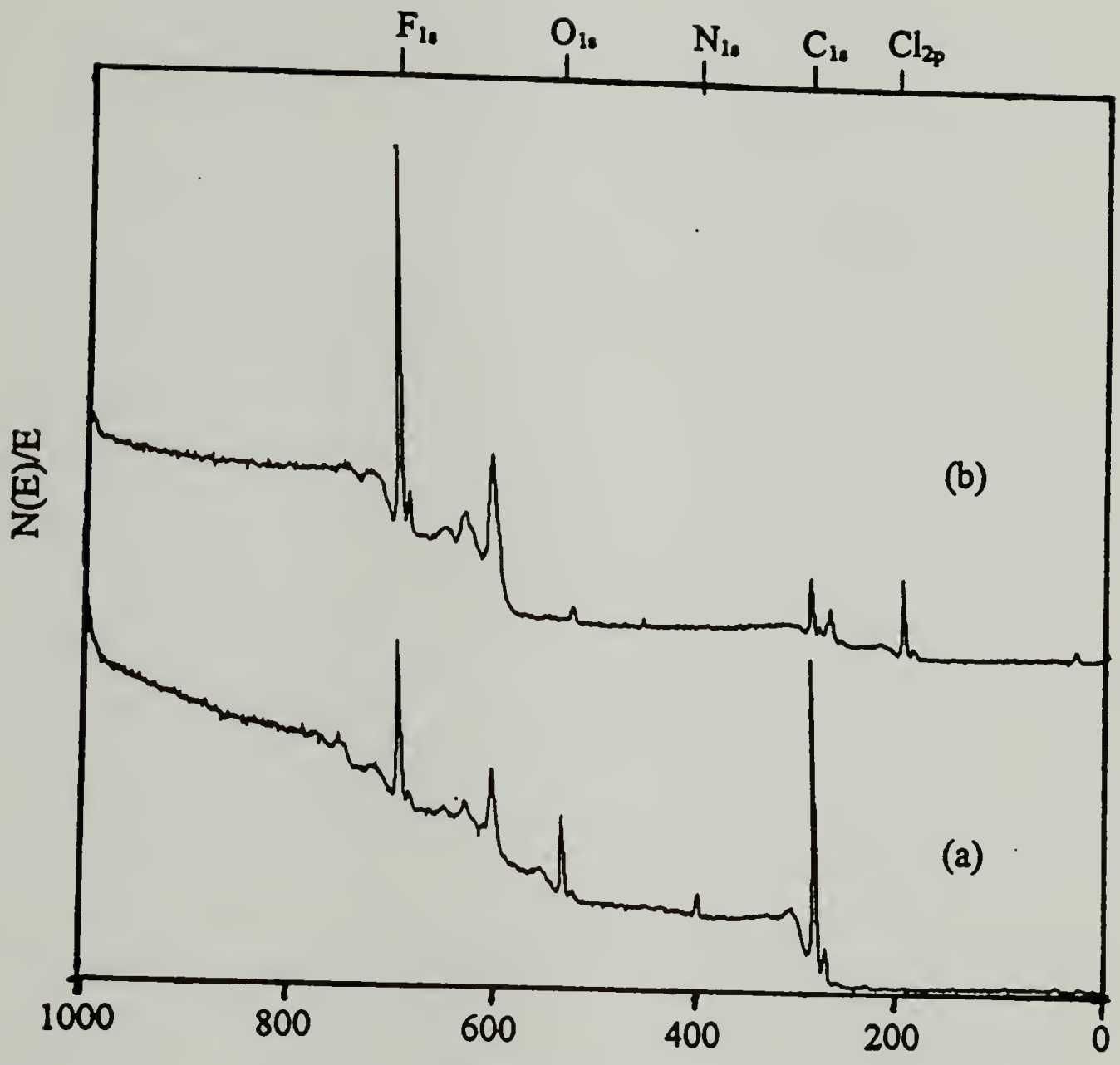

Figure 3.9 XPS survey spectra using 15° take-off angle on epoxy after peeling from (a) PCTFE-Butyl modified in 52.8% heptane/THF for 30 minutes at 0°C and (b) PCTFE-Butyl modified in heptane for 30 minutes at 0°C.

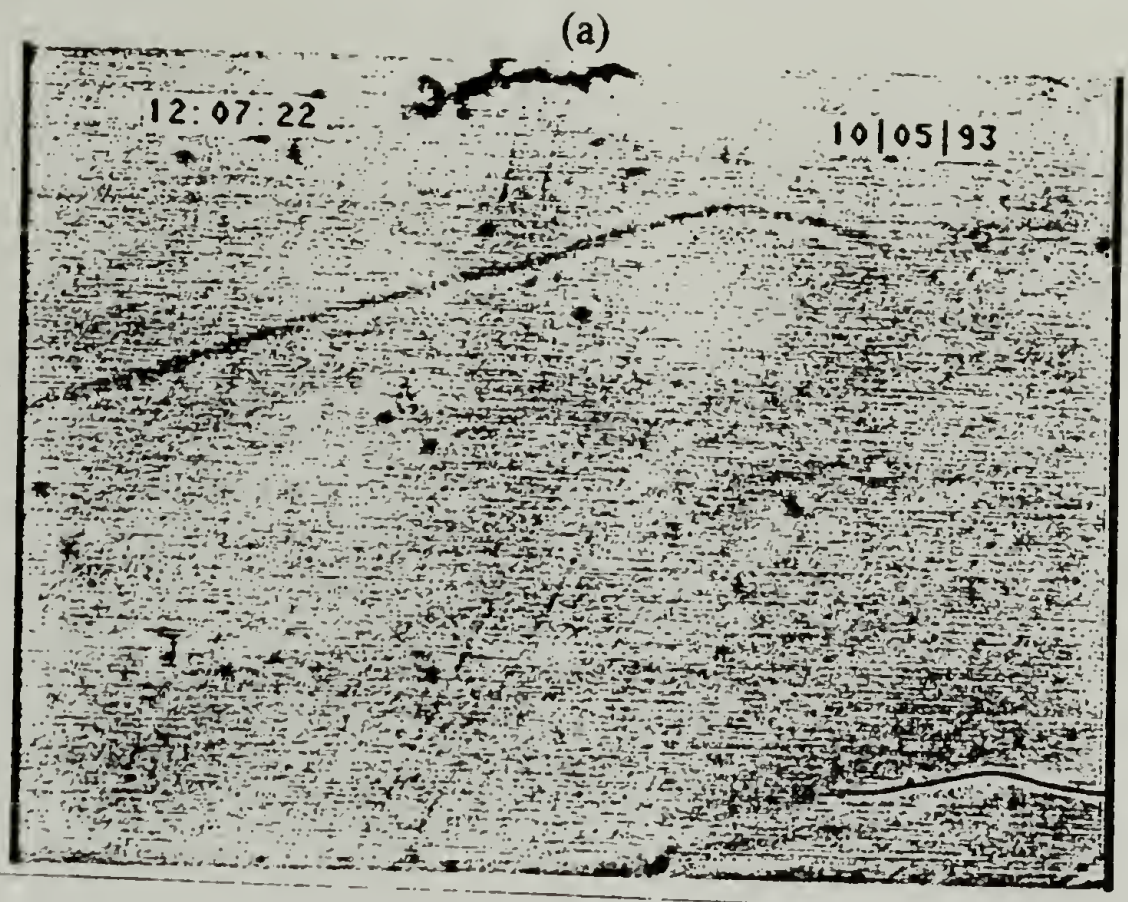

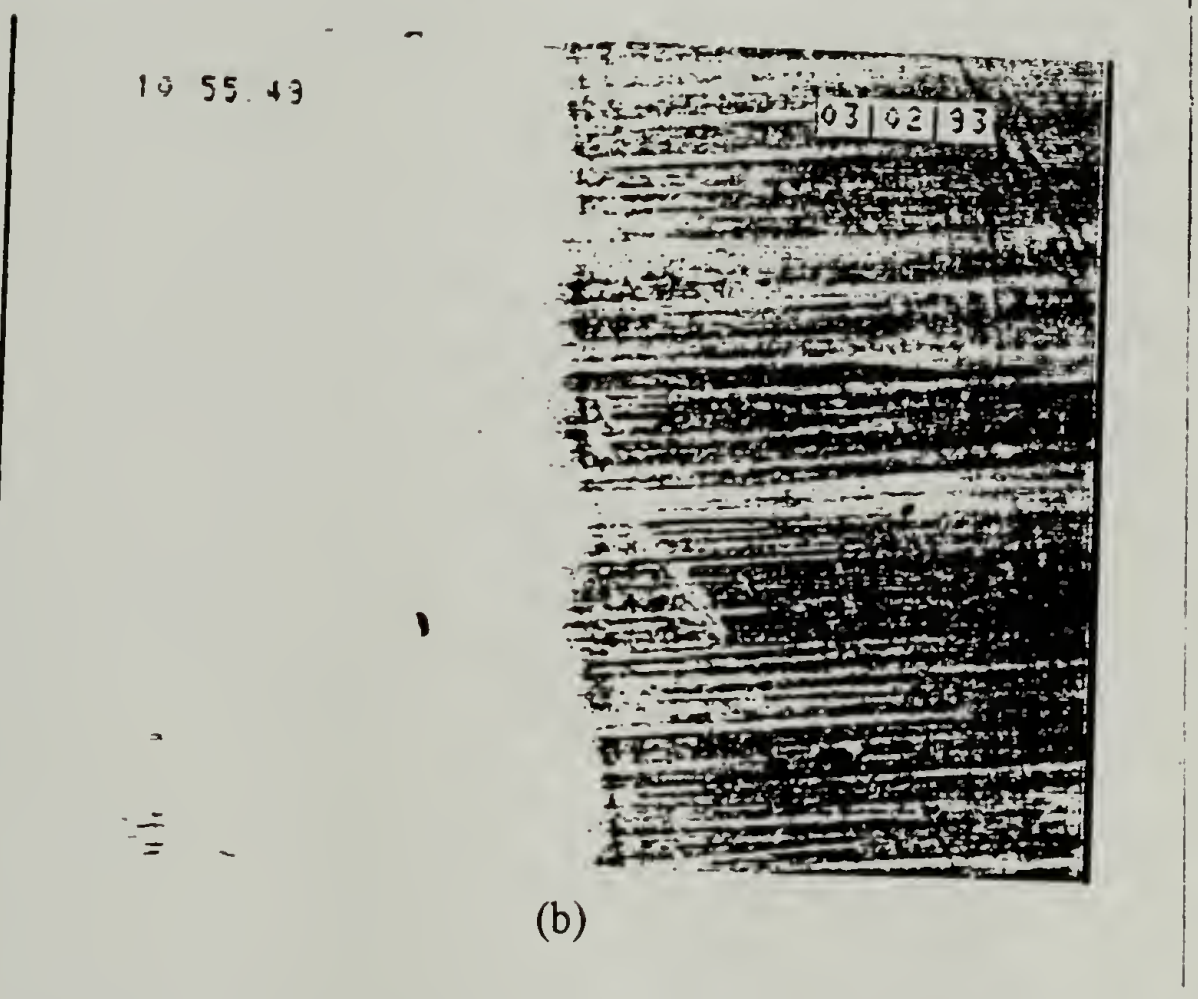

Figure 3.10 Optical micrographs using 100X magnification on (a) virgin PCTFE and (b) PCTFE-Butyl (25°C) after debonding by the DCB test.

Figure 3.11 Optical micrograph using 25X magnification on PCTFE-Butyl (0°C) after debonding by the DCB test.

The peel energy of PCTFE-Butyl to the PSA was 170 J/m^2, essentially identical to that of untreated PCTFE. The failure was also adhesive by XPS. Their was no real difference in peel energies to the PSA between PCTFE-Butyl modified in heptane at 0°C for 30 minutes and PCTFE-Butyl modified in heptane/THF at 25°C for 30 minutes. From surface affinity considerations, it would be predicted that no change in adhesive properties should occur with PCTFE-Butyl surface modification. This is what was observed for PCTFE-Butyl to the PSA and fully modified PCTFE-Butyl to epoxy. The large increases in adhesion to partially modified PCTFE-Butyl surfaces were not predicted from relative surface affinity measurements. This prompted the study of the reactivity of these surfaces with model organic compounds.

Adhesion of PCTFE-Butyl Reacted with Amines

That a partially modified PCTFE-Butyl surface would stick to epoxy while the unmodified and completely modified surfaces would not, was at first puzzling. No changes in surface roughness were detected by SEM or AFM, and no changes in surface affinity were observed by contact angle when water, glycerol, or hexadecane were used as probe fluids (Chapter II). These observations prompted the investigation of covalent bonding across the interface as a possible mechanism of adhesion. Model studies of the reactivity of PCTFE-Butyl surfaces with amines were conducted in Chapter II. Since amines were present in the epoxy curing agent, the possibility of covalent bonding between the curing agent and the PCTFE-Butyl surfaces were investigated. To test this as a possible mechanism of adhesion, partially modified PCTFE-Butyl surfaces were reacted with dimethylamine (Chapter II). Indirect evidence of reaction was observed by the

appearance of a N_{1s} peak at 402 eV in the XPS spectrum (Chapter II). If, in fact, allylic chlorides on the PCTFE-Butyl surface were reacting with the amine in the epoxy curing agent, then PCTFE-Butyl surfaces pre-reacted with dimethylamine before the adhesion tests to epoxy should no longer stick. As seen by figure 3.12 this was, in fact, the case. It should be noted also that surface affinity changes did not occur with the reaction of PCTFE-Butyl with amines. To give more evidence of covalent bonding as the mechanism of adhesion, it would be predicted that PCTFE-Butyl surfaces reacted with hexamethylene diamine should exhibit good adhesion to epoxy. The measured peel energy of PCTFE-Butyl (modified in heptane, for 30 minutes at 0°C) reacted with hexamethylene diamine was ~1,400 J/m^2. These experiments give ample evidence that the adhesion mechanism of partially modified PCTFE-Butyl to epoxy was by covalent bonding between the amine curing agent in the epoxy and allylic chlorides present on the partially modified PCTFE-Butyl surface.

Adhesion to PCTFE-OX

The surface affinity of PCTFE could be increased by modifying PCTFE with *n*-butyllithium, then oxidatively removing the Butyl groups (Chapter II). After oxidation of the PCTFE-Butyl surface, the modified layer was completely removed except for a very thin layer of 1.8% to 5.8% oxygen in the form of carboxylic acid groups. The surface exhibited and increase in surface affinity because of acid-base interactions with the carboxylic groups, the water contact angle was 93/28. The peel energy to epoxy increased to ~1,000 J/m^2. The failure was cohesive in the PCTFE film by XPS and occasionally the PCTFE film tore during peeling. Subsequent reaction of PCTFE-OX

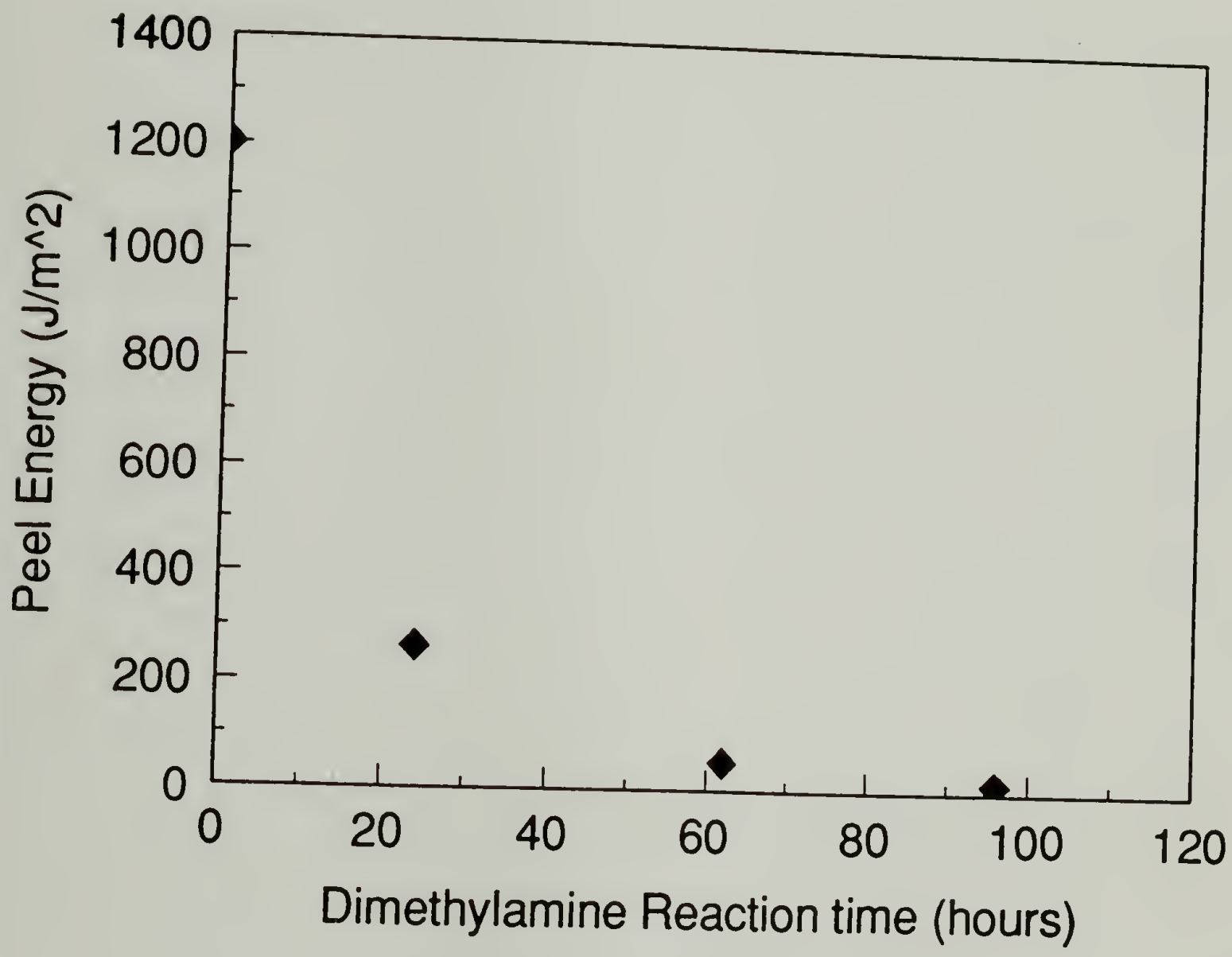

Figure 3.12 Peel energy to epoxy of PCTFE-Butyl (modified in heptane at 0°C for 30 minutes) reacted with dimethylamine in water at ambient conditions for various times.

with *n*-butyllithium (under conditions that give high extents of modification) decreased the surface affinity and the adhesion to epoxy to that of untreated PCTFE.

The peel energy of PCTFE-OX to the PSA was 254 J/m^2, an expected increase also due to acid-base interactions across the interface with the PSA. The failure was predominantly adhesive by XPS, however, a small increase in carbon and oxygen on the PCTFE-OX side indicated the some PSA remained on the PCTFE-OX side after peeling.

Adhesion to PCTFE-PEA

PCTFE-PEA surfaces showed a decrease in the receding water contact angle (Table 3.2) but showed little change in the advancing contact angle, making predictions on surface affinity changes difficult. The adhesion of PCTFE-PEA to epoxy was very poor (~4 J/m^2), and showed primarily cohesive failure in the surface modified region by XPS (Appendix B). The adhesion of PCTFE-PEA to the PSA was 40 J/m^2, and the failure was adhesive by XPS (Appendix C). This is an unexpected result because from the receding water contact angle an increase in adhesion, if any, would be expected. The poor adhesion to epoxy could be explained by a weak boundary layer (which implies that the surface modified region has poor cohesion). However, XPS after peeling the PSA shows that the failure was adhesive not cohesive in the modified layer. Another possible explanation of the apparent poor adhesion to the PSA and epoxy was in regard to the physical structure of the modified layer. It was conceivable that the ethyl acetal groups were flexible enough to reorganize into a surface structure that consists of a smooth layer of methyl groups. The reduction in surface area would account for the reduction in adhesion. Some preliminary AFM experiments, and contact angle measurements support

this explanation. Atomic force micrographs showed a very smooth, liquid-like surface which could be attributed to the effect of the flexible ether-linkages at the surface. The large contact angle hysteresis could also be due to the flexible ether-linkages at the surface reorganizing during the advancing and receding of the water droplet.[23,24]

Table 3.2. Adhesion energy measured by the 180° peel test and contact angle of surface modified PCTFE, surface modifications were deeper than 10 nm.

Surface	Adhesion Energy (J/m^2)		Water Contact Angle	
	Epoxy	PSA	advancing	receding
PCTFE	~4	174	107	75
PCTFE-Butyl	~4	170	106	79
PCTFE-PEA	~4	40	100	40
PCTFE-OH	>1,400	216	69	28
PCTFE-Adipate	~4	241	73	41
PCTFE-Butyrate	57	110	90	44
PCTFE-Heptadecanoate	~4	37	118	77
PCTFE-Stearate	~4	21	106	81

Adhesion to PCTFE-OH

A pronounced increase in surface affinity was evident by water contact angle when the PCTFE-PEA surface was hydrolyzed to the alcohol (Table 3.2). As expected the adhesion to epoxy was very high (>1,400 J/m^2). The PCTFE-OH samples stretched and broke during peeling, this is different from the PCTFE-OX where the failure was cohesive in the PCTFE but near the interface. This difference in the adhesion and loci of failure was likely not due to stronger molecular interactions but the number of molecular interactions. PCTFE-OH surface modifications were on the order of ~150 nm thick, whereas the thickness of the PCTFE-OX layer was on the order of ~4 nm. This increase in the modified layer thickness allowed greater diffusion of the epoxy into the PCTFE-OH layer, hence more molecular interactions. The PCTFE-OH could not be peeled because a crack could not be propagated along the interface, due to the increased bonding. The peel energy to PSA was 216 J/m^2 and the failure was predominantly adhesive with a small amount of PSA on the PCTFE-OH side after peeling.

Adhesion to PCTFE-Ester Surfaces

The PCTFE-Adipate, PCTFE-Hept., and PCTFE-Stearate surfaces showed poor adhesion to epoxy (Table 3.2). The failure was predominantly adhesive by XPS. The adhesion of epoxy to PCTFE-Butyrate was very sensitive to reaction and drying conditions. PCTFE-Butyrate dried 3 days at 45°C (0.05 mm vacuum) had a peel energy of 660 J/m^2 to epoxy. When the drying conditions were increased to 6 days at 95°C the peel energy decreased to 57 J/m^2. The loci of failure after peeling the epoxy also changed with drying conditions. The PCTFE-Butyrate dried 6 days at 95°C gave lower peel

energies and predominantly adhesive failure by XPS, whereas, lower drying times and temperatures, gave cohesive failure. PCTFE-Butyrate reacted with a pyridine catalyst had a contact angle of 102/37 and a peel energy of 7 J/m^2 to epoxy. Even after extensive washing and drying the pyridine remained on the surface as a contaminant.

For the PCTFE-Ester surfaces, surface affinity measurements loosely predicted the trends in adhesion to epoxy and PSA. However, the adhesion to PCTFE-Butyrate surfaces were very sensitive to contaminates such as THF and pyridine. THF effected adhesion of PCTFE-Butyrate by the same plasticizing effect found with PCTFE. Pyridine had the opposite effect of the THF and was more difficult to remove.

Conclusions and Future Work

Introducing functional groups to the surface of PCTFE affected the adhesion to epoxy and a PSA. The adhesion trends roughly correlated with surface affinity measurements, however, other very important factors were found to be important. Solvent swelling (or plasticizing) the PCTFE surface greatly increased its adhesion by making possible the interdiffusion of the adhesive and PCTFE. The nature of the swelling was very sensitive to the surface functionality. Covalent bonding, not predicted from surface affinity measurements, greatly increase the adhesion between partially modified PCTFE-Butyl and epoxy.

For applications other than peeling the peel test is, at best, only a qualitative test. The adhesive energies measured were greatly inflated. When significant adhesion existed the crack was forced into the PCTFE film, making the test less sensitive to the surface functionality. The TDCB test proved to be a very useful test. The amount of

plastic/viscoelastic deformation was minimized and the measured values of adhesion were very sensitive to the surface chemistry.

Future work on fundamental investigations of adhesion should take in consideration important test parameters such as the modes of failure, and the size of plastic/viscoelastic deformations zones. Recent developments in an asymmetric double-cantilever-beam test[21] offer precise control of mode I and II stress components during crack propagation.

Another important parameter in adhesion that could not be precisely investigated was the depth of surface modification. PCTFE surfaces had to be modified deep enough so that allylic chlorides were not present in the surface region, because of their reactivity with epoxy. A fundamental investigation of adhesion would also incorporate control of the depth of the surface modified region, as well as the surface functionality.

References

1. Kinloch, A.J. *Adhesion and Adhesives Science and Technology*, Chapman and Hall: London, **1987**.

2. Kaelble, D.H. *J. Adhesion*, **1992**, 37, 205.

3. Thouless, M.D.; Jensen, H.M. *J. Adhesion*, **1992**, 38, 185.

4. Kim, K-S.; Aravas, N. *Int. J. Solids Structures*, **1988**, 24, 417.

5. Gent, A.N.; Kaang, S.Y. *J. Adhesion*, **1987**, 24, 173.

6. Loukis, M.J.; Aravas, N. *J. Adhesion*, **1991**, 35, 7.

7. Goldfarb, J.L.; Farris, R.J., *J. Adhesion*, **1991**, 35, 233.

8. Goldfarb, J.L. Ph.D. Dissertation, University of Massachusetts, **1992**.

9. Ripling, E.J.; Mostovoy, S. *J. Appl. Polymer Sci.*, **1966**, 10, 1351.

10. Ripling, E.J.; Mostovoy, S.; Corten, H.T. *J. Adhesion*, **1971**, 3, 107.

11. Gledhill, R.A.; Kinloch, A.J. *Polymer Engineering and Science*, **1979**, 19, 82.

12. Bascom, W.D.; Cottington, R.L.; Jones, R.L.; Peyser, P. *J. Appl. Polymer Sci.*, **1975**, 19, 2545.

13. Scott, J.M.; Phillips, D.C. *J. Mater. Sci.*, **1975**, 10, 551.

14. Williams, J.G., *Fracture Mechanics of Polymers*, John Wiley & Sons: New York **1984**.

15. Lau, C.C.; Kinloch, A.J.; Williams, J.G. *The Adhesion Society Proceedings of the Sixteenth Annual Meeting*, February **1993**, 96.

16. Evans, A.G.; Ruhle, M.; Dalgleish, B.J.; Charalambides, P.G. *Metallurgical Transactions A*, **1990**, 21A, 2420.

17. Conversation with Tony Messa, a Technical Sales Representative with Allied-Signal Inc.

18. Allied-Signal Inc., Aclar product bulletin.

19. Schonhorn, H.; Sharpe, L.H. *J. Appl. Polymer Sci.: Part A*, **1965**, 3, 3087.

20. Charalambides, M.; Kinloch, A.J.; Wang, Y.; Williams, J.G. *Inter. J. Fracture*, **1992**, 54, 269.

21. Xiao, F.; Hui, C-Y.; Washiyama, J.; Kramer, E.J. *Macromolecules*, **1994**, 27, 4382.

22. Evans, A.G.; Ruhle, M.; Dalgleish, B.J.; Charalambides, P.G. *Mater. Sci. Eng.*, **1990**, A126, 53.

23. Allen, K.W. *Adhesion*, **1986**, 11, 82.

24. Good, R.J.; Stromberg, R.R. *Surface and Colloid Science*, **1979**, 11, 13.

CHAPTER IV

PREPARATION OF POLY(STYRENE-*B*-1,2-BUTADIENE) AND POLY(STYRENE-*B*-4-HYDROXYBUTENE) FOR ADHESION STUDIES

Introduction

Block copolymers are a unique class of materials that have been found to be very effective adhesives.[1] Block copolymers are polymers composed of two (or more) distinct segments along the backbone of the polymer chain. Unique properties result when segments which vary significantly in physical and chemical properties are joined together.[1] The unique physical properties of block copolymers have been intensively investigated and commercially exploited since the 1960's.[2] Recently, the McCarthy group has been investigating the nature of block copolymers containing a "Sticky Foot"(SF) segment.[3] SF polymers are polymers composed of two distinctly different functional parts. One part of the SF polymer contains organic moieties which are highly interactive with a selected surface (high χ_s); the other part of the SF polymer interacts poorly (low χ_s) with the selected surface. In the McCarthy laboratory, anionic polymerization techniques have been successfully used to prepare SF polymers from block copolymers of well defined structure and compostion.[4-10]

Anionic living polymerization techniques offer the potential to synthesize SF polymers of known molecular weight, narrow polydispersity, and defined number of sticky

feet in known locations. Ziegler[11] was the first to postulate the existence of anionic living polymerization systems. Ziegler proposed that diene monomers could be polymerized with alkali metals and if the reaction vessel was kept free from impurities no termination reactions would take place.[11] Szwarc was the first to show that termination reactions could be eliminated from anionic polymerizations.[12,13] Szwarc showed that after the initial aliquot of monomer was reacted, more monomer or another monomer could be added and the polymer molecular weight would increase linearly. The term 'living polymerization" was used to describe this behavior.[12,13] It was also reported that the molecular weight could be predicted for anionic polymerizations by the equation:

$$DP = [M]/[I]$$

where DP is the degree of polymerization, [M] is the monomer concentration, and [I] is the initiator concentration. For this equation to be valid, the reaction conditions must be such that the rate of initiation is much greater than the rate of propagation.[14] When these conditions are met, not only can the molecular weight be predetermined but the polydispersity will be close to unity.[14]

Block copolymers of predetermined molecular weight and narrow molecular weight distribution have been synthesized by the anionic polymerization of styrene and the subsequent addition of butadiene to the polystyryl anion.[15,16] Butadiene can react with the polystyryl anion to give diene segments in the 1,4- trans, 1,4-cis, or in the 1,2-vinyl configuration.[16] The 1,2-vinyl configuration can be kinetically favored by addition of tetramethylethylenediamine (TMEDA), which functions as a chelating agent for the lithium counterion.[17,18] TMEDA has been reported to give over 90% vinyl addition for

the anionic polymerization of butadiene.[17] This technology demonstrates the ability to synthesize poly(styrene-*b*-1,2-butadiene) with predetermined molecular weight and block sizes.

The mechanical properties of the butadiene and styrene segments differ significantly but their polarity or surface affinity does not.[19] Recent developments in the borane functionalization of dienes have offered many possibilities in functionalizing polymers.[20-25] Chung reported the use of hydroboration-oxidation chemistry to add alcohols to polybutadiene and polyisoprene.[24,25] Kendall extended this work to synthesize poly(styrene-*b*-4-hydroxybutene) from poly(styrene-*b*-1,2-butadiene).[7,8] This work makes the synthesis of SF polymers with varying stick foot surface affinities (χ_s) possible.

The objectives of this chapter are to synthesize block copolymers with a defined number of sticky feet in known location, predetermined molecular weight, low polydispersity, and varying sticky foot χ_s. This chapter discusses the synthesis and characterization of poly(styrene-*b*-1,2-butadiene) and poly(styrene-*b*-4-hyroxybutene) so that adhesion studies can be conducted, investigating the role polymer functionality plays in adhesion.

Experimental

General

The chemicals used were purchased from Aldrich unless otherwise noted. Prepurified nitrogen was supplied by Matheson and used as received. The following chemicals were used as received: *sec*-butyllithium (1.3 M in hexane), benzophenone, methanol, dibutylmagnesium (1.0 M in heptane), calcium hydride, sodium metal, and 9-

borobicyclononane (0.5 M in THF) (9-BBN). Benzene was distilled over calcium hydride and stored under nitrogen. Just prior to polymerization benzene was stirred over polystyryl anion overnight then distilled. The polystyryl anion was generated by adding 4 ml of styrene and 2.5 ml of sec-butyllithium to the benzene (enough to give a persistant orange color). The styrene was purified by vacuum distilling (30 mm Hg) from calcium hydride (the styrene was stored under nitrogen at -20°C). Just prior to polymerization 20-25 ml of styrene was trap-to-trap distilled from dibutylmagnesium (the heptane was first removed from the dibutylmagnesium with vacuum). The butadiene was trapped into a Schlenk tube containing dibutylmagnesium at -196°C (liquid nitrogen bath), then trap-to-trap distilled. Tetramethylethylenediame (TMEDA) was distilled from calcium hydride then trap-to-trap distilled from *sec*-butyllithium just prior to polymerization. The tetrahydrofuran (THF) was distilled from sodium/benzophenone which has a persistant purple color when dry. The isopropanol, 6 N sodium hydroxide, and 30% hydrogen peroxide in water (EM Science) were sparged with nitrogen 30 minutes before using.

All reactions and purifications were run under nitrogen. Considerable care was used to ensure that no contaminates (i.e. air or moisture) were allowed into the reaction system. All glassware was purged with nitrogen, pumped to 0.05 mm Hg, heated with a heat gun, purged with nitrogen, and heated again. All transfers were done under nitrogen by cannulation. All glassware (except the reaction flask) had a teflon stopcock and 14/20 ground glass joint capped with a rubber septum. The reactions were run in a 250 ml flask containing a glass coated magnetic stir bar with a teflon rotoflo valve and a 14/20 ground glass joint capped with rubber septum.

The molecular weights, both number average (Mn) and weight average (Mw), and the polydispersity index (PDI) were determined using gel permeation chromatography (GPC). GPC analysis was performed using a series of Polymer Laboratories PL gel columns (mean pore diameter 10^4, 10^3, 10^2 angstroms) with THF solvent at a constant flow rate of 1 ml/min. GPC data was collected and analyzed using Polymer Laboratories software. The samples were detected on an IBM UV detector. Commercial narrow molecular weight polystyrene standards were used to calibrate the instrument. Infrared (IR) spectra were obtained by casting films of the polymer onto a NaCl plate from dilute solution in chloroform. IR analysis were performed on an Nicolet IR/44 FTIR. Polymers were dissolved in deuterated chloroform (5% by weight/volume) before proton nuclear magnetic resonance (NMR) spectra were obtained using a Bruker NC 80 instrument. Tetramethylsilane was used as an internal standard (set at 0 ppm) for the NMR analysis.

Synthesis of Polystyrene (PS)

The following procedure is an example of a procedure used to synthesize polystyrene (110k molecular weight PS). Polystyryl anion was synthesized by first cannulating 90 ml of benzene to the reaction flask. 0.53 ml of *sec*-butyllithium (diluted to 0.175 M with benzene) was syringed into the reaction flask and then 11.2 ml of styrene was cannulated into the reaction flask. The reaction mixture turned a light orange indicating polystyryl anion formation. The reaction was allowed to continue for 1.5 hours at room temperature. The reaction was terminated by cannulating in 5 ml of isopropanol. The PS was precipitated in methanol, the liquid was then decanted off, and the PS was dissolved in THF. The polymer was then slowly precipitated in methanol. The white PS

powder was filtered and vacuum dried overnight before GPC, NMR, IR, adhesion studies, and subsequent reactions. (Notebook #6 p. 92)

Synthesis of Poly(styrene-*b*-1,2-butadiene)(PS-B)

The following procedure describes the synthesis of a 100k block copolymer containing 20% 1,2-butadiene segments. Polystyryl anion was first synthesized cannulating 35 ml of benzene to the reaction flask. 0.22 ml of *sec*-butyllithium (diluted to 0.182 M with benzene) was syringed into the reaction flask then 3.5 ml of styrene was cannulated into the reaction flask. The reaction mixture turned a light orange indicating polystyryl anion formation. The reaction was allowed to continue for 1.5 hours at room temperature. TMEDA (0.1 ml) was syringed into the reaction flask containing polystyryl anion. The reacton mixture turned from a light orange to a deep red. Butadiene was equilibrated at -55°C in a dry ice/ethanol bath, then 15 ml of butadiene was cannulated into a graduated cylinder containing 46 ml of benzene. Then 5.0 ml of the 24.6% butadiene in benzene solution was cannulated into the polystyryl anion reaction mixture. The color turned from a deep red to a light yellow indicating the initiation of the butadiene. The reaction was terminated with isopropanol 1 hour after the butadiene addition. The PS-B was precipitated and purified in the same manner as the PS. (Notebook #6 p. 96)

Synthesis of Poly(styrene-*b*-4-hydroxybutene)(PS-OH)

The following procedure describes the hydroboration/oxidation of a PS-B 20% butadiene polymer. First, 100 ml of THF were added to a reaction flask containing 0.80 grams of PS-B that had been pumped down with vacuum and purged with nitrogen. The

solution was then equilibrated at 20°C before 4.8 ml of 9-BBN (0.5 M in THF) was syringed into the reaction. After stirring 3 hours at 20°C the reaction mixture was cooled to 0°C. Then 0.48 ml of 6 N NaOH and 1.13 ml of H_2O_2 was syringed into the reaction solution. The reaction was allowed to stir for 1 hour at 0°C and then slowly warmed to 40°C over 1 hour. The PS-OH was precipitated in a water/methanol (70/30) mixture, filtered, and vacuum dried. (Notebook #7 p.59)

Results and Discussion

Effectively using anionic polymerizations to prepare styrene and butadiene block copolymers of predetermined molecular weight and narrow polydispersity is critically dependent on several factors. First, initiation of both the styrene and butadiene monomers must be much faster than their propagation. Second, impurities (typically oxygen and water) must be rigorously removed from monomers, solvent, glassware, cannula, and syringes. Thirdly, the solvent and reaction conditions used must be free of unwanted side reactions which result in termination (i.e. proton extraction from solvent). The presence of any side reactions will result in broad molecular weight distributions. To meet all these requirements, strict purification procedures and handling of all materials coupled with the proper experimental conditions were essential for successful polymerizations. The synthetic procedures used were adapted from those used by Kendall[7] with a few modifications.

Polystyryl Anion and Polystyrene (Scheme 4.1)

Two different molecular weight PS samples were synthesize, 80k and 110k, with PDI's <1.1. A typical GPC chromatogram is given in Figure 4.1. NMR[16,26] and IR[27] spectra are in agreement with previously published data.

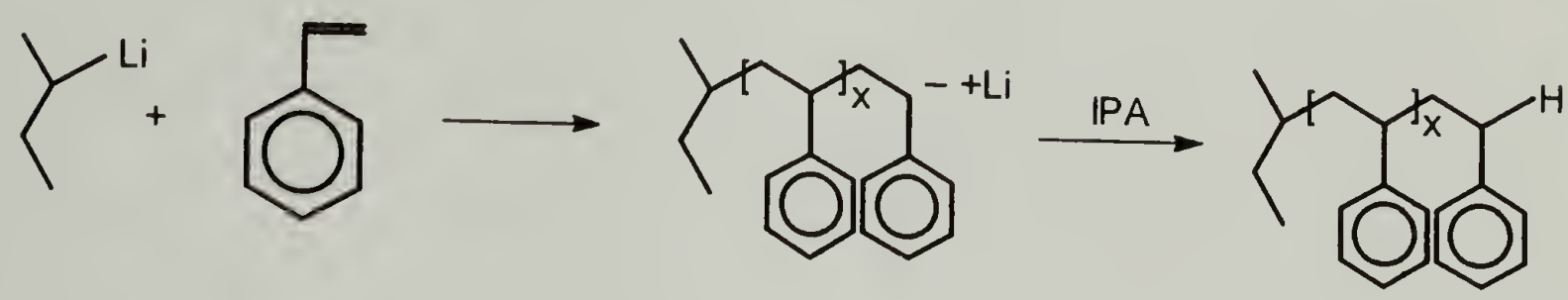

Scheme 4.1 Synthesis of polystyryl anion and termination to give non-functionalized PS.

Poly(styrene-*b*-1,2-butadiene) (PS-B) (Scheme 4.2)

Different PS-B's samples were synthesized varying the % butadiene segments (Table 4.1). Evidence of butadiene block addition was given by the increase in molecular weight by GPC (Figure 4.1). Proton NMR analysis (Figure 4.2) confirmed the addition of the butadiene block and the concentration. Addition of the butadiene in the 1,2- position was confirmed by the observance of vinyl proton resonances at both 4.9 and 5.3 ppm in the correct ratio of 2:1.[26] The IR spectra of PS-B's showed C-H stretching at 910 and 995 cm^{-1} and C=C stretching at 1648 cm^{-1} which confirmed the reaction with butadiene.[27]

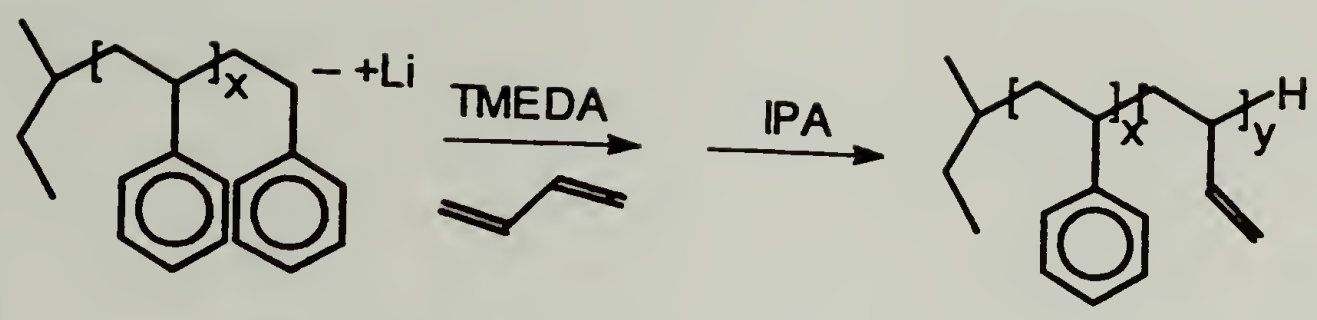

Scheme 4.2 Block copolymerization of polystyryl anion with butadiene to give poly(styrene-*b*-1,2-butadiene).

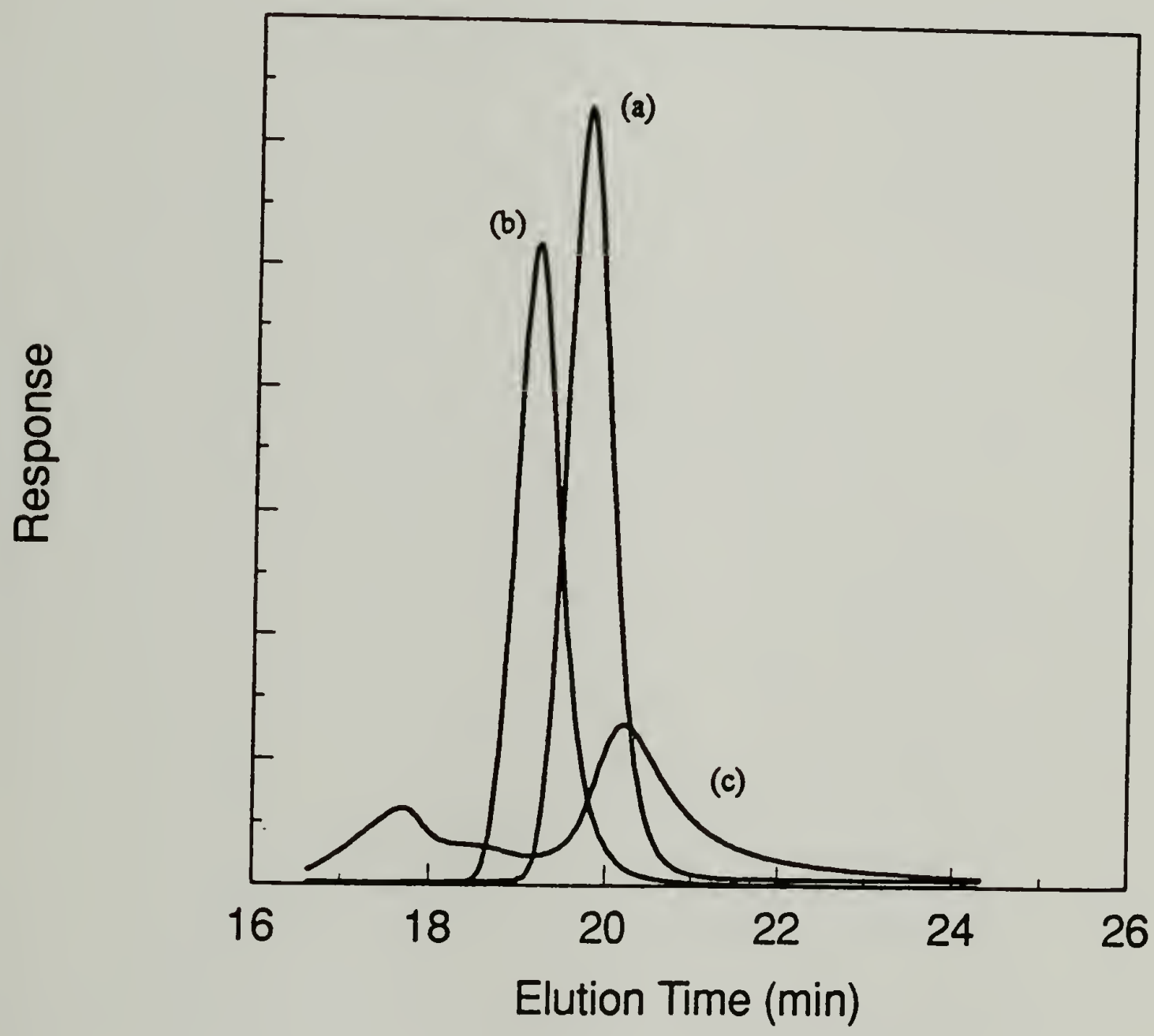

Figure 4.1 GPC chromatograms of (a) PS, (b) PS-B20, and (c) PS-OH20.

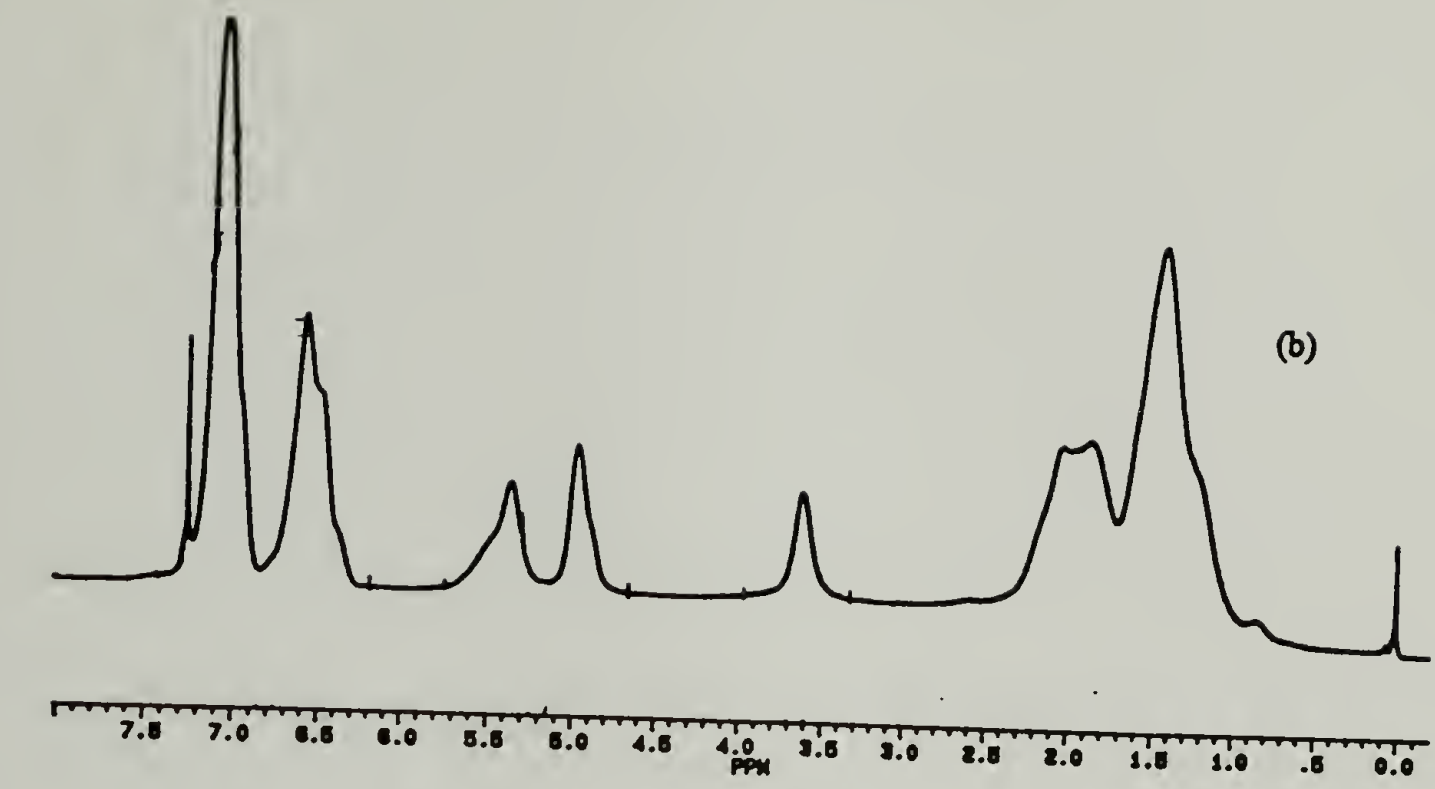

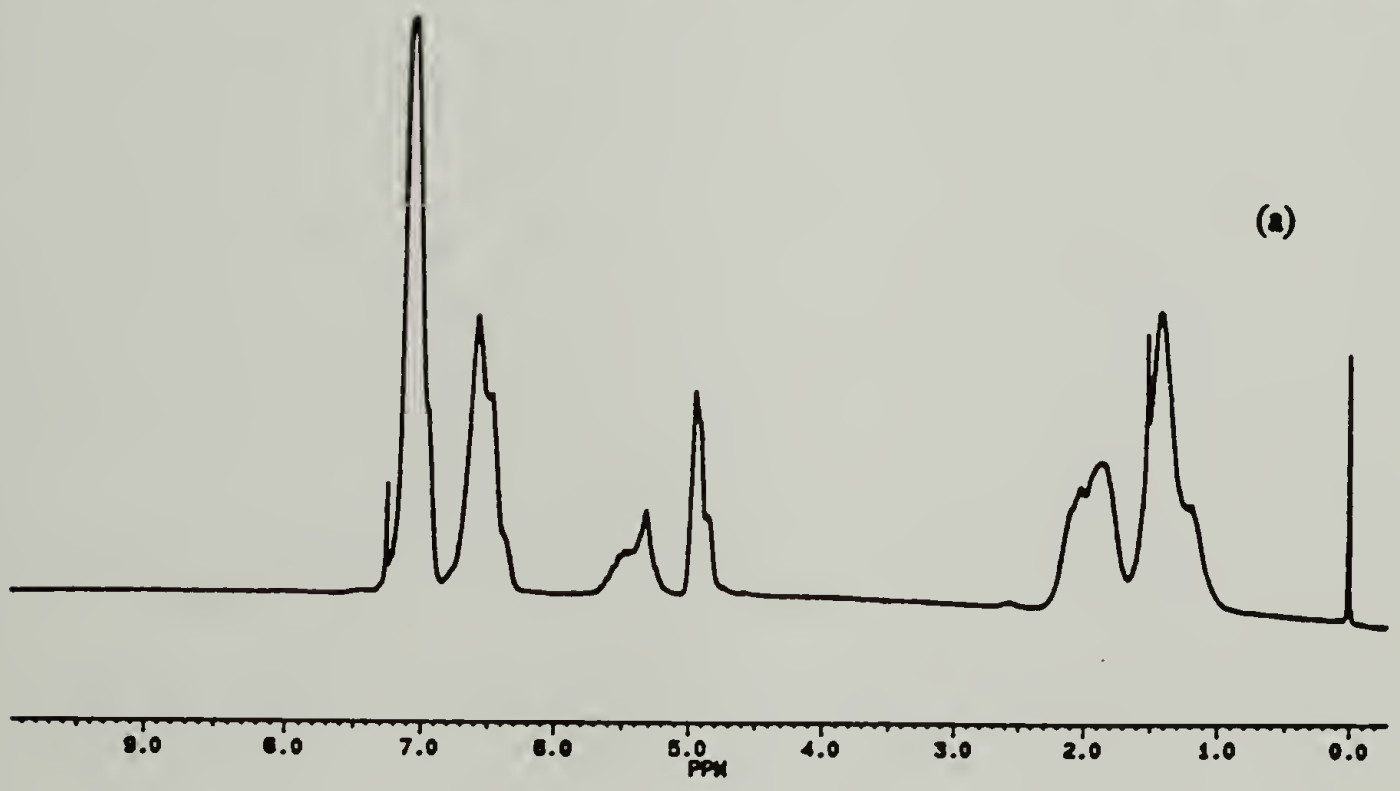

Figure 4.2 Proton NMR spectra of (a) PS-B20 and (b) PS-OH20.

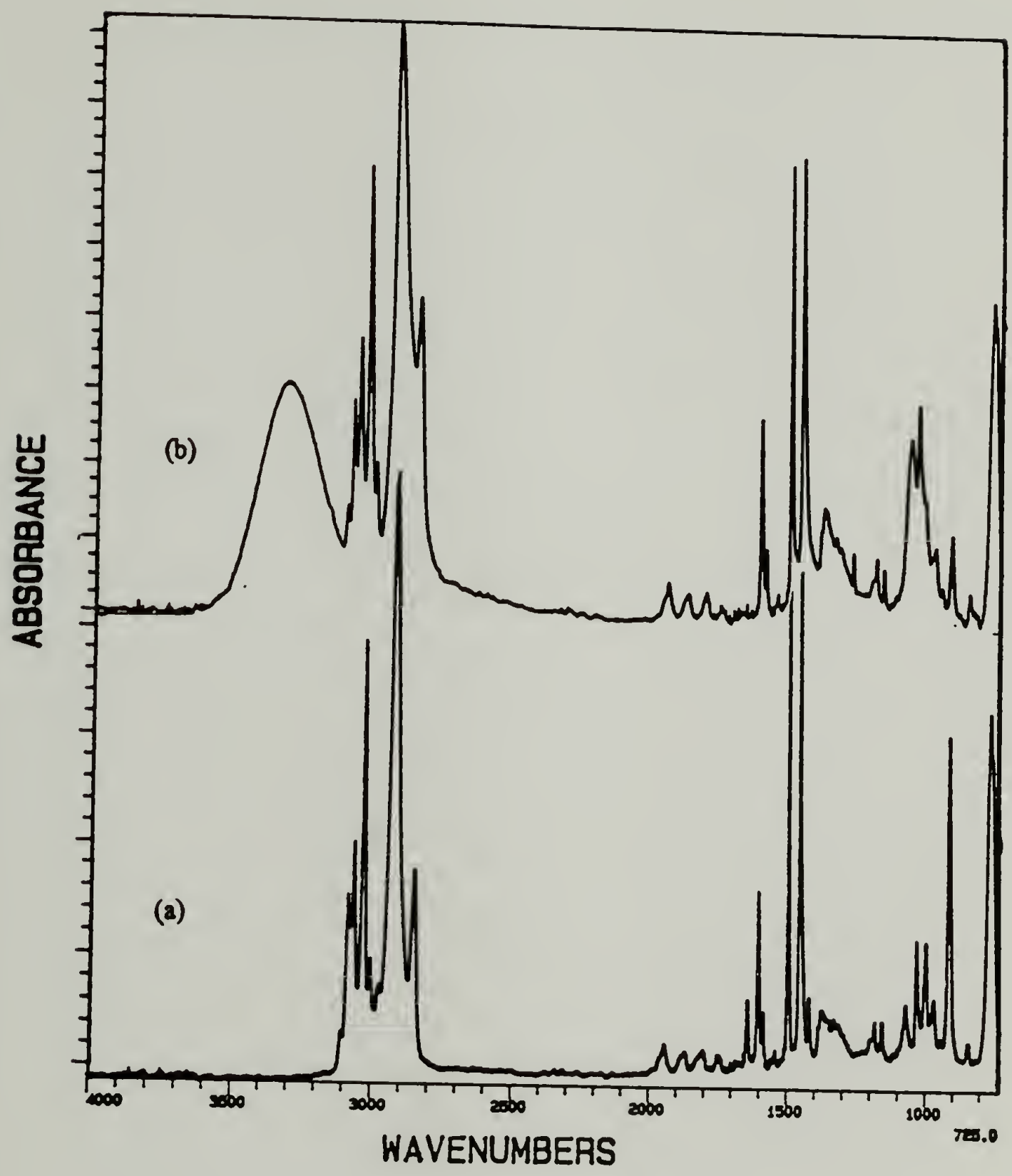

Figure 4.3 IR spectra of (a) PS-B20 and (b) PS-OH20.

Poly(styrene-*b*-4-hydroxybutene) (PS-OH) (Scheme 4.3)

Some cross-linking problems were encountered during the hydroboration /oxidation reaction of PS-B. The PS-B appeared to hydroborate without difficulty because the solution remained homogeneous. Kendall's oxidation reactions were run at -25°C to ensure that no radicals were formed which could cross-link the polymer chains. It was found that under these conditions the PS-B's used were only sparingly soluble in THF. These conditions resulted in a PS-OH polymer that was highly cross-linked and insoluble in THF. To increase the solubility, the oxidation reactions were run at 0°C. This increase in oxidation reaction temperature coupled with using more dilute conditions gave PS-OH polymers soluble in THF. The PS-OH polymers, however, had a high PDI of 1.2 to 2.8 (Figure 4.1), which increased with SF block size. The increase in PDI is partly a result of cross-linking but also partly due to the SF segments sticking to the column of the GPC. The oxidation reactions did not proceed to complete conversion of the butadiene groups to the alcohol as seen by NMR (Figure 4.2) and IR (Figure 4.3). NMR spectra showed an O-H proton peak at 3.6 ppm, but vinyl protons at 5.3 and 4.9 ppm remained. The IR spectra showed an O-H stretch peak at 3200-3500 cm^{-1} and a C-O stretch peak at 1053 cm^{-1} but some C-H stretching at 910 and 995 cm^{-1} also remained.

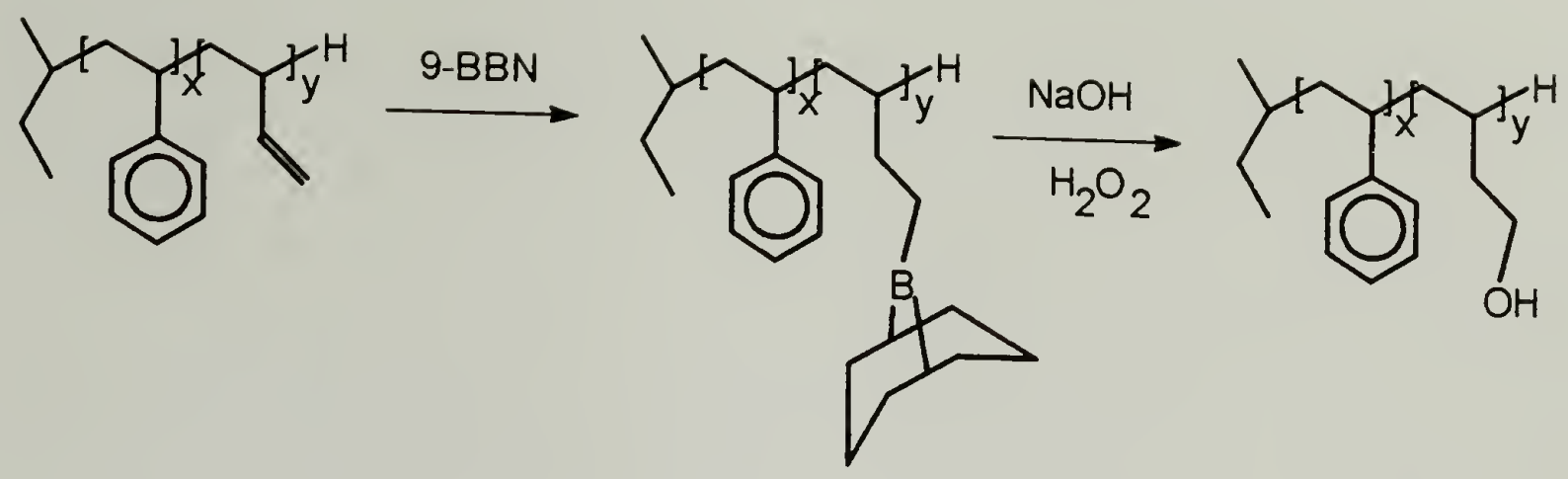

Scheme 4.3 Hydroboration/oxidation of PS-B to PS-OH.

Table 4.1 Summary of PS-B block copolymers synthesized.

Sample	Total Mn		PDI	Mol % Butad.	
	calc.	GPC		calc.	NMR
PS	77	75	1.05	-	-
PS	110	112	1.02	-	-
PS-B20	100	108	1.06	20%	41%
PS-B14	63	63	1.03	14%	20%
PS-B30	100	168	1.04	30%	53%
PS-B5	100	64	1.05	5%	13%
PS-B10	100	147	1.03	10%	15%
PS-B20	100	144	1.04	20%	27%
PS-B40	100	134	1.04	40%	55%

Conclusions and Future Work

Polystyrene, poly(styrene-*b*-1,2-butadiene), and poly(styrene-*b*-4-hydroxybutene) polymers were synthesized. The polymers were characterized by GPC, FTIR, and NMR. PS and PS-B polymers were synthesized with controlled molecular weight, butadiene block size, and low PDI. The synthesis of PS-OH proved to be difficult, near complete conversion of the butadiene to the hydroxybutene was obtained. Cross-linking side reactions occurred that increased the PDI, these side reactions were minimized but could not be eliminated. The oxidation reaction temperature proved to be very important in controlling the conversion to the -OH and minimizing cross-linking. Future studies of this reaction should include finding the optimal temperature that maximized conversion and minimized cross-linking.

References

1. McGrath, J.E. *Anionic Polymerization*, American Chemical Society: Washington, DC, **1981**.

2. Holden, G.; Bishop, E.T.; Legge, N.R. *J. Polymer Sci.: Part C*, **1969**, 26, 37.

3. Definition of Sticky Foot polymes put forth initially by T.J. McCarthy in research discussions and used in this research and the research of Iyengar, D.R., Kolb, B.U., Viviano, K., Franchina, N.F., de Vincenzi, R.D., and Kendall, E.W.

4. Iyengar, D.R. Ph.D. Dissertation, University of Massachusetts, **1992**.

5. Viviano, K. Ph.D. Dissertation, University of Massachusetts, **1994**.

6. Kolb, B.U., Ph.D. Dissertation, University of Massachusetts, **1992**.

7. Kendall, E.W., Ph.D. Dissertation, University of Massachusetts, **1993**.

8. Kendall, E.W.; McCarthy, T.J. *Polym Prepr. (Am. Chem. Soc.,Div. Polym. Chem.)*, **1992**, 33(2), 158.

9. de Vincenzi, R.D. unpublished work, 1994.

10. Kato, T. unpublished work, 1994.

11. Ziegler, K. *Angew. Chem.*, **1936**, 49, 499.

12. Szwarc, M. *Nature*, **1956**, 178, 1168.

13. Szwarc, M; Levy, M.; Milkovich, R. *J. Am. Chem. Soc.*, **1956**, 78, 2656.

14. Morton, M. *Anionic Polymerization: Principles and Practice*, Academic Press, New York, **1983.**

15. Ceresa, R.J., *Block and Graft Copolymerization Volume 1*, John Wiley & Sons, London, **1973.**

16. Morton, M.; Fetters, L.J. *J. Rubber Chem. Technol.*, **1975**, 48, 359.

17. Langer, A.W. *Polym Prepr. (Am. Chem. Soc.,Div. Polym. Chem.)*, **1966**, 7(1), 132.

18. Halasa, A.F.; Lohr, D.F.; Hall, J.E. *J. Polymer Sci. Polymer Chem. Ed.*, **1981**, 19, 1375.

19. Lee, L-H. *Adhesion Science and Technology*, **1975**, 9A, Plenum Press: New York, 199.

20. Chung, T.C.; Ramakrishnan, S.; Berluche, E. *Macromolecules*, **1990**, 23, 378.

21. Chung, T.C; Rhubright, D. *Macromolecules*, **1991**, 24, 970.

22. Chung, T.C.; Janvikul, W.; Bernard, R.; Jiang, G.J. *Macromolecules*, **1994**, 27, 26.

23. Chung, T.C. *Macromolecules*, **1988**, 21, 865.

24. Chung, T.C.; Raate, M.; Berluche, E.; Schulz, D.N. *Macromolecules*, **1988**, 21, 1903.

25. Chung, T.C. *Contemporary Topics in Polymer Science*, Plenum Press: New York, **1989**, 6, 315.

26. Mochel, V.D. *Rubber Chem. Technol.*, **1967**, 40, 1200.

27. Hummel, D.O. *Polymer Spectroscopy*, Verlag Chemie GmbH: Weinheim, **1974**.

CHAPTER V

ADHESION STUDIES OF POLY(STYRENE-*B*-1,2-BUTADIENE) AND POLY(STYRENE-*B*-4-HYROXYBUTENE)

Introduction

At the molecular level, adhesive bonding occurs by the formation of primary bonds, donor-acceptor bonds, and/or secondary bonds across the interface between the adhesive and substrate. These different bonds have different bond energies, and therefore it would predicted that they should exhibit different adhesive energies. However, the measured adhesion does not always correlate with the adhesive energy predicted from molecular bonds. When sufficient adhesion occurs, dissipative irreversible processes are activated during debonding and these processes inflate the measured adhesion.[1,2]

Designing adhesives that allow controlled small-scale dissipation can effectively improve adhesion, but a disadvantage is that the measured adhesion becomes dependent on the adhesion test rate, temperature, and geometry.[3-5] The addition of rubber to epoxy has been shown to effectively improve it's adhesive properties by dissipative type mechanisms.[6,7] Bascom has shown that the adhesive fracture energy of a diglycidyl ether of bisphenol A (DGEBA) type epoxy to aluminum could be increased from 154 J/m^2 to 2250 J/m^2 by the addition of 15% carboxy-terminated butadiene-acrylonitrile (CTBN) rubber.[8]

Much experimental and theoretical work as been conducted investigating the properties of rubber-toughened epoxies, but debate over the macroscopic and microscopic dissipative mechanisms still exists.[7] Early studies of the molecular structure of butadiene-acrylonitrile (BN) rubber modified epoxy showed that polar end-groups on the BN rubber were necessary for adhesion to the epoxy. The optimal properties resulted when epoxied groups in the epoxy were reacted with the carboxy terminal groups of the CTBN rubber forming an alternating block copolymer that precipitated as a rubber domain during curing.[9] Recent investigations have shown that butadiene-acrylonitrile rubbers without functional end groups could toughen epoxy, under certain conditions, almost as well as CTBN.[7] These results are supported by recent developments in the toughening of incompatible polymer interfaces by block copolymers.[10-13]

The adhesive fracture energies between two incompatible homopolymers has been shown to dramatically increase by the addition of block copolymers.[10-13] To reduce the overall free energy, the block copolymer will tend to segregate at the interface and organize with each of its blocks mixed with a compatible or nearly compatible homopolymer. The adhesive fracture energy was found to be dependent on the degree of polymerization of each block, the areal density of block copolymer chains at the interface, the average degree of polymerization between entanglements of the two homopolymers,[12] and the phase angle of loading (mode I/II).[5] The experiments also quantitatively developed the relationship between the measured fracture energy and the fracture mechanism. These well controlled experiments provide the infrastructure for studying polymer functionality and the effect of different types of molecular bonding on adhesion,

which would advance the understanding toughening mechanisms in rubber toughened epoxies.

The adhesion of polymer-polymer interfaces has been shown to be increased by the addition of block copolymers where each segment diffuses into its like homopolymer. These interfaces are very diffuse and adhesion can be enhanced by chain entanglement between the block copolymer segment and the polymer matrix.[10-13] The adhesion of block copolymers at sharp (non-diffuse) interfaces was investigated by Widmaier and Meyer.[14] The adhesion of poly(styrene-b-isoprene) (SI) diblock and SIS triblock copolymers to glass was measured by the lap-shear test as a function of molecular weight and % isoprene. The effect of donor-acceptor bonding was studied by incorporating maleic anhydride groups onto the double bonds of the isoprene blocks. In certain regimes, the donor-acceptor bonding increased the adhesion to glass.[14] The adhesive fracture energies, nor the mechanisms of failure were investigated.

These block copolymer adhesion experiments parallel the polymer adsorption experiments of "sticky foot" (SF) polymers by Kendall.[15,16] Under proper conditions, block copolymers have one block which has a very high surface/segment interaction energy (χ_s) which adsorbs flat on the surface, while the other block has a low surface/segment interaction energy and remains in solution[17] or matrix[18]. The block with the high surface/segment interaction energy is designated the SF. Poly(styrene-*b*-4-hydroxybutene) adsorbed to glass or alumina from solution showed that the amount and structure of adsorbed polymer was effected by molecular weight, % SF, solution concentration, and location of the SF on the polymer backbone.[15,16] It would be predicted

from molecular bonding and the results of the adsorption experiments from solution that polar SF blocks would increase the adhesion to a polar substrate where strong donor-acceptor bonding could occur.

The objectives of this chapter are to investigate the adhesion of SF block copolymers at sharp and diffuse interfaces. First, the double-cantilever-beam test (DCB) and tapered double-cantilever-beam (TDCB) test will be reviewed as methods to measure adhesive fracture energies. Then the effect SF adsorbing segments have on adhesion at sharp interfaces (sharp relative to diffusive polymer-polymer interfaces) will be investigated by measuring the adhesive fracture energy of polystyrene (PS), poly(styrene-*b*-1,2-butadiene) (PS-B), and poly(styrene-*b*-4-hydroxybutene) (PS-OH) to aluminum by the TDCB test. The goal was to develop a relationship between adsorption and adhesion properties. Adhesion at diffuse interfaces was investigated by measuring the adhesive fracture energy of PS, PS-B, and PS-OH to epoxy by the TDCB test. These model studies were used to gain insight on toughening mechanisms in rubber-toughened epoxies. The adhesion of epoxy to a thick spandex layer (the spandex layer was actually knitted spandex fibers) was also investigated to study the use of alternative rubber toughening mechanisms

Experimental

General

The polystyrene (PS), poly(styrene-*b*-1,2-butadiene) (PS-B) and poly(styrene-*b*-4-hydroxybutene) (PS-OH) synthetic routes were described in Chapter IV. The epoxy used for the adhesion tests was Epon 828, a diglycidyl ether of Bisphenol A type epoxy, with

V-40 curing agent, an oligomeric diamine, mixed in a ratio of 2:1 (by weight). Both are products from Shell Chemical Company. The aluminum beams used were alclad 2024, T3 temper, with a mill finish. The steel beams used were stainless steel. All adhesion tests were run at ambient conditions on an Instron Tensile Tester at 0.2 cm/minute. The equations used to calculate adhesive fracture energies for the DCB tests will be discussed. The equation used to calculate the adhesive fracture energy with the TDCB test was:[19,20]

$$G_c = (4P_c^2 m)/Eb^2)$$

where P_c is the critical load for crack growth, m is the taper of the beams ($m=3a^2/h^3 + 1/h = 1.165\ m^{-1}$), E is the modulus of aluminum, and b is the width of the beams.

Surface Pretreatment of Metal Beams

The beam surfaces were treated so that reproducible adhesion tests could be obtained. Two different surface pretreatments were investigated for the aluminum beams. Method A consisted of using a solvent to remove any visible polymer on the surface, then the beams were washed with soap, rinsed with hot water, then hot air dried with a heat gun. Method B was modeled after ASTM D2651-79. The beams were first sanded with 100 grit sandpaper, then solvent washed by placing in THF at 68°C for 20 minutes. The beams were then oxidized by placing in a solution of 300 ml distilled water, 54 ml concentrated sulfuric acid, and 10 grams sodium dichromate. The beams were oxidized for 10 minutes at 68°C, washed with warm water, washed with distilled water, then dried 1-3 days at 70°C under a continuous flow of dry air. (Notebook #5 p.87)

Adhesion of Epoxy to Aluminum and Steel Measured by the Double-Cantilever-Beam (DCB) Test

This test was modeled after ASTM D3433 (see Figure 3.1). Two aluminum or steel beams each 2.54 cm wide, 1.27 cm thick, 35.6 mm long, and surface treated by method A were blade coated with epoxy, which had been centrifuged to remove air bubbles. PCTFE spacers, 2.5 cm x 2.5 cm x 0.025 cm were inserted at each end of the beams to maintain constant epoxy thickness and act as a precrack. The epoxy was cured 7 days at ambient conditions. (Notebook #5 p.10, 30)

Adhesion of Epoxy to Aluminum Measured by the Tapered Double-Cantilever-Beam (TDCB) Test

The aluminum beams were tapered as described in ASTM D3433 (see Figure 3.2), the beams were 24.13 cm long, 2.54 cm wide, and the taper was from 1.27 cm to 3.175 cm over a distance of 14.498 cm. The aluminum surface was treated by method A and the epoxy was cured at ambient conditions for 7 days, or the aluminum surface was treated by method B and the epoxy cured 7 hours at ambient conditions then cured 14 hours at 65°C. Before curing, spacers 2.5 cm x 2.5 cm x 0.025 cm were inserted at each end of the beams to maintain constant epoxy thickness and act as a precrack. (Notebook #5 p.38, Notebook #8 p.50)

Adhesion of Polystyrene (PS) to Aluminum

The adhesion of polystyrene to aluminum was measured by the TDCB Test. The beams were surface treated by method B. The PS used was 112,000 g/mol with a PDI of 1.02. PS (0.19 gms) was dissolved in 4 ml of MEK/THF solution (10% THF). 2 ml of

solution was coated onto one face of each beam, the beams were then vacuum dried 1 hour at 70°C. The beams were then put together and annealed at 138°C or 169°C for 12 or 22 hours under vacuum or nitrogen. (Notebook #5 p.88-100)

Adhesion of Poly(styrene-*b*-1,2-butadiene) (PS-B) to Aluminum

The Adhesion of PS-B to aluminum was measured by the TDCB Test. The beams were surface treated by method B. The PS-B polymers studied were PS-B30 (53% butadiene, 168k g/mol), PS-B20 (27% butadiene, 144k g/mol), and PS-B10 (15% butadiene, 147k g/mol). The polymers were applied to the beams, dried, annealed, and tested the same as above for PS. (Notebook #5 p.88-100)

Adhesion of Poly(styrene-*b*-4-hydroxybutene) (PS-OH) to Aluminum

The adhesion of PS-OH to aluminum was measured in the same manner as above. The polymers studied were PS-OH30, PS-OH20, and PS-OH10, all from their corresponding PS-B's. (Notebook #5 p.88-100)

Adhesion of PS, PS-B, and PS-OH to Epoxy Measured by the TDCB Test

The tapered aluminum beams were surface treated by method B. The PS, PS-B, and PS-OH polymers tested were the same as above. The polymer (0.19 grams) was dissolved into 4 ml of 10% THF/MEK. 2 ml of solution was coated onto the face of each beam then dried/annealed 8 hours at 138°C under vacuum. After the beams were allowed to cool overnight the polymer surface was coated with epoxy and the beams were put together after inserting a 2.5 cm x 2.5 cm x 0.0127 cm spacer at each end of the beams to maintain constant epoxy thickness and act as a precrack. The epoxy was cured 7 hours at

ambient conditions then post cured at 65°C for 4 or 15 hours. The beams were cooled at least 3 hours before testing. (Notebook #8 p.5-30)

Adhesion of Epoxy Filled with PS-B

The tapered aluminum beams were surface treated by method B. PS-B30 (0.19 gms) was dissolved into 3 ml of THF, then 3 gms of Epon 828 was added to the solution. The THF was then removed with vacuum. V-40 curing agent (1.5 gms) was added and the solution was stirred until a homogeneous mixture resulted. The epoxy/PS-B mixture was coated onto the beams then the beams were put together after inserting a 2.5 cm x 2.5 cm x 0.0127 cm spacer at each end of the beams to maintain constant epoxy thickness and act as a precrack. The epoxy was cured 7 hours at ambient conditions then post cured at 65°C for 15 hours. The beams were cooled at least 3 hours before testing. (Notebook #8 p.47)

Spandex Epoxy Adhesion Measurement via the DCB Test

The steel beams used in the epoxy adhesion tests were surface treated by method A then coated with epoxy. A spandex fiber knit (from DuPont) was placed between the beams and cured 7 days at ambient conditions. (Notebook #3 p.133)

Results and Discussion

Aluminum Epoxy Adhesion Measured by the DCB Test and TDCB Test

The aluminum-epoxy adhesive fracture energy was measured using the DCB test. The fracture energy (G_c) can be calculated using the general equation (equation 1) assuming only that force vs. displacement is linear.[21]

$$G_c = (P_c^2/2b)(dC/da) \qquad (1)$$

P_c is the critical force for crack growth, the width is b, and dC/da is the change in compliance with the change in crack length. Figure 5.1 shows a typical DCB test force-displacement diagram. The fracture energy to epoxy calculated using the general equation was 149.6 J/m^2 with a standard deviation of 42.7 J/m^2. The ASTM standard test (D3433) makes the assumption that simple beam theory is valid and that the compliance can be related to the modulus by the equation:[21]

$$C = v/P = 8a^3/Eh^3b \qquad (2)$$

where C is the compliance, v is the opening displacement at force P, a is the crack length, E is the modulus (E=72.4 GPa for aluminum and 200 GPa for steel), h is the beam thickness, and b is the width. Substituting equation (2) into the general equation, another expression for the fracture energy can be derived.

$$G_c = (12P_c^2a^2)/(Eb^2h^3) \qquad (3)$$

Using equation (3) the fracture energy to epoxy was calculated to be 106.1 J/m^2 with a standard deviation of 27.4 J/m^2. Note that the contributions due to shear are neglected because they were found to be less than 2 J/m^2. Mostovoy and Ripling[19] found that beam theory was not valid by measuring the force vs. displacement for clamped beams, and then calculating the crack length from equation (2). They found that the calculated crack length was larger than the measured crack length by a factor, a_0. This showed that simple beam theory is not completely valid for the DCB Test due to rotations past the crack tip. To circumvent this problem the "effective crack length" term, a_0, was introduced to equation (3) and the fracture energy becomes:

$$G_c = 12P_c^2(a-a_0)^2 / Eb^2h^3 \qquad (4)$$

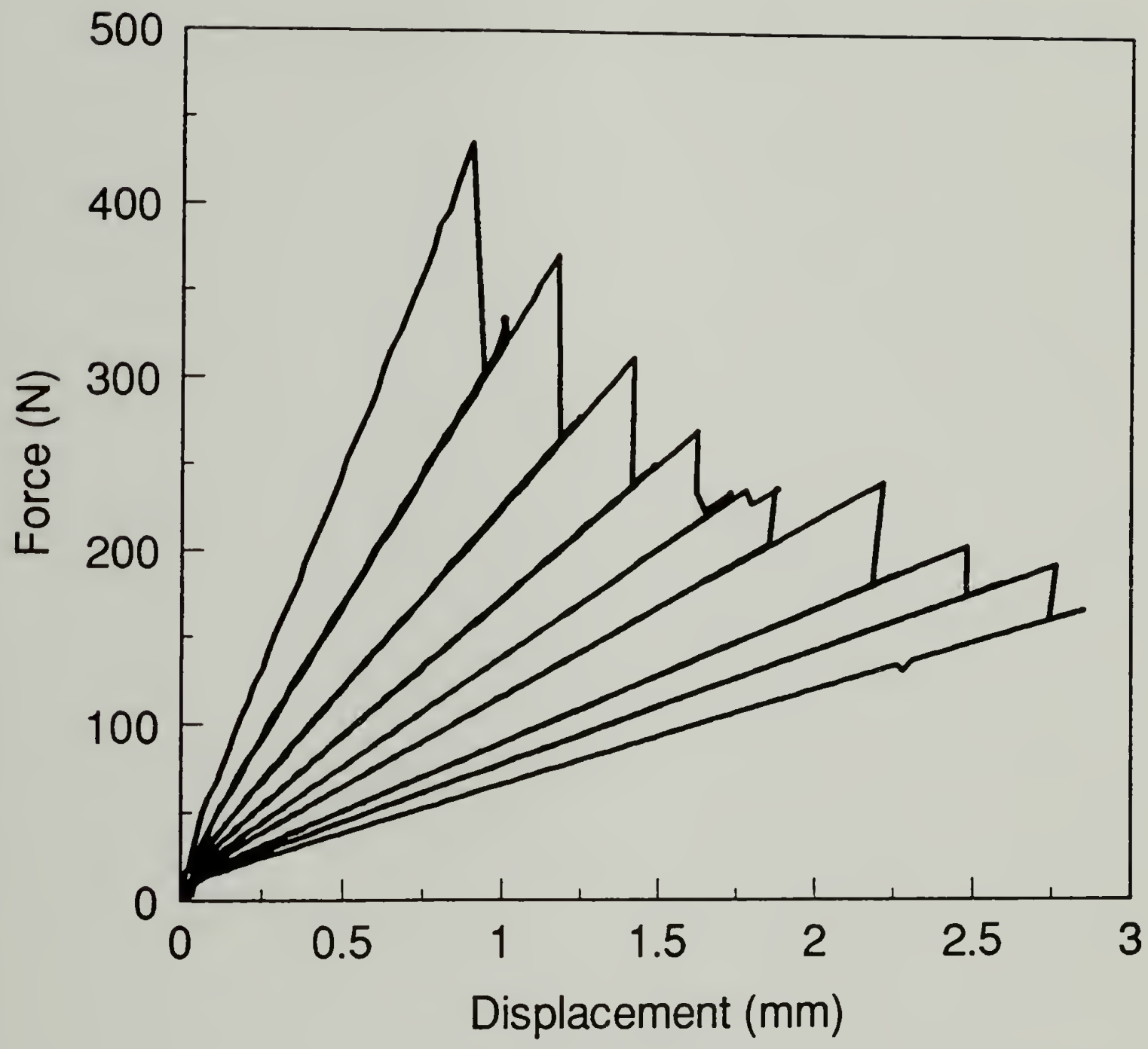

Figure 5.1 Force vs. displacement for the epoxy-aluminum DCB test.

The "effective crack length", a_0, was determined experimentally for this system by measuring the force vs. displacement of the clamped aluminum beams and found to be 35.7 mm. Using equation (4) the fracture energy was calculated to be 179.7 J/m^2 with a standard deviation of 28.1 J/m^2. The fracture energy can also be measured using the area method described by Whitney.[22]

$$G_c = (P_1 v_2 - P_2 v_1) / 2b(a_2 - a_1) \qquad (5)$$

P_1 and v_1 are the critical load and opening displacement at crack length a_1 to grow a new crack, a_2. Using equation (5) the fracture energy was found to be 148.1 J/m^2 with a standard deviation of 45.0 J/m^2.

These results show that even though the same test and in some cases the exact same data was used to calculate the adhesive fracture energy using the DCB test, the calculated fracture energy varied from 106.1 J/m^2 to 179.9 J/m^2 depending on the equation used. However, the variability was to high to infer real differences between the tests. Adhesive fracture energies were also measured using the TDCB test. The TDCB test assumes simple beam theory and also assumes $a^2/h^3+1/h$ is a constant m, which means that the fracture energy is independent of crack length.[19,20] Figure 5.2 shows experimentally that the critical load, and therefore the fracture energy, was independent of crack length for adhesion measurement between epoxy and aluminum. Using the TDCB test the aluminum epoxy fracture energy (aluminum surface treated by method A) was calculated to be 121.2 J/m^2 with a standard deviation of 11.7 J/m^2 (Figure 5.2), which agrees well with the DCB test when the general equation is used. This data showed that the TDCB test was an experimentally advantageous test because of its good comparison to the DCB

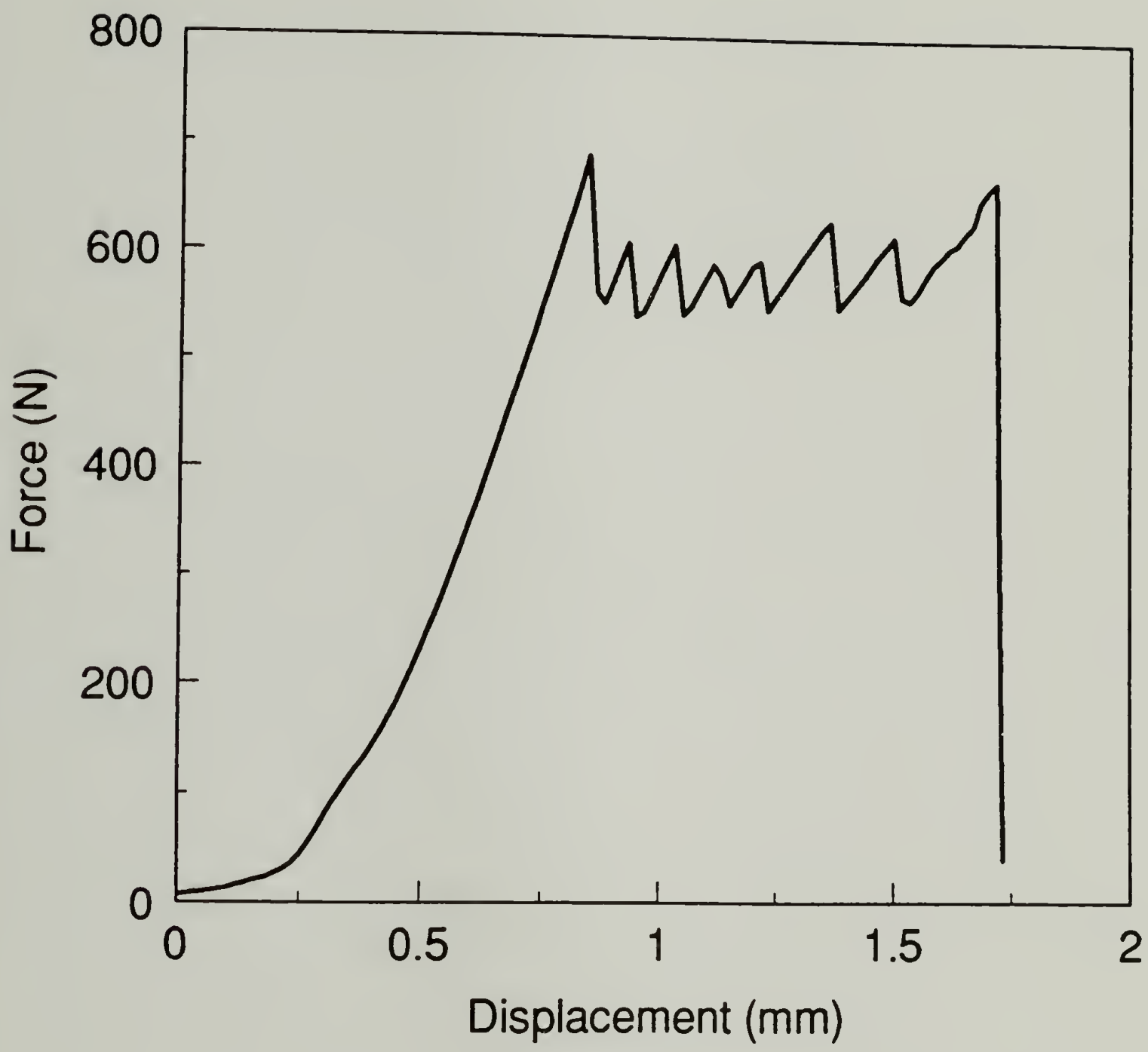

Figure 5.2 Force vs. displacement for the epoxy-aluminum TDCB test.

test, its experimental ease, and lower standard deviation. When the tapered beams were surface treated by method B and cured 7 hours at ambient conditions then 14 hours at 65°C, the fracture energy was 119.0 J/m^2. This showed that the alternative surface pretreatment and curing procedure had little effect on the measured aluminum-epoxy fracture energy.

The adhesive fracture energy was measured between epoxy and steel using the DCB test. The fracture energy was calculated using equation (3) and found to be 132.1 J/m^2 with a standard deviation of 48.1 J/m^2.

The measured adhesive fracture energies of epoxy using the DCB test was highly variable and depended more on the equation used to calculate G_c than the beam composition, surface pretreatment, or curing conditions. The failure after fracture in all cases was cohesive in the epoxy, which explains why the fracture energy is not dependent on the beams treatment or composition. The fracture energies measured are in close agreement with those reported by Bascom, considering a different curing agent was used.[8] The TDCB test was found to be the most useful test for measuring adhesive fracture energies because of its low experimental variability.

Adhesion of PS, PS-B, and PS-OH to Aluminum

The adhesion tests of PS, PS-B, and PS-OH to aluminum using the TDCB test were all problematic. All samples tested exhibited excellent adhesion to the aluminum. The force required for crack propagation was high and the failure was cohesive in the polymer. The force required for crack growth was not independent of crack length (Figure 5.3), this makes the equation for calculating fracture energies from the TDCB test

invalid. There was considerable scatter in the forces required for crack growth, making the test irreproducible. Table 5.1 reports the adhesion as the force required for crack growth. Various annealing conditions were investigated to eliminate the scatter in the measured forces for crack propagation, but this was unsuccessful. Figure 5.3 shows a typical force-displacement diagram for PS-B10 and PS-OH10. It is important to note in Figure 5.3 that their was no real difference in the force required to cause crack propagation between PS-B and PS-OH. Because adhesion of the styrene block and the scatter in the data was so high, the effect of the SF block to aluminum could not be evaluated.

Adhesion of PS, PS-B, and PS-OH to Epoxy

The PS-B and PS-OH block copolymers showed a substantial increase in adhesion to epoxy over PS homopolymer. Figure 5.4 shows at typical force-displacement TDCB test diagram. It was observed from the diagrams that the force for crack growth was independent of crack length. Figure 5.4 also shows that the failure between the epoxy and PS-B was more ductile, whereas the failure for the PS-OH and PS was more brittle. Stress-whitening and plastic deformation in the PS-B layer could be observed visually after fracture for polymers with high butadiene content. Figure 5.5 shows the effect of fracture energy on % Sticky Foot and Table 5.2 shows the effect of cure conditions on the fracture energy. The increase in the adhesive fracture energy closely parallels that of rubber toughened epoxies. The layer of PS-B has fracture energies almost identical to those of epoxy filled with carboxy-terminated butadiene-acrylonitrile elastomers with the same rubber content.[23] The PS-OH contains functional groups that interact stronger

Table 5.1 Adhesion of PS, PS-B, and PS-OH to aluminum.

Sample	Annealing Conditions			Force for Crack Growth
	hours	°C	cond.	newtons
PS	12	138	vac.	1180
PS	22	138	vac.*	2450
PS	22	169	vac.	390
PS-B53	12	138	N_2	390
PS-B53	22	138	vac.*	740
PS-OH53	22	138	vac.*	150
PS-B27	12	138	vac.	880
PS-B15	12	138	N_2	490, 740
PS-B15	12	138	vac.	1080
PS-B15	22	169	vac.	690, 1080
PS-OH15	12	138	N_2	980, 690
PS-OH15	22	169	vac.	880, 1080

* denotes that these samples were annealled under compression

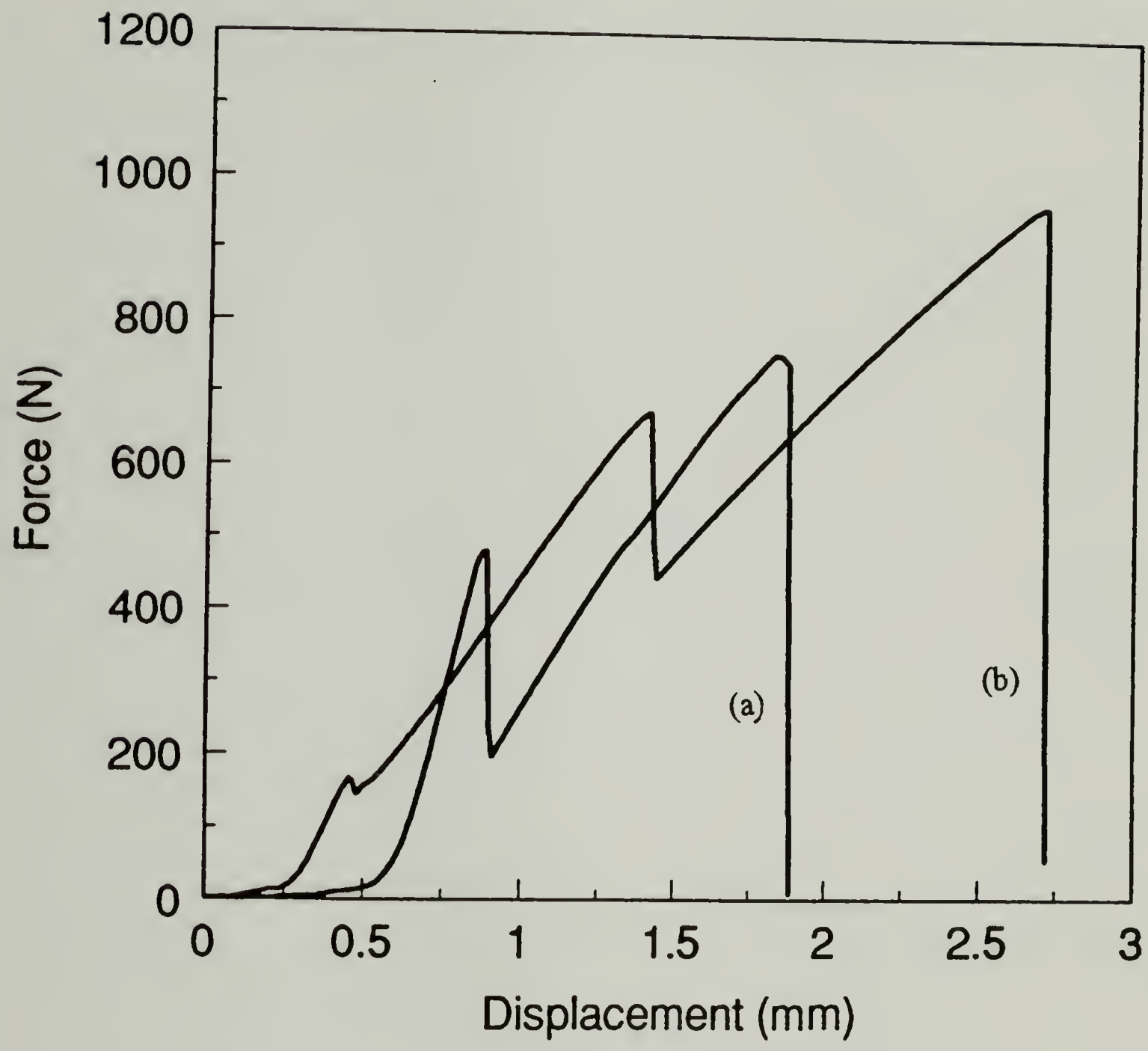

Figure 5.3 Force vs. displacement for the (a) PS-B15 and (b) PS-OH15 adhesion to aluminum by the TDCB test.

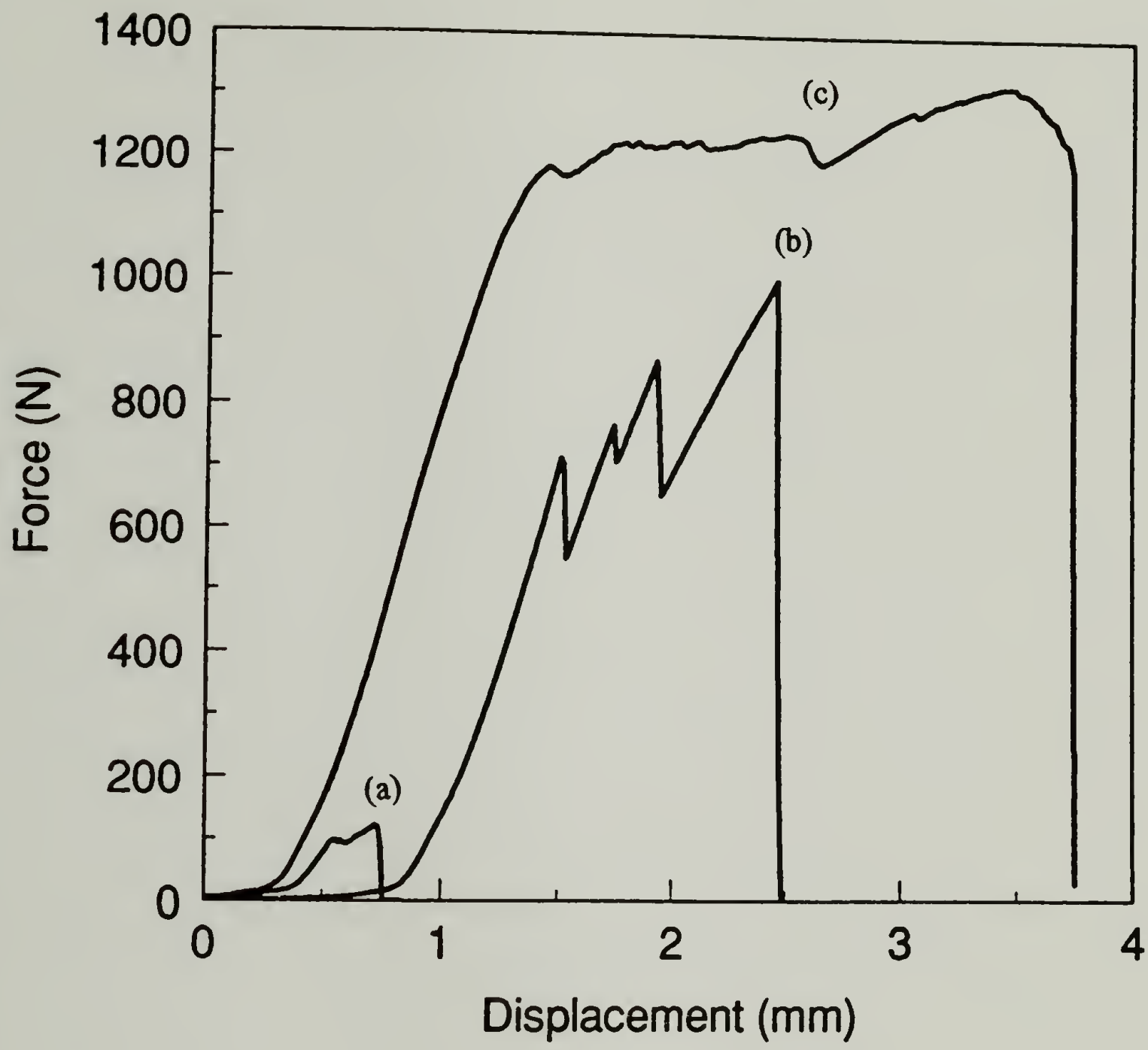

Figure 5.4 Force vs. displacement for (a) PS, (b) PS-OH20, and (c) PS-B20 adhesion to epoxy by the TDCB test.

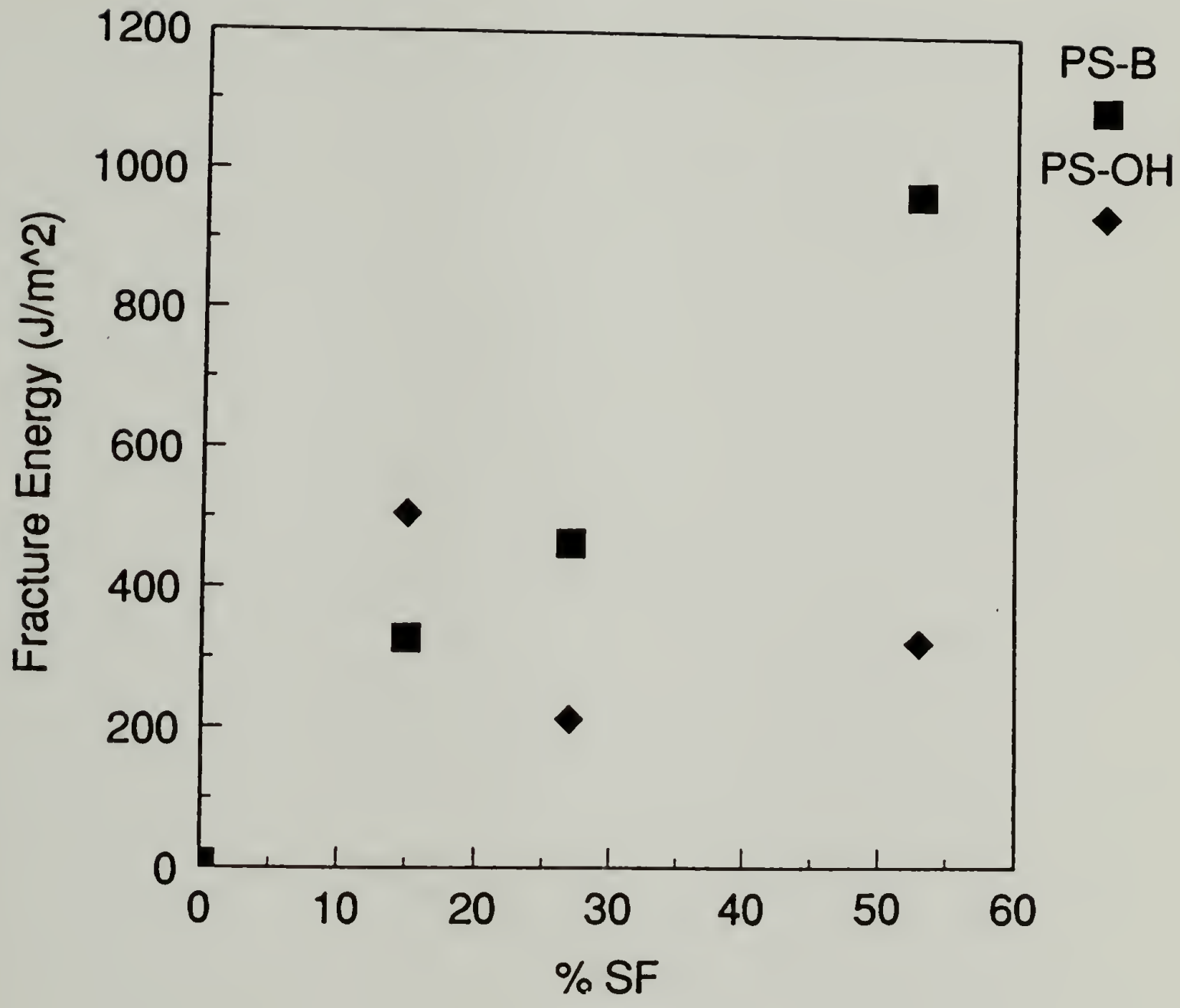

Figure 5.5 Adhesive fracture energy of PS-B and PS-OH to epoxy measured by the TDCB test as a function of SF content, SF being %B or %OH.

Table 5.2 Adhesive fracture energies of PS, PS-B, and PS-OH to epoxy.

Sample I.D	%Butad. by NMR	Epoxy Curing Conditions		Fracture Energy (J/m^2)
		Temp.(°C)	Time (hr)	
PS	0	60	4	10
PS	0	66	14	4
PS-B30	53	60	4	831
PS-B30	53	69	15	968
PS-OH30	53	60	4	447
PS-OH30	53	69	15	322
PS-B20	27	66	16	462
PS-OH20	27	66	14	212
PS-B10	15	69	15	327
PS-OH10	15	69	15	505

molecularly with the epoxy than butadiene groups because hydroxy groups can bond by stronger donor-acceptor interactions. The PS-OH, however, does not exhibit as high fracture energy to the epoxy except at very low %SF contents. Studies of poly(styrene-isoprene) block copolymers show that the polymer organizes with the isoprene segment at the polymer-air interface.[24] This data and the fracture data gives evidence that the butadiene diffuses into the epoxy, forming chain-entanglements which act as an effective energy dissipation mechanism.[10-13] Likewise, the PS-OH shows poor adhesion, not

because of weaker molecular interactions, but because the SF segment cannot diffuse into the epoxy and dissipate energy as effectively.

PS-B dissolved into the epoxy showed similar fracture behavior as when the PS-B was coated onto the aluminum beams then coated with the epoxy (Figure 5.6). This supports the assumption that coating the aluminum beams with the block copolymer for basic investigations on toughening mechanisms in rubber-toughened epoxies is valid.

Spandex Epoxy Adhesion via the DCB Test

Figure 5.7 shows the force-displacement diagram for spandex knit-epoxy using steel double-cantilever-beams. Because the spandex interlayer consisted of knitted fibers, the fibers were able to deform axially and no discrete crack growth occurred, so fracture energies were not calculated. The force and displacements for failure, and therefore the energy for failure, where much greater with the spandex layer than with just epoxy. The adhesion between the epoxy and spandex was sufficient such that the energy went into stretching the spandex fibers, expending energy like the above mentioned block copolymers but on a much larger scale. This allowed for a greater amount of energy required for separation.

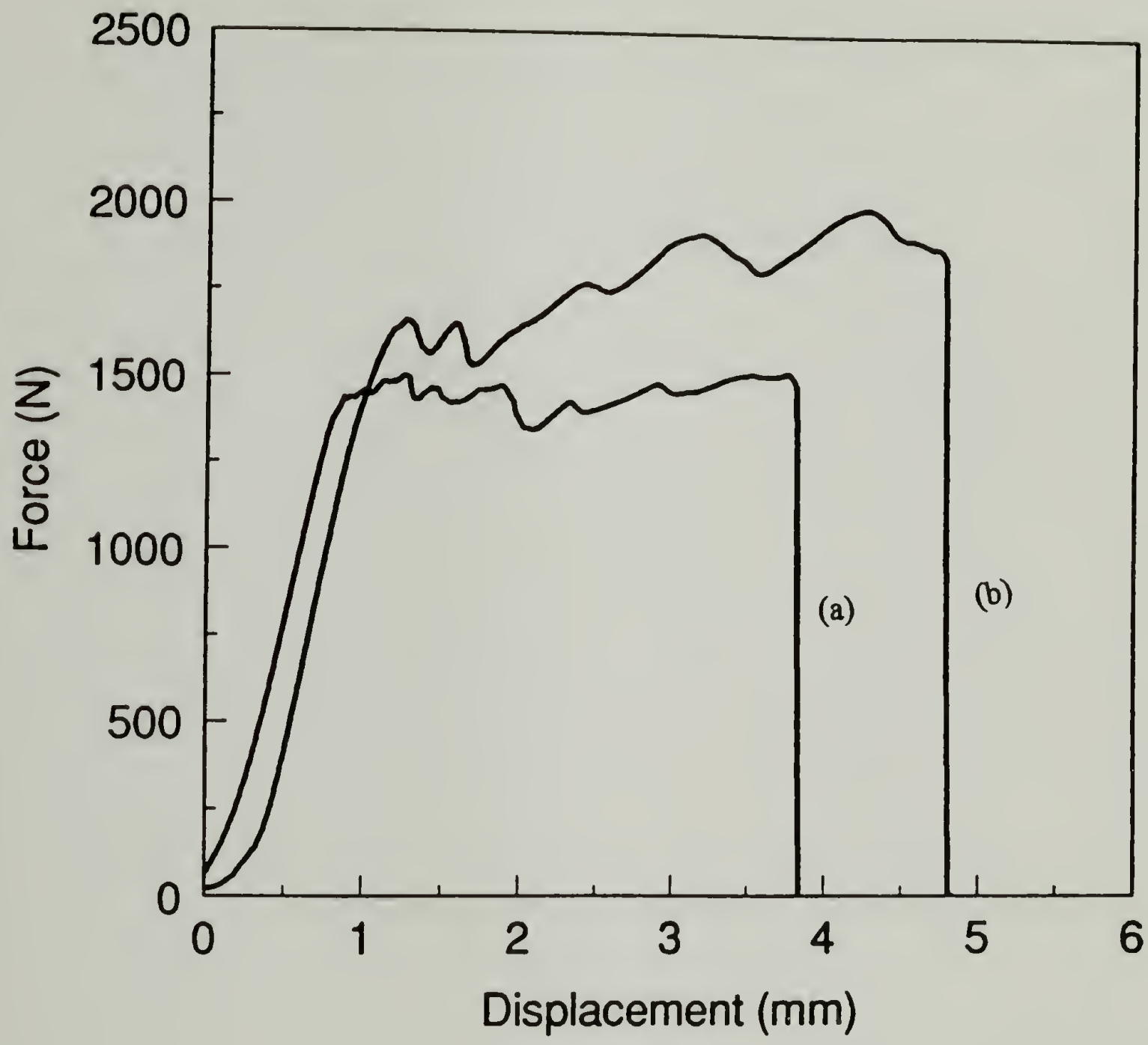

Figure 5.6 Force vs. displacement for adhesive fracture between epoxy and aluminum by the TDCB test toughened by (a) PS-B30 dissolved into the epoxy and (b) PS-B30 coated onto the aluminum before coating with epoxy.

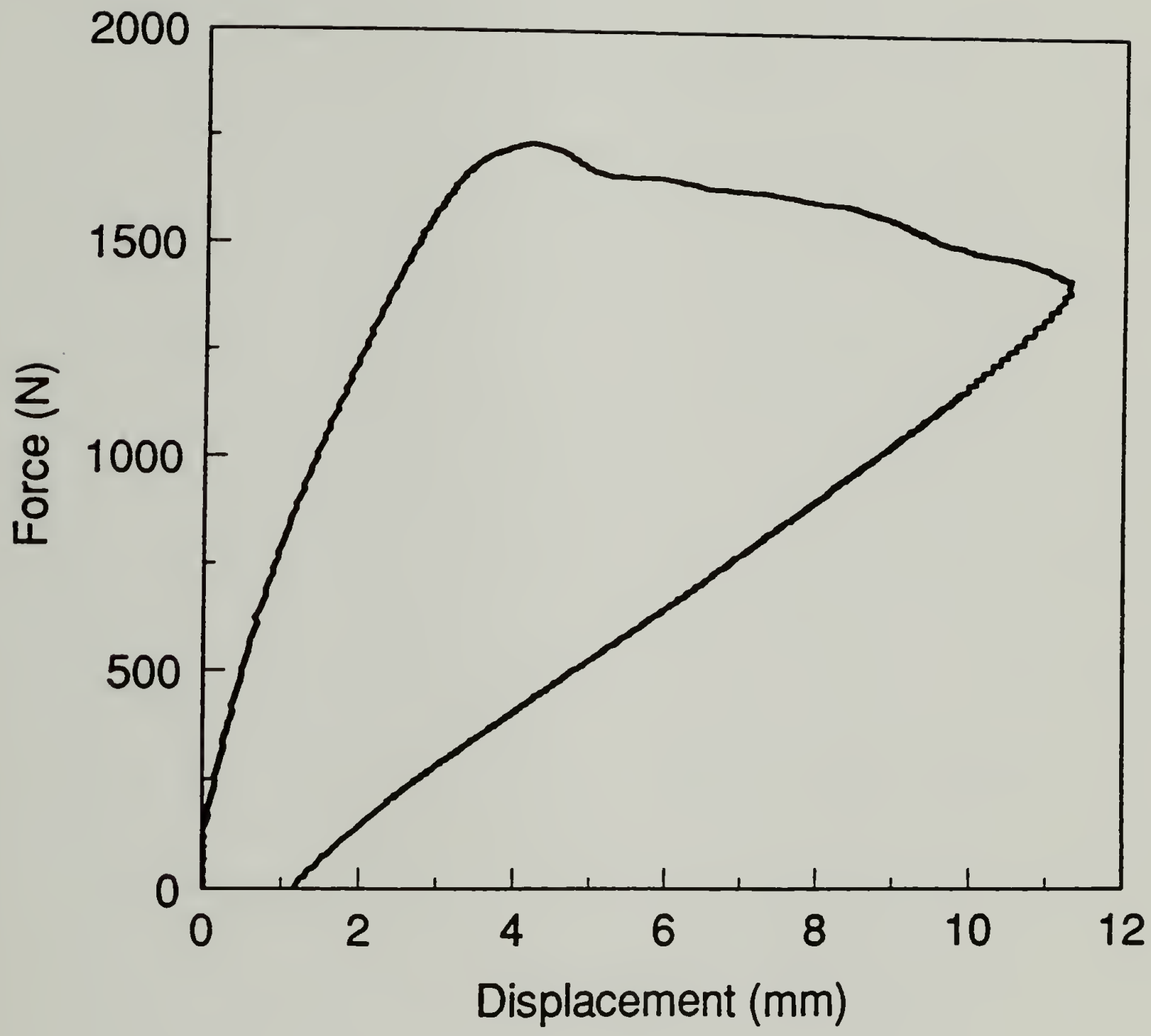

Figure 5.7 Force vs. displacement for adhesion of epoxy to steel by the DCB test with a spandex interlayer.

Conclusions and Future Work

The adhesion of SF polymers to aluminum had no effect compared to polystyrene alone. This system did not parallel SF polymer adsorption because the polystyrene exhibited good adhesion to aluminum. A better system would be one in which the polystyrene exhibited poor adhesion to the substrate. PS-B and PS-OH showed an increase in adhesion with increased SF block size. A plateau value was not obtained with SF blocks as high as 53%, however, one would predict a decrease in adhesion at very high SF because polybutadiene is a viscous liquid at room temperature. PS-OH did not show as good adhesion as PS-B. Even though -OH groups can molecularly interact stronger with the epoxy than the butadiene, the butadiene groups can dissipate more energy during debonding, thus high fracture energies are measured. This similar "energy absorbing" layer could also be observed when a spandex layer was inserted into a steel-epoxy joint.

Future work would consist of better quantifying the failure after fracture, i.e. chain scission vs. chain pull-out and the size of the dissipation zone. It is also possible that the -OH groups could not diffuse into the epoxy at the cure temperatures used, thus making a sharper interface. Curing profiles and TEM studies should be conducted to investigate the effect of the depth of diffusion into the epoxy on fracture properties.

Experiments conducted measuring the epoxy fracture energy by the DCB Test showed that care needs to be taken when interpreting these results. The calculated fracture energy varied with the equations used so one must fully understand the assumptions used and the limitations of these equations. The TDCB test proved to be an experimentally simpler test with lower variability than the DCB test. This lower variability

is most likely due to the elimination of the need to measure the crack length. The adhesive fracture energies of epoxy to aluminum measured by the TDCB test were comparable to the DCB test and previously reported literature values. However, the TDCB test was found to be unsuitable for measuring fracture energies between polystyrene and aluminum. This result reinforces the point that care must be taken to choose the proper adhesion test for the materials being evaluated.

References

1. A.J. Kinloch *Adhesion and Adhesives*, Chapman and Hall: New York, **1987**.

2. Wu, S. *Polymer Interface and Ahesion*, Marcel Dekker, Inc.: New York, **1982**.

3. Andrews, E.H.; Kinloch, A.J. *Proc. R. Soc. Lond.A.*, **1973**, 332, 385.

4. Gledhill, R.A.; Kinloch, A.J. *Polymer Eng. Sci.*, **1979**, 19(2), 82.

5. Xiao, F.; Hui, C-Y.; Washiyama, J.; Kramer, E.J. *Macromolecules*, **1994**, 27, 4382.

6. Riew, C.K.; Gillman, J.K. *Rubber-Modified Thermoset Resins*, Advances in Chemistry Series 208, American Chemical Society: Washington, D.C., **1984**.

7. Riew, C.K.; Kinloch, A.J., Ed.; *Toughened Plastics*, Advances in Chemistry Series 233, American Chemical Society: Washington, D.C., **1993**.

8. Bascom, W.D.; Cottington, R.L.; Jones, R.L.; Peyser, P. *J. Appl. Polymer Sci.*, **1975**, 19, 2545.

9. Deanin, R.D.; Crugnola, A.M. *Toughness and Brittleness in Plastics*, Advances in Chemistry Series 154, American Chemical Society: Washington, D.C., **1976**.

10. Creton, C.; Kramer, E.J.; Hui, C-Y.; Brown, H.R. *Macromolecules*, **1992**, 25, 3075.

11. Brown, H.R.; Char, K.; Deline, V.R.; Green, P.F. *Macromolecules*, **1993**, 26, 4155.

12. Creton, C.; Brown, H.R.; Deline, V.R. *Macromolecules*, **1994**, 27, 1774.

13. Creton, C.; Brown, H.R.; Shull, K.R. *Macromolecules*, **1994**, 27, 3174.

14. Goodman, I., Ed.: *Developments in Block Copolymers -2*; Elsevier Applied Science Publisher: New York, **1985**.

15. Kendall, E.W., Ph.D. Dissertation, University of Massachusetts, **1993**.

16. Kendall, E.W.: McCarthy, T.J. *Polym. Prepr. (Am. Chem. Soc. Div. Polym. Chem.)*, **1992**, 33(2), 158.

17. Marques, C.; Joanny, J.F. *Macromolecules*, **1989**, 22, 1454.

18. Shull, K.R. *J. Chem. Phys.*, **1991**, 94(8), 5723.

19. Ripling, E.J.; Mostovoy, S.; Corten, H.T. *J. Adhesion*, **1971**, 3, 107.

20. Mostovoy, S.; Ripling, E.J. *J. Appl. Polymer Sci.*, **1966**, 10, 1351.

21. Williams, J.G. *Fracture Mechanics of Polymers*, John Wiley & Sons: New York, **1984.**

22. Whitney, J.M. *J. Reinf. Plastic Comp.*, **1982**, 1, 297.

23. Riew, C.K. *Rubber-Toughened Plastics*, Advances in Chemistry Series 222, American Chemical Society: Washington, D.C., **1989**.

24. Ishizu, K.; Yamada, Y.; Fukutomi, T. *Polymer*, **1990**, 31, 2047.

CHAPTER VI

LAYER-BY-LAYER ADSORPTION OF POLY(SODIUM 4-STYRENESULFONATE) AND POLY(ALLYLAMINE HYDROCHLORIDE) ONTO GLASS

Introduction

Molecular films are currently finding applications in many areas such as integrated optics, sensors, friction-reducing coatings,[1] and electrically conducting layers.[2] Molecular films are ordered thin organic films that have thicknesses from a few nanometers (a monolayer) to several hundred nanometers. The attachment of the film to a solid substrate is usually accomplished by one of three procedures: spontaneous adsorption of molecules from a vapor environment, spontaneous adsorption of molecules from a solution environment, and forced interfacial transfer processes, such as the Langmuir-Blodgett (LB) procedure.[1]

A new technique, layer-by-layer adsorption, has been developed for constructing multilayer ultrathin films. The layered films were first built on substrates by consecutive alternating adsorption of anionic and cationic bipolar amphiphiles.[3,4] This technique was later extended to polyelectrolytes (Figure 1).[5-12]

The layer-by-layer deposition technique has certain advantages over other deposition methods such as the LB procedure, or those based on chemisorption. The LB

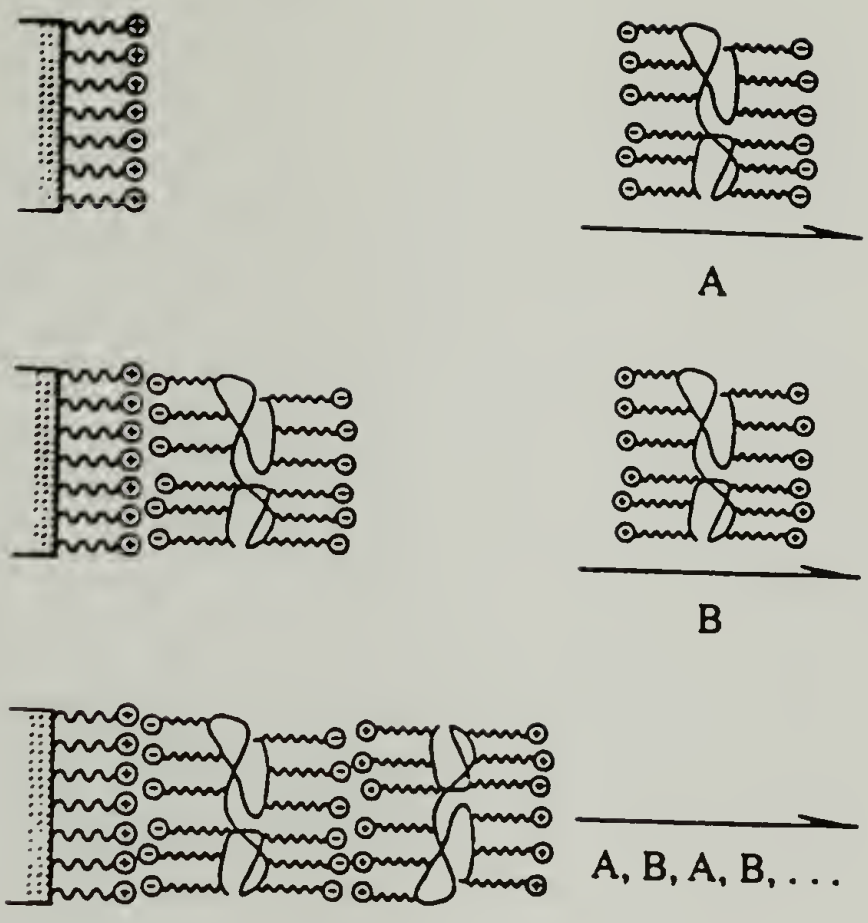

Figure 6.1 Layer-by-layer adsorption of anionic and cationic polyelectrolytes onto a solid surface.[6]

technique has produced some examples of highly organized monolayer and multilayer films, however, these films are not necessarily thermodynamically stable. Binding to the surface usually does not occur by strong chemical bonds, and only amphiphilic molecules which form assemblies at the air-water interface are suitable.[1] This technique is also rather inconvenient for automation and large scale application. Chemisorption techniques

require a 100% reaction yield or lateral cross-linking to maintain a constant surface functional density after each deposition step. The layer-by-layer deposition method utilizes electrostatic attraction between the surface and the molecules, offering the ability to build alternating molecular layers on surfaces by adsorption from solution.

In principle, any multilayer structure of molecules containing opposite charges can be built on any charged substrate. Before the alternating anionic and cationic layers can be adsorbed to the surface of a substrate, the surface must first be electrostatically charged. Many polymers, metals, and glass surfaces can be reacted with silane coupling agents containing ionizable functional groups.[13] Glass surfaces can also be charged by methane-plasma treatment.[10] The surface of gold can be electrostatically charged by the reaction of thiols or disulfides containing ionizable functional groups.[14] Multilayer films were first built onto silicon and gold using small organic molecules.[3,4] Later, alternating layers of polyelectrolytes on glass were prepared.[5,6,9,10] Recently alternating layers of (ionizable) conductive polymers have been built on silicon wafers.[7] The layer-by-layer deposition technique has been used successfully for building layers of poly(styrene sulfonate) sodium salt, poly(vinyl sulfate) potassium salt, DNA, poly(thiophene-3-acetic acid), poly(aniline sulfonate), poly(pyridium acetylene), polypyrrole, polyaniline, poly(allylamine hydro-chloride), poly[4-vinylbenzyl-(N,N-diethyl-N-methyl)-ammonium iodide], polylysine, polyuracil, and polyadenine. An attempt to adsorb alternating layers of poly(diallyl-ammoniumchloride) and poly(styrenesulfonate) sodium salt onto mica, however, was not successful. The first poly(diallylammoniumchloride) layer adsorbed but the poly(styrene

sulfonate) layer did not.[15] The authors did not suggest reasons as to why the second layer failed to adsorb, and the conditions of the experiments were not reported.

Multilayers of poly(styrene sulfonate) sodium salt (PSS) and poly(allylamine hydrochloride) (PAA) have been the most extensively characterized. A linear increase in UV absorbance at 225 nm with the number of layers indicates an increase in the amount of PSS deposited.[6] Small angle X-ray reflectivity[6] studies show a bilayer thickness of 2.27 nm (later studies showed the layer thickness varies with salt concentration in the adsorption solution[11]). Detailed neutron and X-ray reflectivity studies of PSS and PAA adsorbed at high salt concentrations show that continous molecular layers are formed with well-defined supramolecular structure.[12] The thickness of the PAA layer was found to be ~2.0 nm, and the PSS layer ~3.5 nm. The distance between the neighboring polymer chain backbones was estimated to be 1.2 nm. The layer thickness decreased upon heating due to removal of water trapped inside the multilayer structure.[5] The amount of water trapped was found to be four water molecules per styrene sulfonate repeat unit.[12]

The question arises as to what is the driving force for polyelectrolyte adsorption onto surfaces, since it is well documented that both nonionic and ionic polymers adsorb under certain conditions. Polyelectrolyte adsorption theory was developed by Van der Schee and Lyklema[16] and extended to include weakly dissociated polyelectrolytes by Evers *et al.*[17] Their theories were based on the self consistent field approaches of Scheutjens and Fleer[18] where a lattice model was used to explain the segment-substrate (χ_s) and segment-solvent (χ) interactions. The electrostatic component plays an important role, affecting polymer solution and adsorption conformations. Experimental evidence of electrostatic

attraction between a charged surface and charged adsorbing segments has been given by electrophoresis[19] and surface force measurements.[20.20] These experiments indicated that the electrostatic attraction between an oppositely charged surface and polyelectrolyte can be the driving force for adsorption. This is different from nonionic polymers where secondary bonding is the driving force for adsorption (secondary bonding may also be important in polyelectrolyte adsorption under certain conditions).

Many factors can contribute to polyelectrolyte adsorption. These factors are: (a) properties of the surface (surface area and charge density); (b) properties of the polyelectrolyte (degree of polymerization and dissociation); (c) interaction of the polyelectrolyte and surface (net adsorption energy, χ_s); (d) properties of the solution (ionic strength and polymer concentration, χ).[22] Few of these variables have been investigated in multi-layer systems. Recently, the effect of ionic strength on layer thickness was investigated by Decher.[12] He found that as the ionic strength was increased by the addition of NaCl, the layer thickness increased. This effect agrees with theory and was explained by screening of the electrostatic repulsion between the ionic groups fixed on the polyelectrolyte chain. At low salt concentrations the repulsion between ionic groups on the chain forced the chain into an extended conformation making it adsorb flat onto the surface. At higher salt concentrations the electrostatic repulsion was screened so the polymer chain assumed a more random conformation, and therefore adsorbed in a more random or "loopy" conformation. The same trend has been found by others using surface force microscopy to study polyelectrolytes adsorbed onto mica.[21.23] Dahlgren found that

the adhesion force decreased with increasing ionic strength,[23] which also indicates that the ionic strength is an important factor in the adsorption of polyelectrolytes onto surfaces.

As discussed above the layer-by-layer adsorption of polyelectrolytes has been characterized by UV-Vis spectroscopy, neutron reflectivity, and X-ray reflectivity. However, many questions remain unanswered concerning, the mechanism by which they adsorb, their solid-state properties, and the factors which contribute to these properties. The objectives of this research were to study the layer-by-layer deposition of poly(sodium 4-styrenesulfonate) (PSS) and poly(allylamine hydrochloride) (PAA) onto glass by X-ray photoelectron spectroscopy (XPS) and contact angle. Atomic compositions of the top 1.6 to 5.8 nm of the surface were determined by XPS. The effect of surface charges on wettability were determined by contact angle. The "mechanical intergrity" of these layers and their influence on adhesion was investigated by peeling a pressure sensitive adhesive (PSA) from the layered surfaces and measuring the adhesive fracture energy between glass containing adsorbed layers and epoxy. The surfaces were then examined by XPS for polymer transfer.

Experimental

General

The procedure used was adapted from that described by Decher.[6] Glass microscope slides (Fischer Scientific) were used as the substrate. The poly(allylamine hydrochloride) (Aldrich, high mol. wt.), poly(sodium 4-styrenesulfonate)(Aldrich, mol. wt. ~70,000), 3-aminopropyltriethoxysilane (Aldrich), ammonium hydroxide (Fisher),

concentrated sulfuric acid (Fisher), 30% hydrogen peroxide (Fisher), 1 N hydrochloric acid (Fisher), manganese chloride (Fisher), and methanol (Fisher) were used as received. Toluene (Fisher) was distilled from calcium hydride under nitrogen before using. The ultrapure water used for all cleaning steps and as a solvent for the adsorption steps was obtained by reverse osmosis (Milli-RO 6 Plus, Millipore) followed by ion-exchange and filtration steps (Milli-Q UF Plus, Millipore).

X-ray photoelectron spectra (XPS) were recorded using a Perkin Elmer-Physical Electronics 5100 spectrometer with Mg Kα excitation (400 W); data in Table 6.1 used an Al Kα anode. The samples charged variably during analysis, and the reported binding energies are not corrected for charging. Spectra were recorded at take-off angles of 15, 30, 45, and 75 degrees from the glass surface (some samples were also analyzed at 5 degrees). Much debate in the literature exists over the exact electron mean free paths (or escape depth) for carbon and silicon. From experimental and theoretical data, escape depths have been estimated between 0.7 and 4.4 nm.[24] For this work we will assume an escape depth for carbon and silicon to be 2.0 nm. This means that at take-off angles of 15 and 75 degrees, 95% of the signal originates from the outer 1.6 nm and 5.8 nm, respectively.

UV data was obtained using a Perkin Elmer Lambda 2 UV/Vis Spectrometer. Contact-angle measurements were obtained with a Rame-Hart telescopic goniometer and a Gilmont syringe with a 24-gauge flat-tipped needle. Aqueous buffer solutions of pH 2-12, was used as probe fluids.[25] The pressure sensitive adhesive (PSA) used for the adhesion tests was Scotch Brand #750 from 3M.

Glass Preparation

Three glass slides were placed into a Schlenk tube with glass dividers to maintain separation of the glass slides. Concentrated sulfuric acid (75 ml) and 30% hydrogen peroxide (35 ml) were added to the Schlenk tube and sonicated for 1 hour. After the glass slides were washed with water, ammonium hydroxide (100 ml), hydrogen peroxide (20 ml), and water (100 ml) were added to the Schlenk tube. The Schlenk tube was then sonicated for 30 minutes and washed with water. (Notebook #7 p.79)

Reaction of Glass Surface with 3-Aminopropyltriethoxysilane (glass-NH_2)

The glass slides were prepared for amination by rinsing with 100 ml of the following reagents: water, methanol, 50% methanol/toluene, and toluene. All transfers were done under nitrogen by cannulation. A solution of 5 ml aminopropyltriethoxysilane, in 95 ml toluene was cannulated into the schlenk tube. After reacting 20 hours, the glass slides were washed by cannulating in 100 ml of the following solvents: toluene (let soak 1 hour), toluene, 50% (by volume) toluene/methanol, methanol, and water. (Notebook #7 p.79)

Adsorption of the First Poly(sodium 4-syrenesulfonate) (PSS) Layer

PSS (0.20 grams), water (99ml), and 1 N HCl (0.5 ml) were added to a 100 ml beaker. The solution was equilibrated in an ice bath to 0°C, then a glass slide was placed into the beaker for 20 minutes. After adsorption the glass slide was removed and washed with water (3 x 100 ml). (Notebook #7 p.79)

Adsorption of Poly(allylamine hydrochloride) (PAA) Layers

The glass slide with a PSS top layer was placed into a 100 ml beaker containing the following: 0.125 grams PAA, 1.0 ml 1N HCl, 99 ml water. The PAA adsorptions were run at ambient conditions for 20 minutes. (Notebook #7 p.79-113)

Adsorption of Subsequent PSS Layers

After PAA adsorption the glass slide was rinsed with water (3 x 100 ml) and placed into a beaker containing: PSS (0.30 grams), 1 N HCl (1.0 ml), $MnCl_2 \bullet 4\ H_2O$ (20.0 grams), and water (99 ml). The subsequent PSS adsorptions were for 20 minutes at ambient conditions. (Notebook #7 p.79-113)

Adhesion of Layers to a PSA Measured by the Peel Test

A PSA-layered glass laminate was prepared by sticking the PSA to the glass (containing PSS and PAA layers) and rolling 50 times with a roller. The laminate was placed into an Instron Tensile Tester and peeled in a 180° geometry at a rate of 25 mm/min. The force for peeling was averaged over a 10 mm length and divided by the width to give an average peel energy in J/m^2. (Notebook #8 p.35-46)

Adhesion of Layers to Epoxy Measured by the Assymetric Double-Cantilever-Beam Test

Epon 828 epoxy and V-40 curing agent, both products of Shell Chemical Co., were mixed in a ratio of 2:1 by weight. The epoxy was stirred until a homogeneous mixture then centrifuged 15 minutes at 1000 rpm to remove air bubbles. The glass slides containing PSS and PAA layers, precut into 10 mm x 40 mm x 1 mm sizes, were placed into a polethylene mold with a 10 mm x 40 mm x 3 mm opening. The epoxy was poured

into the mold coating the glass slide and cured under nitrogen for 8 hours at 60°C. The adhesive fracture energy was calculated using the assymetric double-cantilever-beam (ADCB) test. The validity and use of this test has been demonstrated by Brown[26] and Janarthanan.[27] By driving a wedge into the interface until a crack propagates, the adhesive fracture energy, G_c, can be calculated using the equation:

$$G_c = (3u^2ED^3) / 8a^4[1+0.64(D/a)]^4$$

where u is the wedge thickness, E is the modulus of the epoxy (2.1 GPa), D is the thickness of the top layer, and a is the crack length. (Notebook #9 p.31)

Results and Discussion

Layer-by-layer deposition of PSS and PAA was confirmed by UV spectroscopy XPS and contact angle. UV spectra showed an increase in adsorption at 225 nm with increasing number of PSS layers. The data had a high scatter because glass absorbs in the UV region, so no quantitative information could be inferred from the UV data. UV spectroscopy has been shown to be useful for quantifying the adsorbed amount of PSS on the surface,[6] however a UV transparent substrate such as quartz should be used.

XPS spectra showed the appearence of a nitrogen (N_{1s}) peak at 401 eV, and an increase in the relative intensity of the carbon (C_{1s}) peak at 285 eV upon reaction with 3-aminopropyltriethoxysilane (Figure 6.2). The first PSS adsorption induced the appearence of a sulfur (S_{2p}) peak at 166 eV and S_{2s} peak at 230 eV in addition to a sodium Na_{1s} peak at 1072 eV and Auger peak at 264 eV. Adsorption of the first PAA layer showed an increase in the N_{1s} peak intensity but only small amounts of the chlorine counter ion (Cl_{2p})

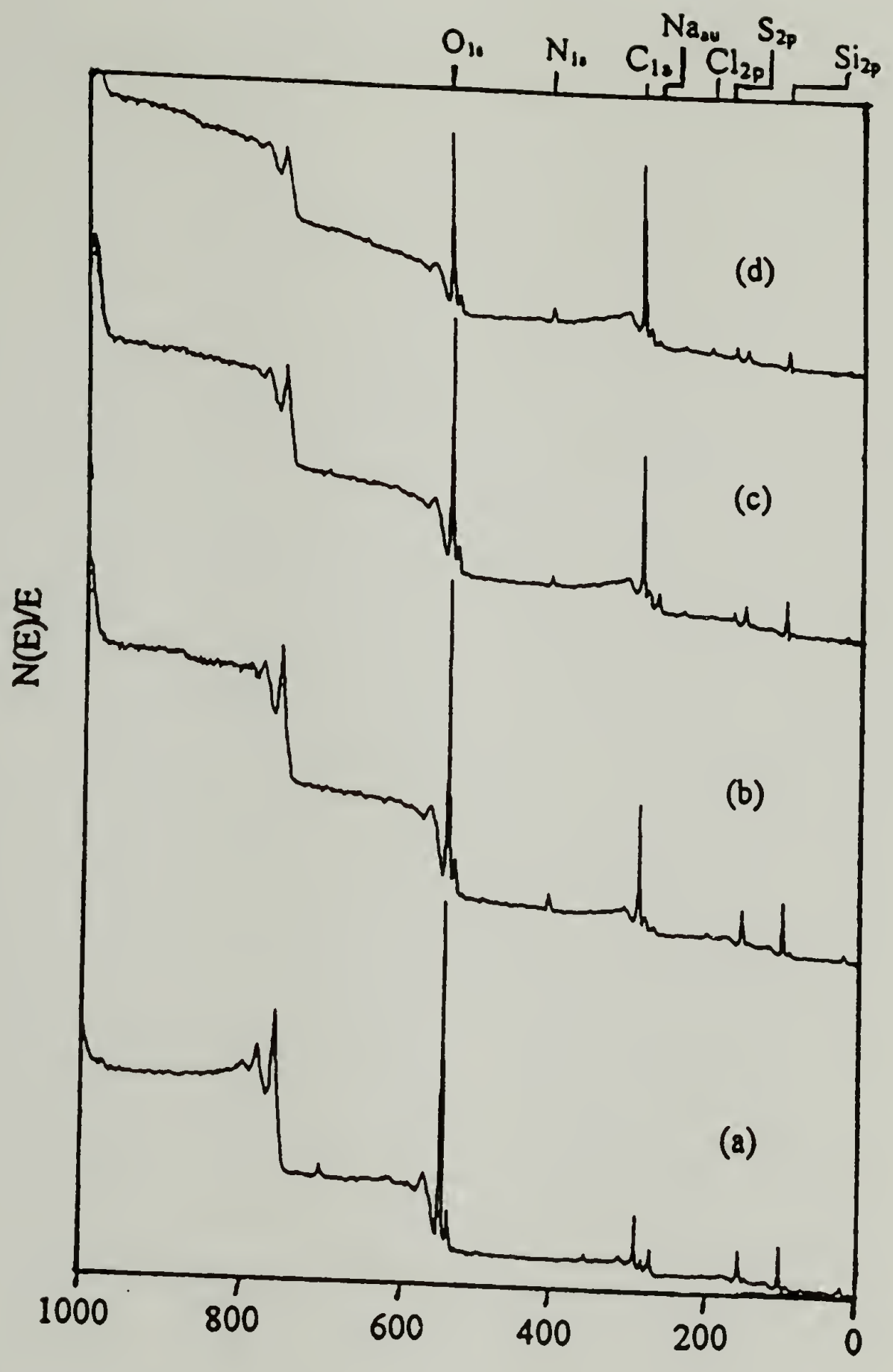

Figure 6.2 XPS survey spectra with a 15° take-off angle of (a) glass, (b) glass-NH_2, (c) glass-NH_2 with 1 PSS layer, and (d) glass-NH_2 with 1 PSS and 1 PAA layer.

peak at 200.0 eV were observed (Figure 6.2). The chlorine peak was only observed for the first PAA layer, all other PAA layers showed no chlorine, when properly rinsed. It was not clear why such little chlorine was observed. It was expected that a significant amount of ammonium chloride would be present because sodium sulfate was observed. When glass-NH_2 was converted to the ammonium chloride with dilute HCl then vacuum dried, XPS showed ~1% chlorine. This indicated that the ammonium chloride eliminated HCl during drying or during the XPS experiment due to X-ray beam damage. It would also be predicted that the electron binding energy should be different between the amine and ammonium. An attempt was made using XPS to quantify the shift in binding energy, but a statistically significant shift could not be deduced because of the low concentrations of nitrogen. The long acquisitions times required to increase the signal to noise ratio would have resulted in significant X-ray beam damage of the surface.

XPS spectra of additional PSS layers showed small manganese (Mn_{2p}) peaks at 642 and 654 eV (from the $MnCl_2$ salt residue). The Mn_{2p} peaks were only observed when PSS was the top layer, but again no chlorine was observed. The intensity of the silicon Si_{2s} peak at 153 eV and Si_{2p} peak at 102 eV decreased with increasing number of layers. Figure 6.3 shows XPS survey spectra at higher layer numbers and Table 6.1 gives representative atomic compositions of PSS and PAA layers adorbed onto glass.

From Table 6.1 it can be observed that very small amounts of the counter ion are present, particularly when PAA was the top surface. This XPS data indicates that during the PSS adsorption process, approximately 80% of the sulfonate groups bond to the surface and 20% exist as loops and tails with a sodium or manganese counterion attached.

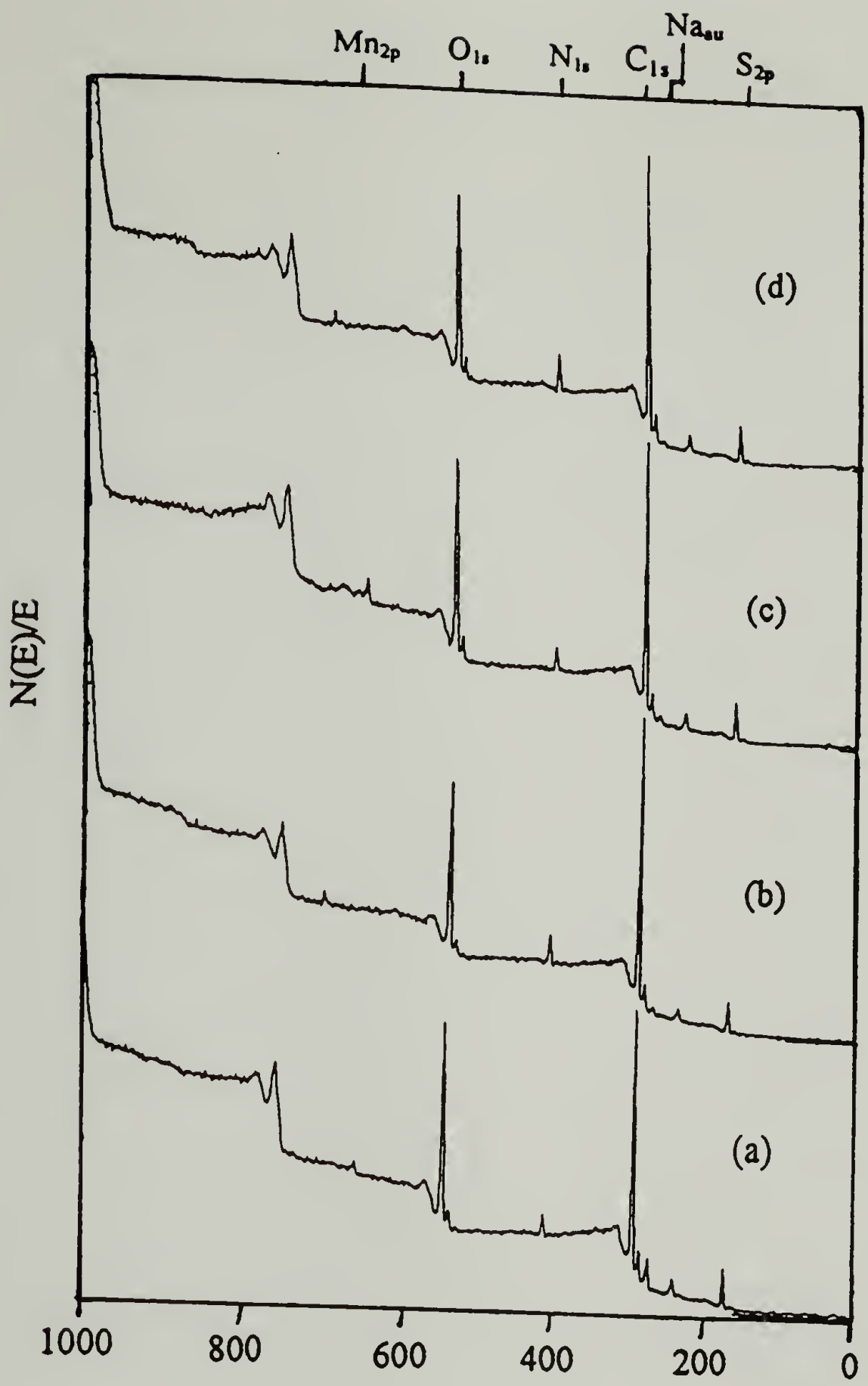

Figure 6.3 XPS survey spectra with a 15° take-off angle of (a) 9 layers, (b) 10 layers, (c) 33 layers, and (d) 34 layers adsorbed onto glass-NH_2.

Table 6.1 Atomic concentration by XPS of PSS and PAA layers adsorbed onto glass-NH_2.

Sample	Atomic Concentration, % (15°/75° take-off angle)							
	C_{1s}	O_{1s}	N_{1s}	S_{2p}	Si_{2p}	Cl_{2p}	Na_{1s}	Mn_{2p}
glass-NH_2	32.8/ 19.9	46.2/ 56.9	3.8/ 2.4	0/0	17.0/ 20.7	0/0	0.1/ 0	0/0
glass-NH_2•HCl	37.9/ 24.4	39.5/ 50.5	5.3/ 3.3	0/0	16.4/ 20.9	1.0/ 0.8	0 / 0.1	0/0
9 layers	68.9/ 64.9	20.8/ 24.6	3.8/ 3.6	5.1/ 5.3	-	0/0	0.8/ 0.9	0.7/ 0.8
10 layers	70.9/ 66.8	19.3/ 22.4	5.0/ 6.0	4.6/ 4.8	-	0/0	0.4/ 0.1	0/0
19 layers	69.7/ 67.2	20.6/ 22.1	3.8/ 4.1	5.1/ 5.7	0/0	0/0	0/0	0.8/ 0.9
20 layers	73.6/ 71.2	17.0/ 18.5	5.0/ 5.3	4.3/ 5.1	0/0	0/0	0/0	0.1/0

It was not possible to accurately asses the adsorption process of the PAA because of spontaneous elimination of chlorine during or just prior to the XPS experiment. However,the data does suggest that most, if not all of the amine groups bond to the underlying sulfonate groups with little or no loops and tails. From the adsorption mechanism proposed by Decher[6,10] it was predicted that higher concentrations of counterions would be present. The XPS data presented here suggests that most of the sulfonate groups are bound to the ammonium groups and when an additional layer was added some of the ammonium sulfonate bonds break apart and form new bonds with the added layer. This mechanism would account for the small amounts of counter ions

observed by XPS, however it was possible that some of the chlorine was not properly accounted for because of elimination during drying or upon bombardment with X-rays.

The deposition of very thin layers was evident by the gradual decrease in silicon to carbon ratios from the XPS data (Figure 6.4). The 15° take-off angle data showed that the Si_{2p} peaks due to the underlying glass substrate dissappearred after 5 layers were deposited. Using a 75° take-off angle, 10 layers were deposited before the Si_{2p} peaks dissappearred. Assuming an electron mean free path for carbon and silicon of 2.0 nm, the carbon/silicon ratio of the added layers was calculated using the uniform overlayer model:[28]

$$I_C/I_{Si} = \lambda_C/\lambda_{Si}[e^{t/\lambda c \sin\theta} - 1]$$

t was the layer thickness, I_C was the concentration of carbon, I_{Si} was the concentration of silicon, λ_C was the mean free path of carbon, and θ was the take-off angle. The I_C/I_{Si} ratio was calculated assuming a layer thickness of 0.6 and 0.8 nm. Figure 6.5 gives the I_C/I_{Si} ratio (carbon to silicon ratio) vs. the number of layers. The 15° data was not accurate past the first 2 layers and the 75° data was not accurate past 10 layers because the layer thickness then became greater than the sampling depth, making the carbon/silicon ratio inaccurate.

By comparing the measured carbon/silicon ratios to the calculated ratios it became apparent that the layer thickness was on the order of 0.6 to 0.8 nm. For this system, Decher[6] calculated an average layer thickness of 1.14 nm using X-ray reflectivity data, but the X-ray reflectivity data was conducted on hydrated samples, whereas this XPS

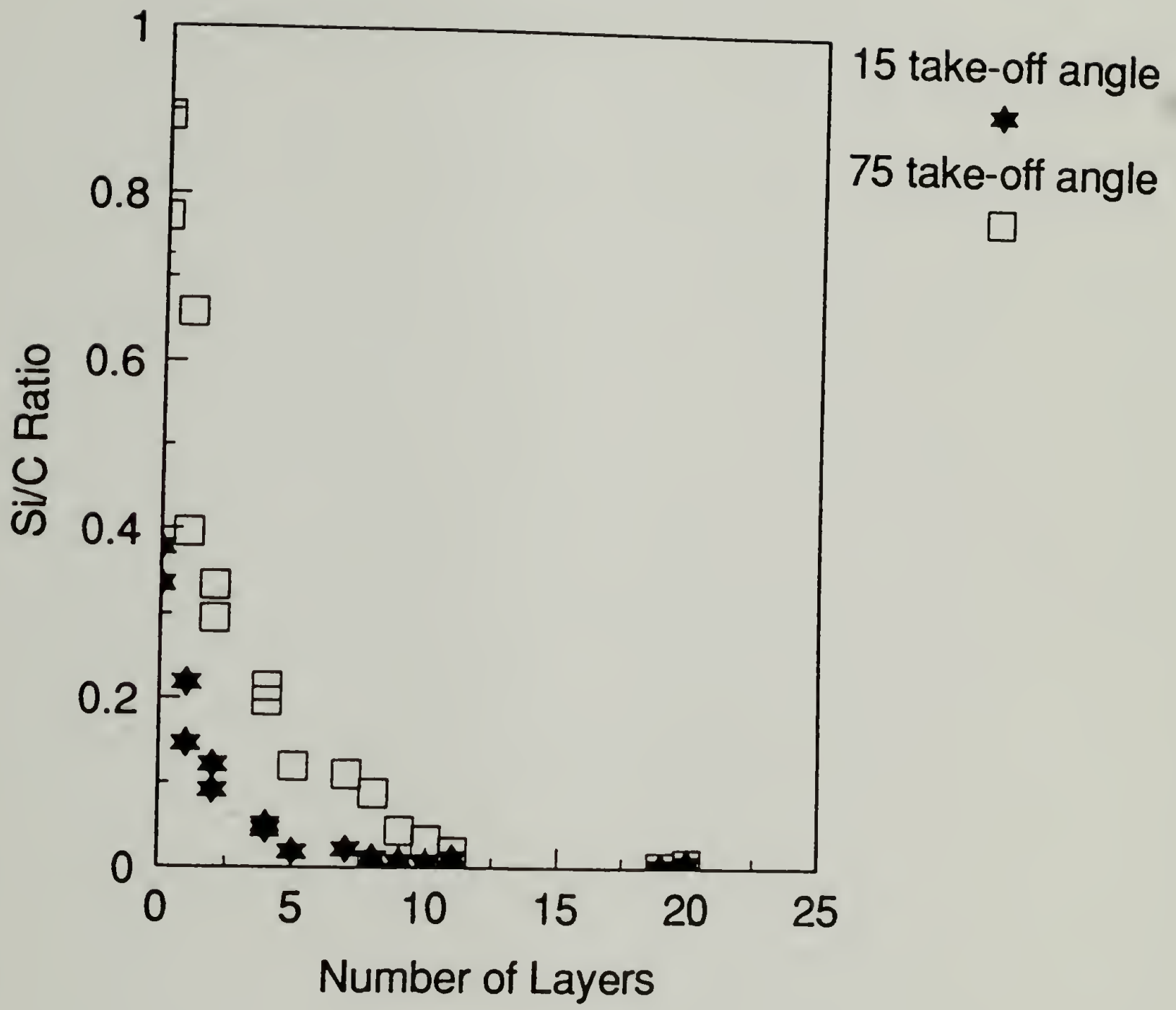

Figure 6.4 Silicon to carbon ratios determined by XPS using a 15° and 75° take-off angle vs. the number of PSS and PAA layers on glass-NH_2.

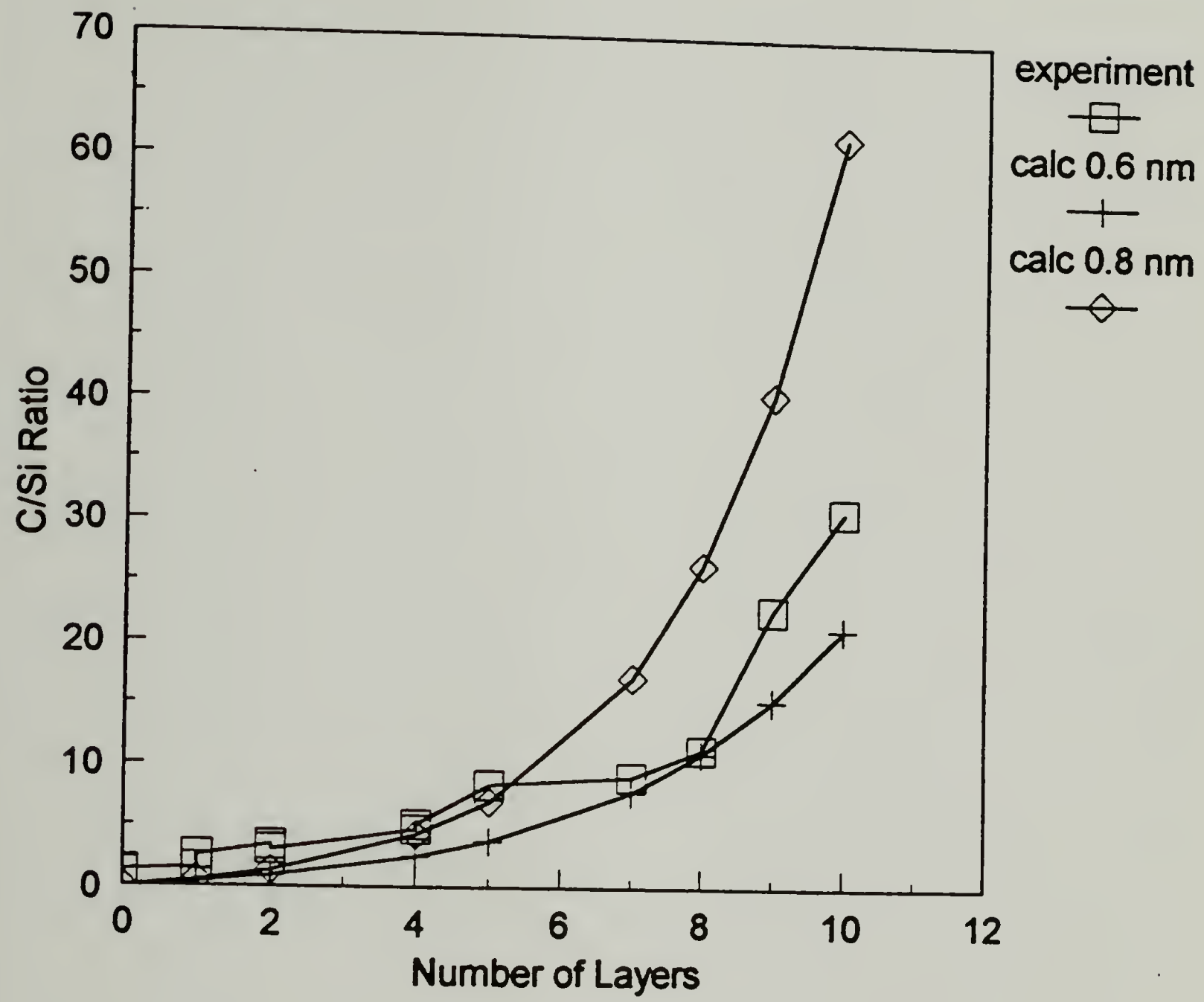

Figure 6.5 The carbon/silicon ratio of the added PSS and PAA layers onto glass measured experimentally by XPS using a 75° take-off angle and calculated assuming a layer thickness of 0.6 nm and 0.8 nm.

data was on completely dry samples (XPS was run at 10^{-9} torr). This indicated that the loopy, hydrated layers collapsed into thin layers with drying. This was in agreement with X-ray reflectivity data on similar systems where the layers were heated to promote drying.[5,9]

Plots of carbon and nitrogen (C/N) ratios (Figure 6.6), carbon and sulfur (C/S) ratios (Figure 6.7), and nitrogen and sulfur (N/S) ratios (Figure 6.8) showed a stratification between the odd and even number layers. This stratification was because the odd numbered layers had a PSS outer surface and the even numbered layers had a PAA outer surface. If the layers were not stratified (into organized layers) but mixed, the C/N ratios and C/S ratios would not be dependent on the PAA or PSS outer layer. The C/S and N/S ratios were inflated for the first few layers, due to the underlying aminopropyl-silane layer. The average N/S ratio was 1.32 for even layer numbers and 0.76 for odd layer numbers. Since the even layer numbers deviate more from theoretical value of one than the odd layers, the PAA layers must be thinner and/or more nitrogen dense.

Angle dependent XPS data showed the stratification of the C/S, C/N, and N/S holds at 5°-75° take-off angles. Both the C/S and C/N ratios exibited a more carbon-enriched surface at lower angles than at higher angles (Figures 6.9-6.12). A small angle dependence was observed in the N/S ratios when PSS was the outer surface) (Figures 6.13, 6.14). This implies the PSS layer could be thick enough to be resolved at low angles, whereas the PAA layer is to thin to be resolved, even at very low angles. This was consistent with the N/S ratio that deviates from one more when PAA was the top layer because the sampling depth at a 15° take-off angle comes from 2 PAA layers and 1 PSS

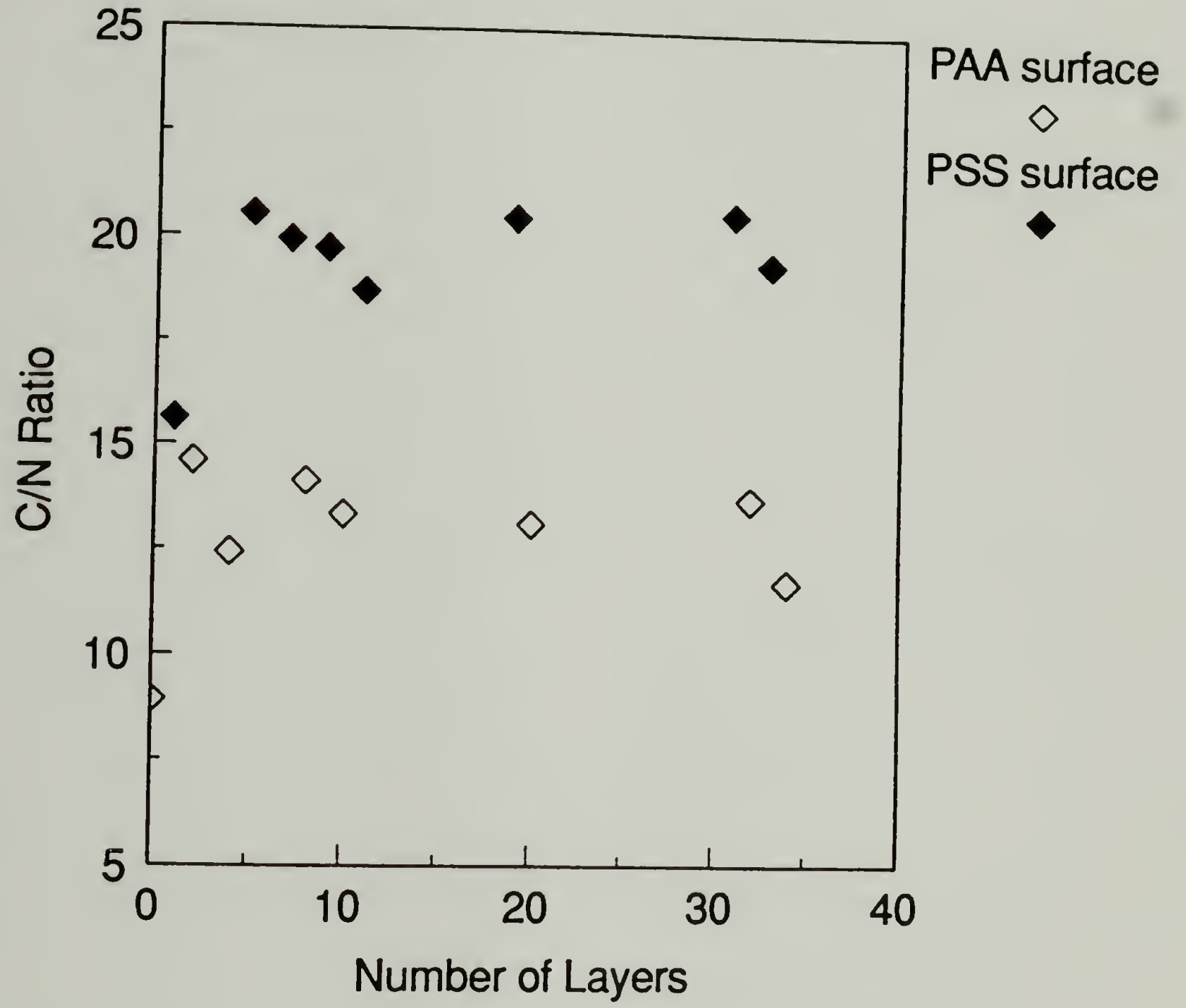

Figure 6.6 Carbon to nitrogen ratios measured by XPS using a 15° take-off angle vs. the number of layers.

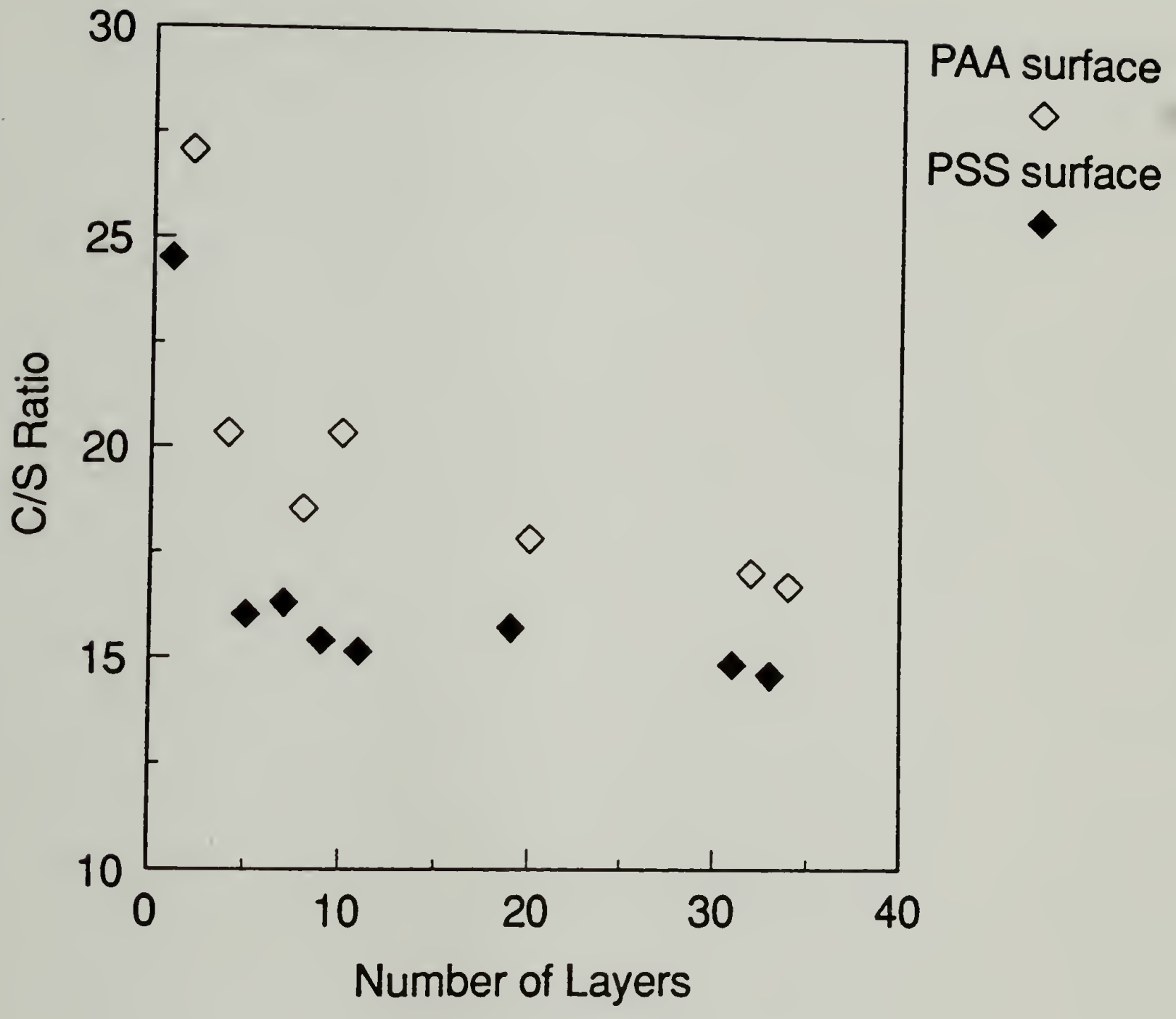

Figure 6.7 Carbon to sulfur ratios measured by XPS using a 15° take-off angle vs. the number of layers.

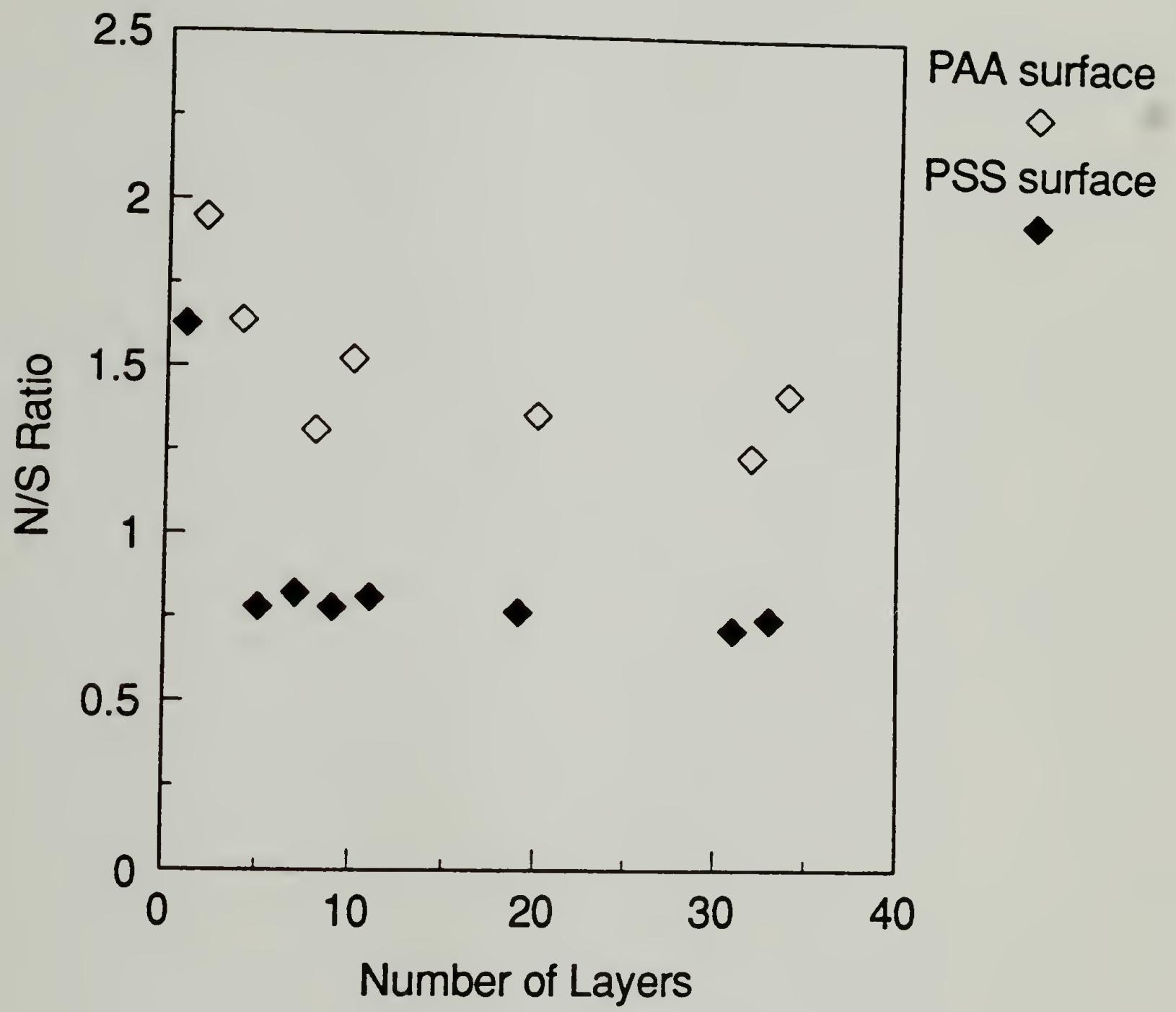

Figure 6.8 Nitrogen to sulfur ratios measured by XPS using a 15° take-off angle vs. the number of layers.

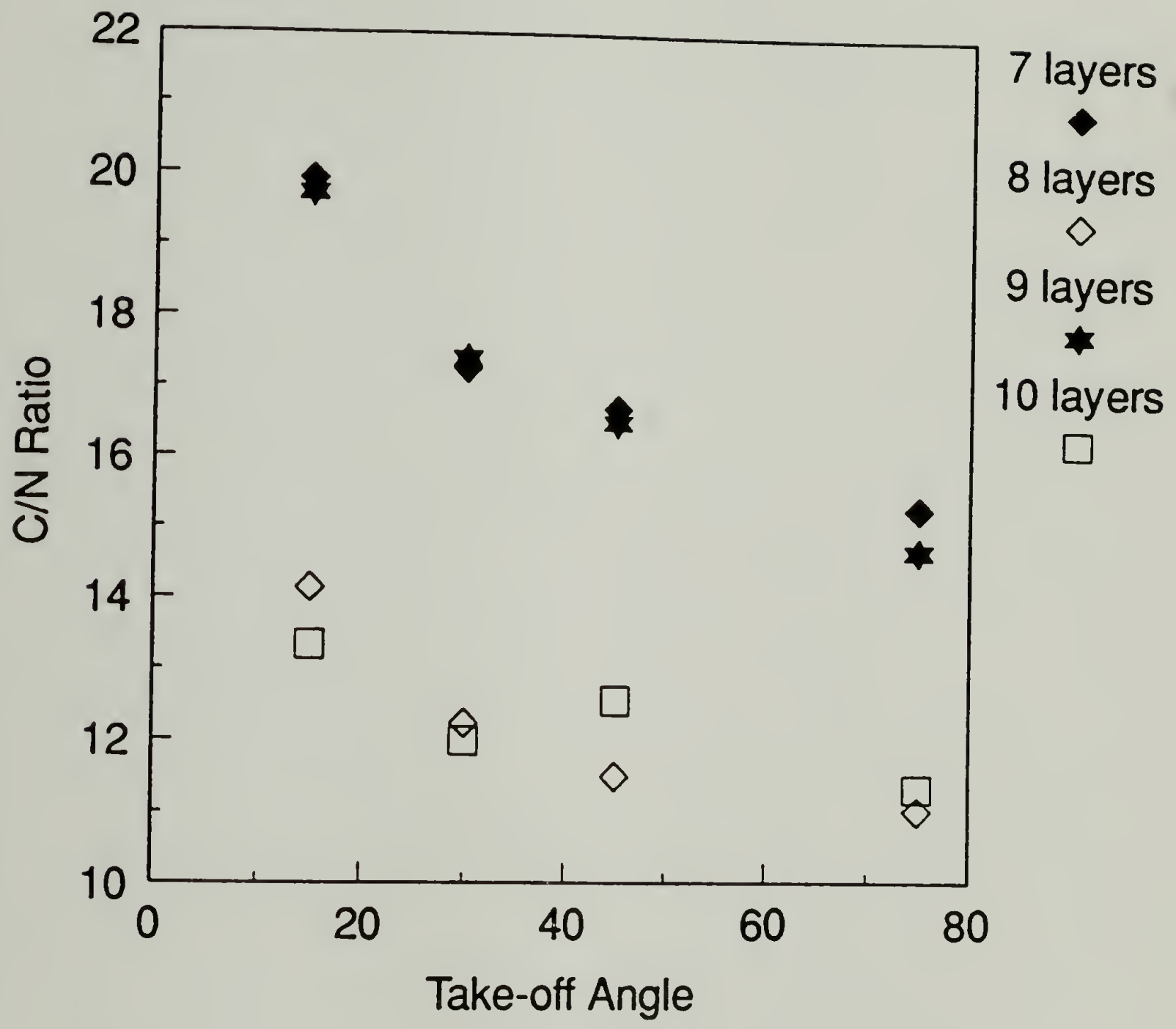

Figure 6.9 Carbon to nitrogen ratios at different XPS take-off angles for 7-10 layers on glass-NH_2.

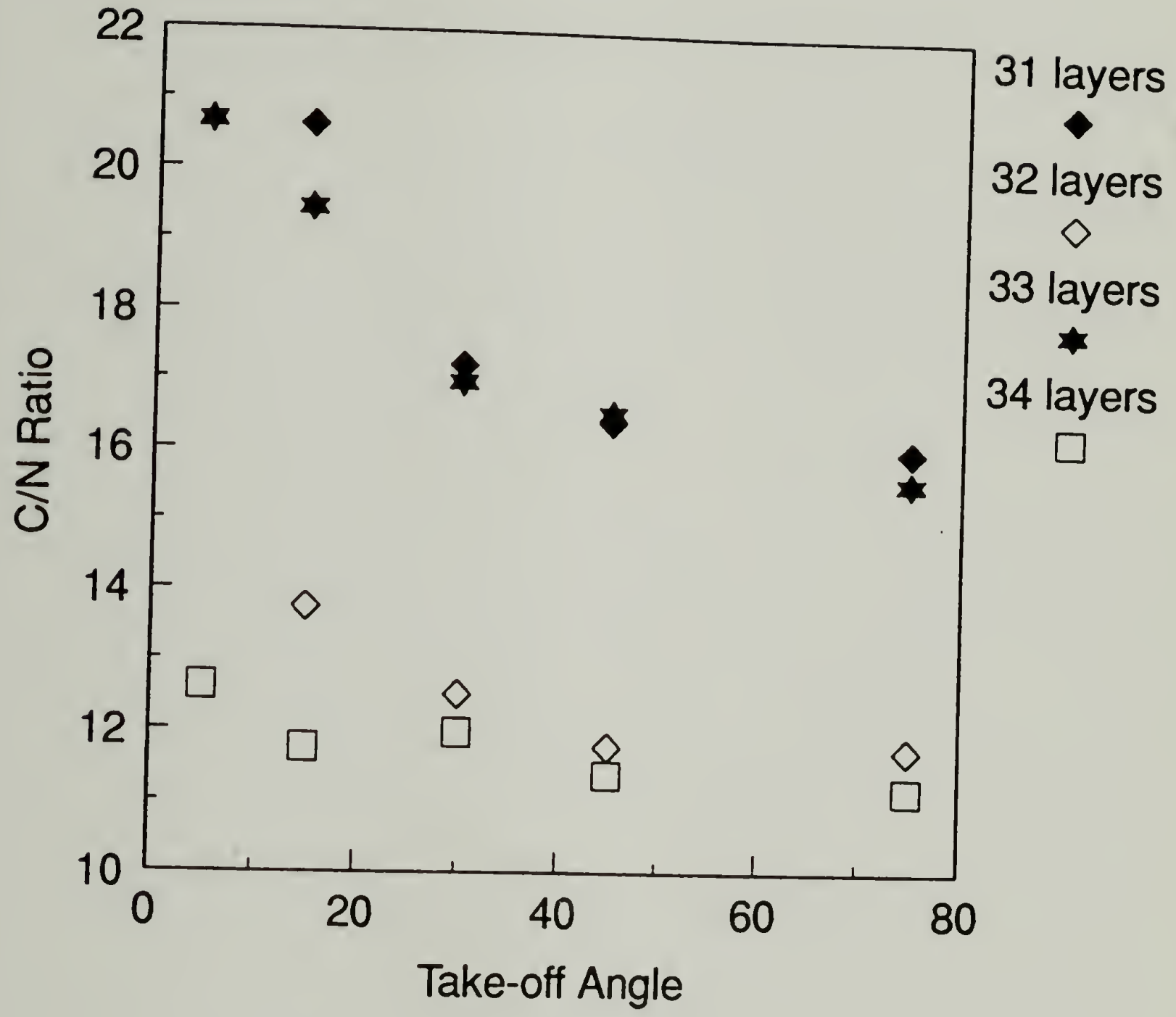

Figure 6.10 Carbon to nitrogen ratios at different XPS take-off angles for 31-34 layers on glass-NH_2.

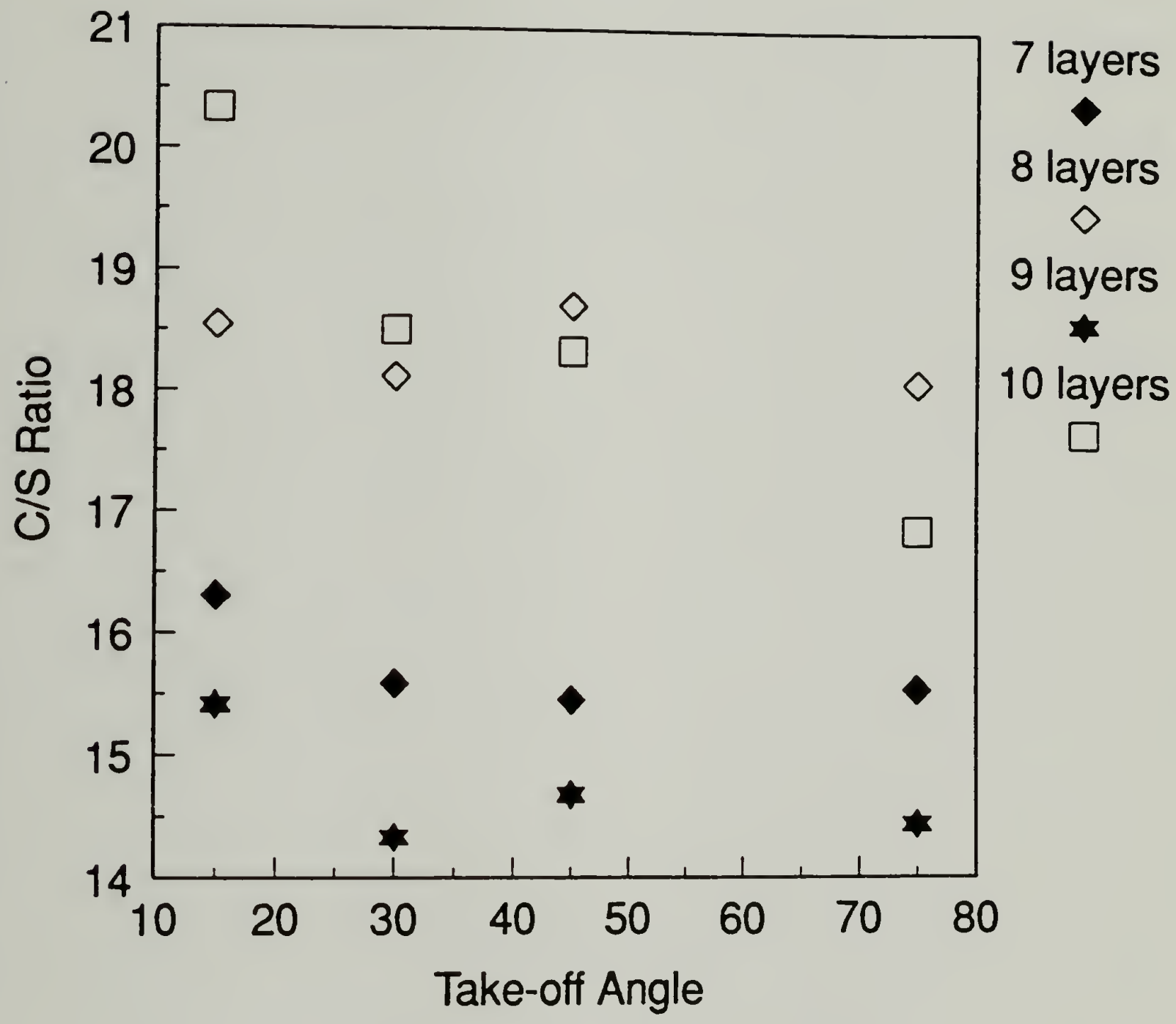

Figure 6.11 Carbon to sulfur ratios at different XPS take-off angles for 7-10 layers on glass-NH_2.

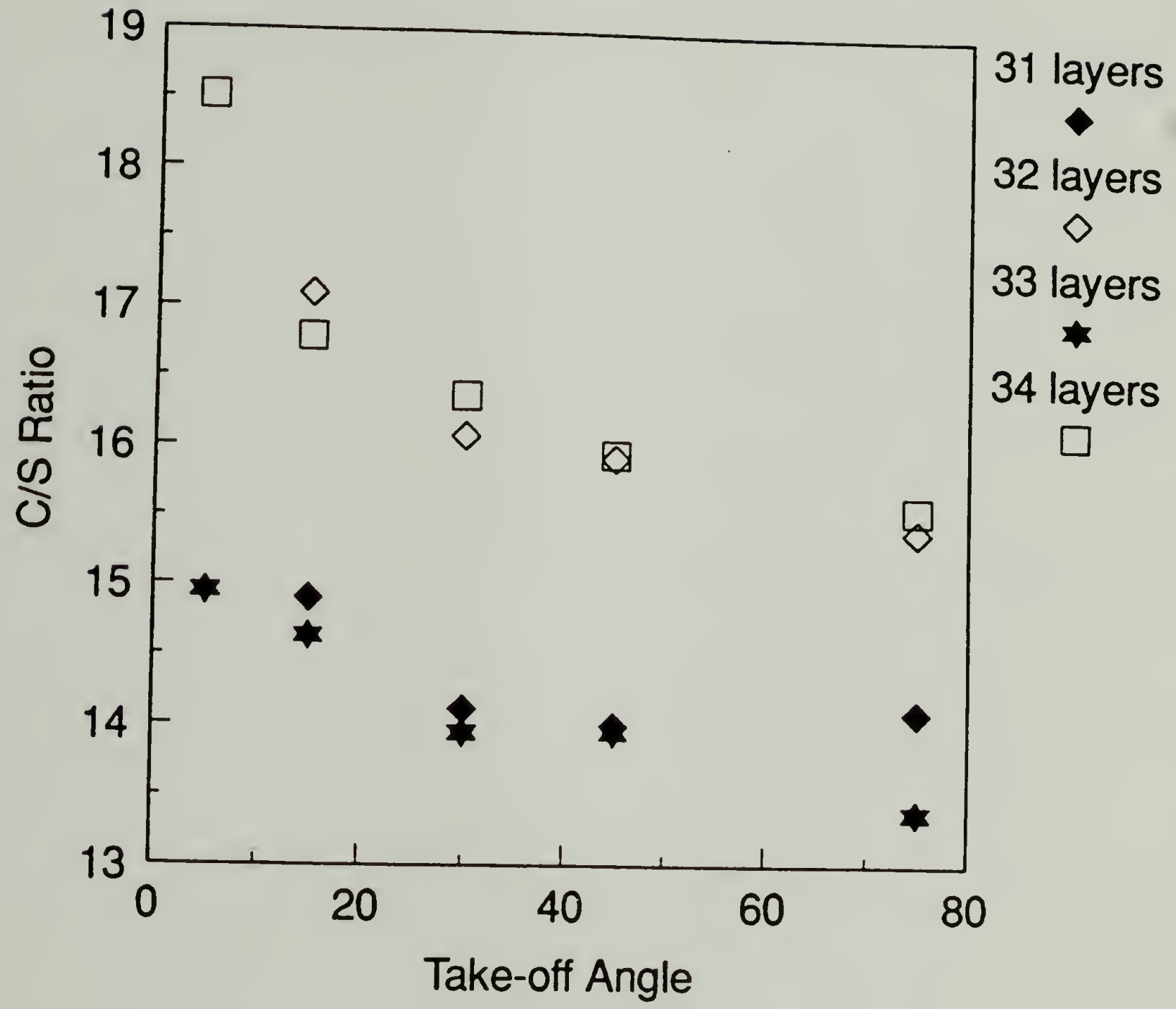

Figure 6.12 Carbon to sulfur ratios at different XPS take-off angles for 31-34 layers on glass-NH_2.

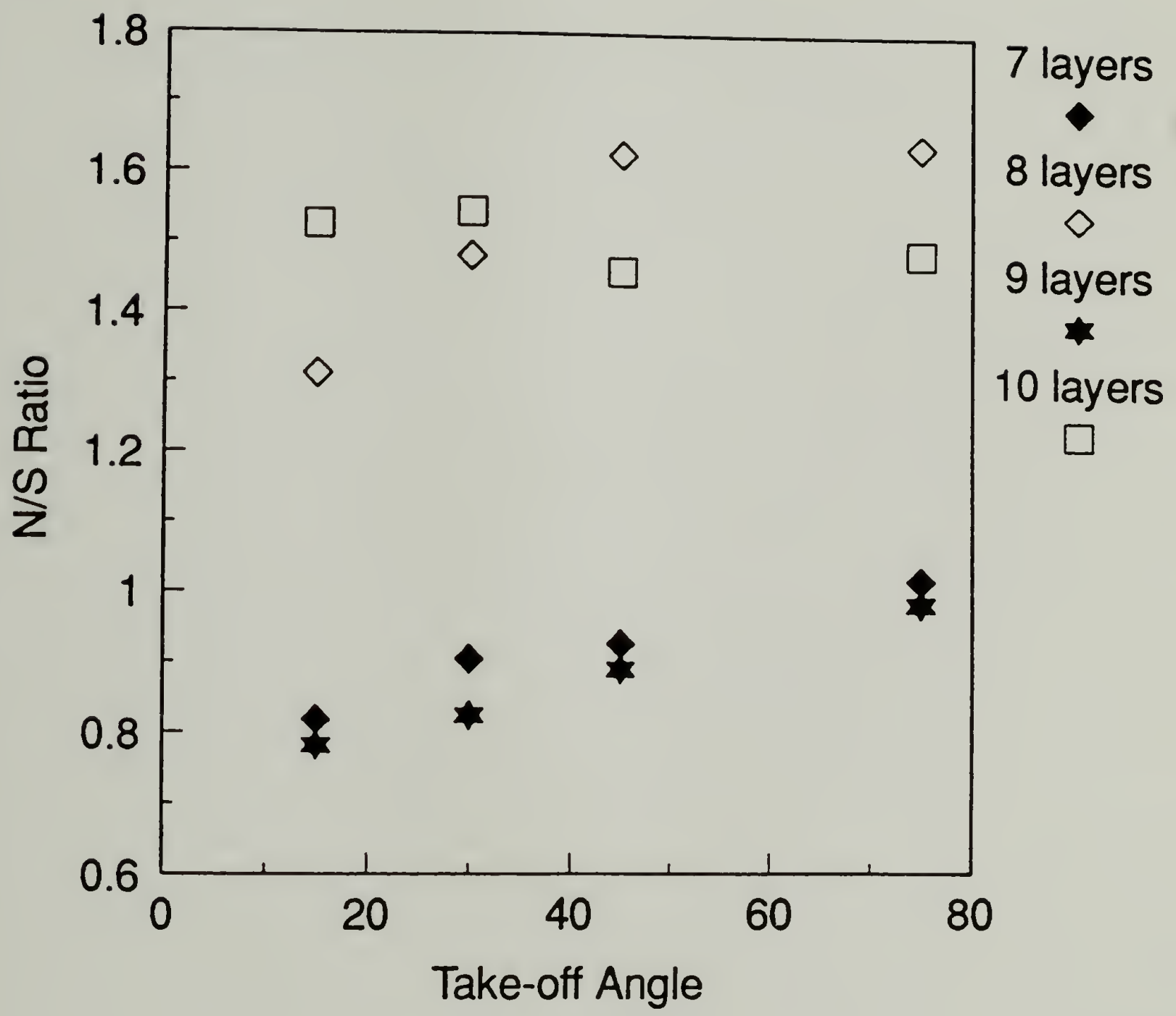

Figure 6.13 Nitrogen to sulfur ratios at different XPS take-off angles for 7-10 layers on glass-NH_2.

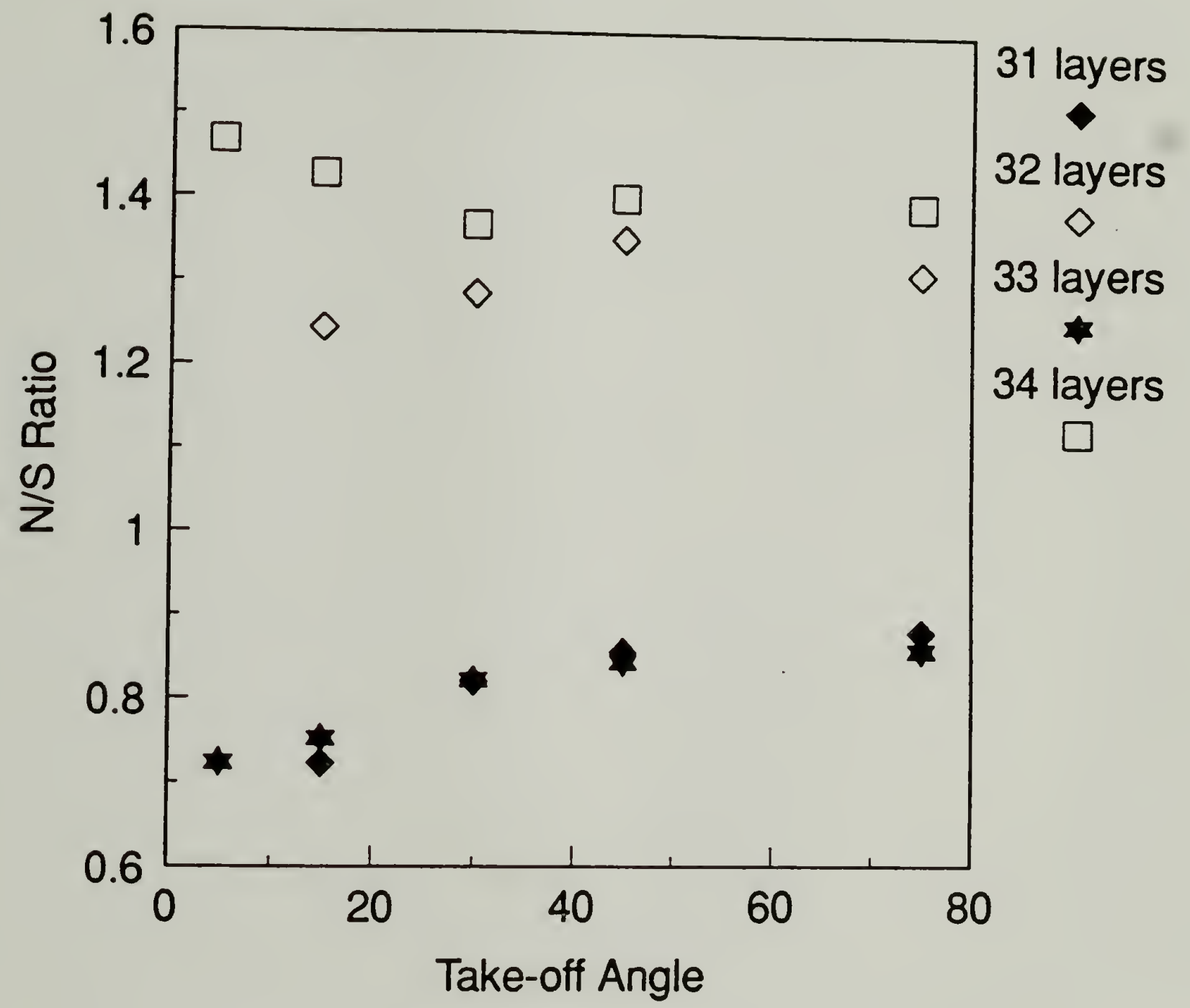

Figure 6.14 Nitrogen to sulfur ratios at different XPS take-off angles for 31-34 layers on glass-NH_2.

layers when PAA was the top surface, but when PSS was the top surface the sampling depth was 1 PAA layers and 1.5 PSS layers. The observation that the PAA layers were thinner than the PSS layers is consistent with the neutron reflectivity data by Decher.[12]

Contact angle data also showed a stratification between the odd and even numbered layers. The advancing contact angles were higher when PAA was the top surface (Figures 6.15-6.17). This trend was also observed by Suter[15] when poly(diallyl-ammoniumchloride) was adsorbed onto mica, and by Whitesides[29.30] on surface modified polyethylene containing amine surface functional groups (50° advancing contact angle) and sulfate groups (34° advancing contact angle). The receding contact angle was essentially zero for all surfaces. The contact angle was essentially independent of pH between 2 and 10 for all the surfaces. All layers exhibited a decrease in advancing contact angle a pH's greater than 10. This was possibly due to the breaking up of the ionic bonds between the ammonium and sulfonate to form the free sulfonate ion. The reader is referred to references 29 and 30 on the relationship between extent of ionization and contact angle.

Adhesion of the adsorbed polyelectrolyte layers to a commercial PSA (3M Scotch Brand #750) was investigated by peeling in a 180° geometry. The peel energy to clean glass was 371 J/m^2, aminated glass was 246 J/m^2. The decrease in adhesion was what would be predicted from the contact angle data, the aminated glass had a higher contact angle and therfore a lower surface energy. The peel energy to glass with 19 adsorbed layers was 348 J/m^2, and the peel energy to glass with 20 adsorbed layers was 360 J/m^2.

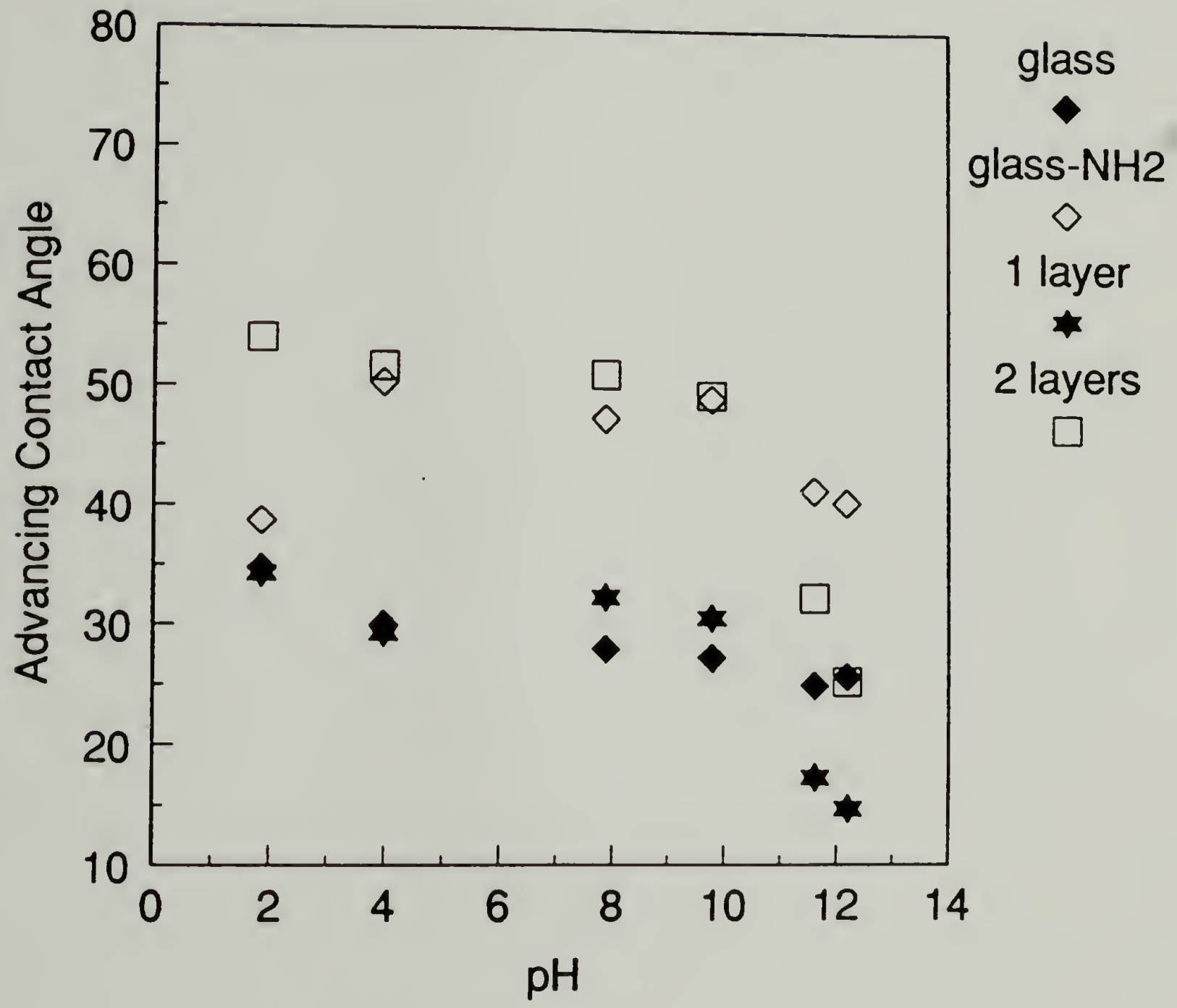

Figure 6.15 Advancing contact angle of water buffered at various pH values on glass, glass-NH_2, 1 layer, and 2 layers.

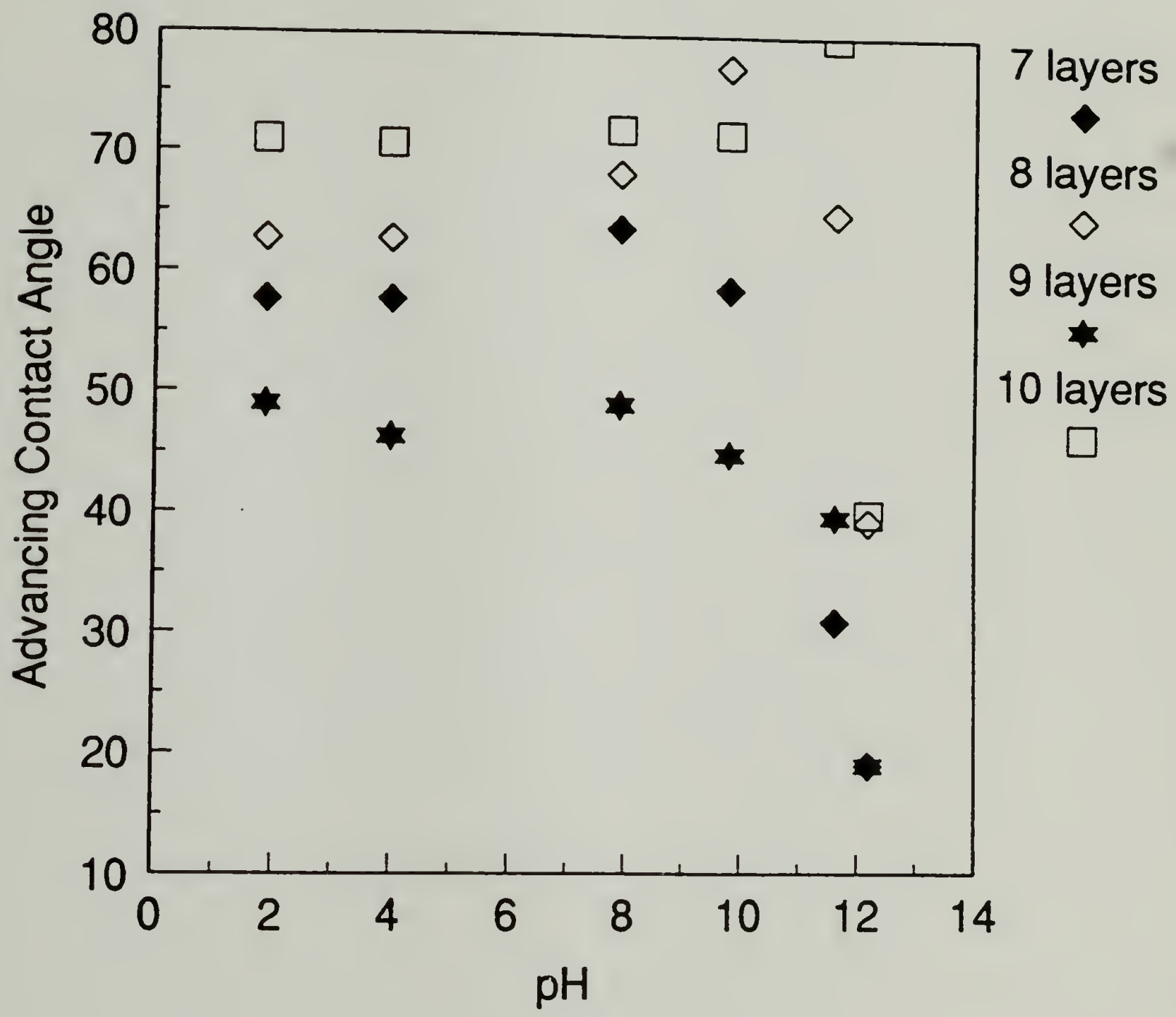

Figure 6.16 Advancing contact angle of water buffered at various pH values on 7-10 layers.

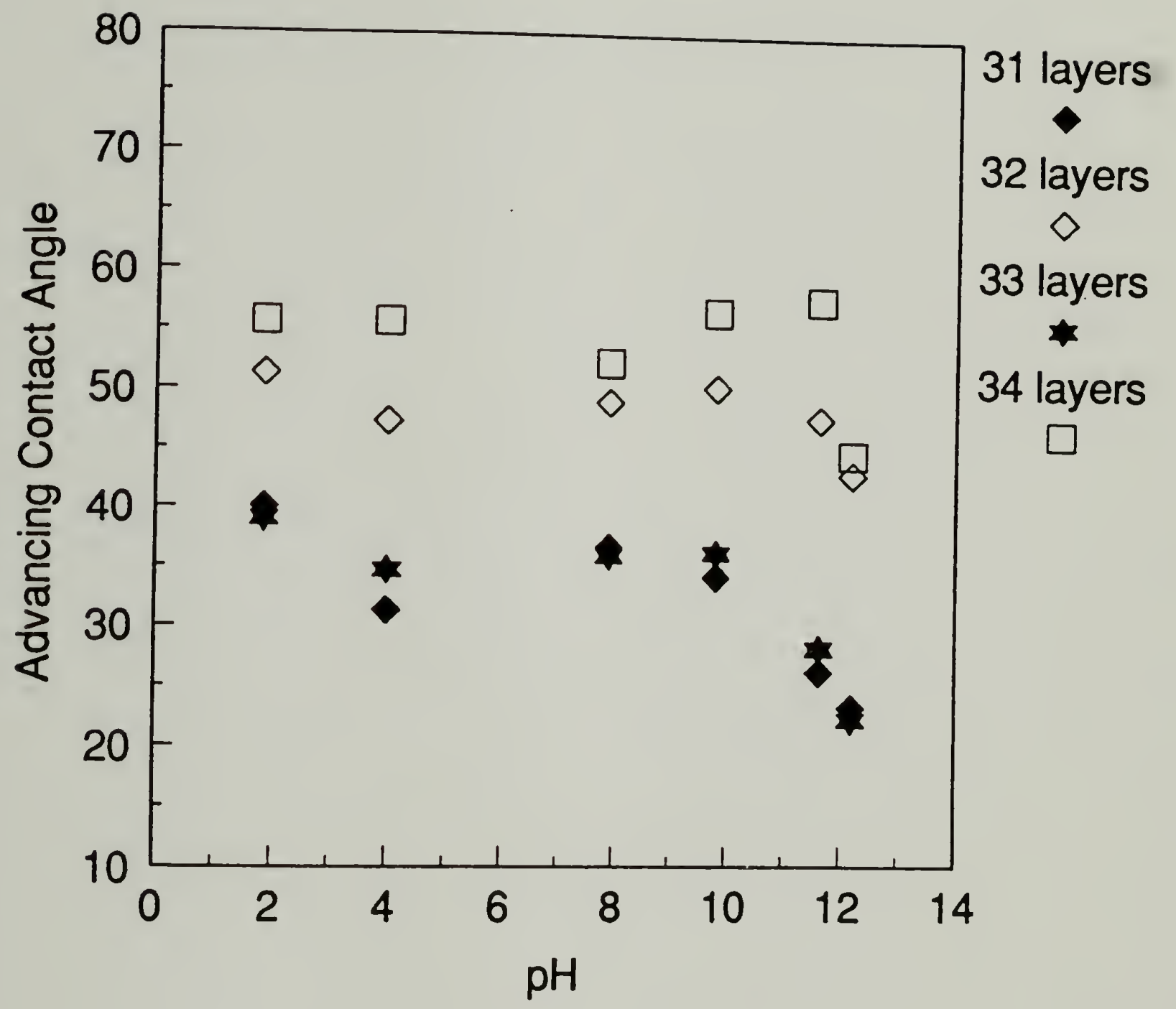

Figure 6.17 Advancing contact angle of water buffered at various pH values on 31-34 layers.

The difference in peel energy between 19 and 20 layers was within the experimental error, the standard deviation was 24.4 J/m^2. From the contact angle data, it would be predicted that the 19 adsorbed layers would stick better than the 20 adsorbed layers, however, this was not observed. XPS analysis after peeling the PSA showed PSA was transfered to the glass, glass-NH_2, 19 layers, and 20 layers during peeling. XPS on the PSA side showed that no PSS or PAA chains were removed from the glass substrate. This result indicated that the PAA and PSS layers were strongly bound to the glass surface and had good "mechanical integrity". The loci of failure by XPS also explains why the peel energy did not change with the different surfaces. Adhesion to the adsorbed polyelectrolytes was not being measured, the cohesion of the PSA was.

The adhesion of layered structures to epoxy was also qualitatively investigated. The fracture energy, G_c, between epoxy and glass, glass-NH_2, 18 layers, and 21 layers were measured using the assymetric double-cantilever-beam (ADCB) test. The fracture energy between epoxy and glass was 63 J/m^2. The fracture energy between epoxy and glass-NH_2 was very high, the glass would break before a crack would propagate along the interface. The fracture energy of 18 layers on glass to epoxy was 5 J/m^2 and 21 layers was 145 J/m^2. These studies of the fracture energy to epoxy were preliminary and have not been reproduced.

Conclusions and Future Work

Alternating layers of poly(sodium 4-styrenesulfonate) and poly(allylamine hydrochloride) were adsorbed onto glass. XPS data showed that each polyelectrolyte organized into a ~0.7 nm layer. The wettability of the surface was affected by the layers,

the, PAA surfaces had a higher advancing contact angle than the PSS surfaces. The "mechanical integrity" or adhesion of the layers was assesed to be very good by peeling a PSA from the layers. XPS showed that the layers were not removed by peeling the PSA. The ADCB test was shown to be a potentially useful test in measuring adhesion of the layers on glass to epoxy. Preliminary experiments showed that the adhesion of 21 layers on glass to epoxy was very good, which gave more evidence of the good "mechanical integrity" of the layers. However, more work needs to be done to quantify the adhesion and the loci of failure.

The next step in this research is to assess some of the variables in polyelectrolyte adsorption on their solid state properties. Polyelectrolytes adsorbed from solutions of low ionic strengths should give layers that are more organized and ionized. This should have an increased effect on their wettability (pH dependence should be more pronounced) and adhesive properties because of less screening of the ionized groups. The effect of charge density on polyelectrolyte adsorption could be investigated by adsorbing block copolymers containing ionizeable and nonionizable groups. Glass is known to be rigid and flat, the surface being an ideal two-dimensions. Surface modified polymers contain an "interphase" that can be characterized by adsorbing PSS and PAA layers. If the polymer surface acts as a sponge soaking up the layers until the "interphase" is full, its properties can be more fully understood by the layer-by-layer adsorption technique.

References

1. Swalen, J.D.; Allara, D.L.; Andrade, E.A.; Chandross, E.A.; Garoff, S.; Israelachvili, J.; McCarthy, T.J.; Murray, R.; Pease, R.F.; Rabolt, J.F.; Wynne, K.J. *Langmuir*, **1987**, 3, 932.

2. Stockton, W.B.; Rubner, M.F.; *Polymr. Prepr. (Am. Chem. Soc., Div. Polym. Chem.)*, **1994**, 35(1), 319.

3. Lee, H.; Kepley, L.J.; Hong, H-G.; Akhter, S.; Mallouk, T.E. *J. Phys. Chem.*, **1988,** 92, 2597.

4. Decher, G.; Hong, J-D. *Makromol. Chem. Macromol. Symp.*, **1991**, 46, 321.

5. Decher, G.; Lvov, Y.; Mohwald, H. *Langmuir*, **1993**, 9, 481.

6. Decher, G.; Hong, J-D.; Schmitt, J. *Thin Solid Films*, **1992**, 210/211, 831.

7. Rubner, M.F.; Cheung, J.H.; Fou, A.F.; Ferreira, M. *Polym. Prepr. (Am. Chem. Soc., Div. Polym. Chem.)*, **1993**, 34(2), 757.

8. Rubner, M.F.; Fou, A.C.; Ellis, D.; Ferreira, M. *Polymr. Prepr. (Am. Chem. Soc., Div. Polym. Chem.)*, **1994**, 35(1), 221.

9. Decher, G.; Lvov, Y.; Sukhorukov, G. *Macromolecules*, **1993**, 26, 5396.

10. Decher, G.; Lvov, Y.; Haas, H.; Mohwald, H. *J. Phys. Chem.*, **1993**, 97, 12835.

11. Decher, G.; Schmitt, J. *Progr. Colloid Polym. Sci.*, **1992**, 89, 160.

12. Decher, G.; Schmitt, J.; Grunewald, T.; Pershan, P.; Kjaer, K.; Losche, M. *Macromolecules*, **1993**, 26, 7058.

13. Plueddmann, E.P. *Silane Coupling Agents*, Plenum Press, New York, **1982**.

14. Nuzzo, R.G.; Allar, D.L. *J. Am. Chem. Soc.*, **1983**, 105, 4481.

15. Pireaux, J.J.; Bertrand, P.; Bredas, J.L. editors *Polymer-Solid Interfaces*, IOP Publishing Ltd, London, **1992** p. 131.

16. Van der Schee, H.A.; Lyklema, J. *J. Phys. Chem.*, **1984**, 88, 6661.

17. Evers, O.A.; Fleer, G.J.; Scheutjens, J.M.H.M.; Lyklema, J. *J. Colloid Interface Sci.*, **1985**, 111, 446.

18. (a) Scheutjens, J.M.H.M.; Lyklema, J. *J. Chem. Phys.*, **1979**, 83, 1619.
(b) Scheutjens, J.M.H.M.; Lyklema, J. *J. Chem. Phys.*, **1980**, 84, 178.

19. Adamson, A.W. *Physical Chemistry of Surfaces, fifth edition*, John Wiley & Sons Inc., New York, **1990**.

20. Berndt, P.; Kurihara, K.; Kunitake, T. *Langmuir*, **1992**, 8, 2486.

21. Marra, J.; Hair, M.L. *J. Phys. Chem.*, **1988**, 92, 6044.

22. Parfitt, G.D.; Rochester, C.H. editors, *Adsorption From Solution at the Solid/Liquid Interface*, Academic Press, New York, **1983** p.392.

23. Dahlgren, M.A.G. *Langmuir*, **1994**, 10, 1580.

24. Clark, D.T.; Thomas, H.R. *J. Polym. Sci.: Polym. Chem. Ed.*, **1977**, 15, 2843.

25. Weast, R.C. editor, *CRC Handbook of Chemistry and Physics 67th edition*, CRC Press Inc., Boca Raton, **1986**.

26. Brown, H.R. *J. Mater. Sci.*, **1990**, 25, 2791.

27. Janarthanan, V.; Stein, R.S.; Garrett, P.D. *J. Polymer Sci.: Part B: Polymer Physics*, **1993**, 31, 1995.

28. Andrade, J.D. *Surface and Interfacial Aspects of Biomedical Polymers*, Plenum Press: New York, **1985**, 184.

29. Holmes-Farley, S.R.; Bain, C.D.; Whitesides, G.M. *Langmuir*, **1988**, 4, 921.

30. Holmes-Farley, S.R.; Reamy, R.H.; McCarthy, T.J.; Deuth, J.; Whitesides, G.M. *Langmuir*, **1985**, 1, 725.

APPENDIX A

ATOMIC RATIOS BY XPS OF PCTFE-BUTYL AND EPOXY AFTER PEELING

Initial Reaction Conditions			C_{1s}/F_{1s} Atomic Ratio by XPS After Peeling			
Time (hrs.)	Temp. (°C)	Solvent	Epoxy Side		PCTFE-Butyl Side	
		% hept/THF	15°angle	75°angle	15°angle	75°angle
unreacted			1.05	1.27	0.67	0.68
0.5	-78	100	0.86	1.06	0.77	0.72
0.5	-15	100	0.75	0.87	0.69	0.70
0.5	0	100	0.77	0.76	0.68	0.69
0.5	25	100	0.85	0.86	0.79	0.73
3.0	25	100	1.70	1.87	1.52	1.47
18	25	100	8.12	9.20	4.80	4.45
0.5	0	99.96	0.80	0.65	0.76	0.66
0.5	0	99.87	0.75	0.80	1.45	0.94
0.5	0	99.20	7.09	5.80	6.35	5.99
0.5	0	96.7	7.47	6.49	7.31	5.98

APPENDIX B

ATOMIC COMPOSITIONS BY XPS OF SURFACE MODIFIED PCTFE AND EPOXY AFTER PEELING

Surface	Atomic Composition of Epoxy Side After Peeling (75° angle)				Atomic Composition of PCTFE Side After Peeling (75° angle)			
	$\%C_{1s}$	$\%O_{1s}$	$\%N_{1s}$	$\%F_{1s}$	$\%C_{1s}$	$\%O_{1s}$	$\%N_{1s}$	$\%F_{1s}$
PCTFE	47.3	4.0	2.4	37.2	33.6	0.8	0	49.1
PCTFE-PEA	71.8	16.7	0	11.6	71.8	16.8	0	11.4
PCTFE-Butyrate, pyridine cat., dried 3 days at 45°C,	74.1	17.3	0.6	8.0	72.5	17.8	0	9.4
PCFTE-Butyrate, no catalyst, dried 3 days at 45°C,	72.8	19.0	1.8	6.4				
PCTFE-Butyrate, no catalyst, dried 6 days at 95°C	76.8	18.1	2.7	2.4				
PCTFE-Adipate	80.4	13.3	3.7	1.8	73.3	19.0	0.4	6.7
PCTFE-Hept.	84.9	9.1	2.6	3.0	86.2	7.8	0	5.2
PCTFE-Stearate	86.1	8.5	3.3	2.0				

APPENDIX C

ATOMIC COMPOSITIONS BY XPS OF SURFACE MODIFIED PCTFE AND A PSA AFTER PEELING

Surface	Atomic Composition of PSA Side After Peeling (75° angle)			Atomic Composition of PCTFE Side After Peeling (75° angle)			
	$\%C_{1s}$	$\%O_{1s}$	$\%F_{1s}$	$\%C_{1s}$	$\%O_{1s}$	$\%F_{1s}$	$\%Cl_p$
PCTFE	81.1	18.4	0.1	35.6	1.3	47.6	15.6
PCTFE-Butyl (reacted in hept., 0°C, 30 min.)	80.2	19.3	0.1	69.0	6.5	19.8	4.6
PCTFE-Butyl (reacted in 98.1% hept/THF, 21°C, 30 min.)	75.1	24.8	0.0	79.3	18.3	2.2	0.0
PCTFE-OX	79.5	19.2	0.2	48.6	8.2	31.5	11.1
PCTFE-PEA	78.5	20.0	0.0	73.1	16.6	10.1	0.2
PCTFE-OH	81.3	18.4	0.0	68.8	17.9	12.0	0.0
PCTFE-Butyrate	82.0	18.1	0.0	72.8	18.0	9.2	0.0

BIBLIOGRAPHY

1. A.J. Kinloch *Adhesion and Adhesives*, Chapman and Hall: New York, **1987**.

2. Adamson, A.W. *Physical Chemistry of Surfaces, fifth edition*, John Wiley & Sons Inc., New York, **1990**.

3. Allen, K.W. *Adhesion*, **1986**, 11, 82.

4. Allied-Signal Enc., Aclar Product Bulletin.

5. Amouroux, J.; Goldman, M.; Revoil, M.F. *J. Polym. Sci.: Polym. Chem. Ed.*, **1982**, 20, 1373.

6. Andrade, J.D., *Surface and Interfacial Aspects of Biomedical Polymers*, Volume 1, Plenum Press: New York, **1985**.

7. Andrews, E.H. *Developments in Fracture -1*, Applied Science Publishers LTD: London, **1979.**

8. Andrews, E.H.; Kinloch, A.J. *Proc. R. Soc. Lond.A.*, **1973**, 332, 385.

9. ASTM D2093-62T.

10. Banks, B.A.; Sovey, J.S.; Miller, T.B.; Crandall, K.S. *NASA*, TM-7888 (June **1978**).

11. Barker, D.J.; Brewis, D.M.; Dahm, R.H. *J. Mat. Sci.*, **1979**, 14, 749.

12. Bascom, W.D.; Cottington, R.L.; Jones, R.L.; Peyser, P. *J. Appl. Polymer Sci.*, **1975**, 19, 2545.

13. Baszkin, A.; Ter-Minassian-Saraga, L. *J. Polym. Sci.: Part C*, **1971**, 243.

14. Bee, T.G. Ph.D. Dissertation, University of Massachusetts, **1993**.

15. Bee, T.G.; McCarthy, T.J. *Macromolecules*, **1992**, 25, 2093.

16. Benderly, A.A. *J. Appl. Polym. Sci.*, **1962**, 6, 221.

17. Bening, R.C.; McCarthy, T.J. *Macromolecules*, **1990**, 23, 2648.

18. Berndt, P.; Kurihara, K.; Kunitake, T. *Langmuir*, **1992**, 8, 2486.

19. Bikerman, J.J. *The Science of Adhesive Joints*, Academic Press: New York, **1961**.

20. Brecht, H.; Mayer, F.; Binder, H., *Angew. Makromol. Chem.*, **1973**, 33, 89.

21. Brennan, J.V.; McCarthy, T.J. *Polym. Prepr. (Am. Chem. Soc., Div. Polym. Chem.)*, **1987**, 29(2), 338.

22. Brennan, J.V.; McCarthy, T.J. *Polym. Prepr. (Am. Chem. Soc., Div. Polym. Chem.)*, **1989**, 30(2), 152.

23. Brewis, D.M. *J. Adhesion*, **1992**, 37, 97.

24. Brewis, D.M.; Barker, J.D.; Dahm, R.H.; Hoy, L.R.J. *Electrochim. Acta.*, **1978**, 23, 1107.

25. Brewis, D.M.; Dahm, R.H.; Konieczko, M.B. *Angew. Makromol. Chem.*, **1975**, 43, 191.

26. Briggs, D.; Brewis, D.M.; Konieczko, M.B. *J. Mat. Sci.*, **1979**, 14, 1344.

27. Brown, H.R. *J. Mater. Sci.*, **1990**, 25, 2791.

28. Brown, H.R.; Char, K.; Deline, V.R. *Macromolecules*, **1993**, 26, 4164.

29. Brown, H.R.; Char, K.; Deline, V.R.; Green, P.F. *Macromolecules*, **1993**, 26, 4155.

30. Cagel, C.V., *Handbook of Adhesive Bonding*, McGraw-Hill Pub.: New York, **1973**, 16.

31. Ceresa, R.J., *Block and Graft Copolymerization Volume 1*, John Wiley & Sons, London, **1973.**

32. Charalambides, M.; Kinloch, A.J.; Wang, Y.; Williams, J.G. *Inter. J. Fracture*, **1992**, 54, 269.

33. Chung, T.C. *Contemporary Topics in Polymer Science*, Plenum Press: New York, **1989**, 6, 315.

34. Chung, T.C. *Macromolecules*, **1988**, 21, 865.

35. Chung, T.C.; Janvikul, W.; Bernard, R.; Jiang, G.J. *Macromolecules*, **1994**, 27, 26.

36. Chung, T.C.; Raate, M.; Berluche, E.; Schulz, D.N. *Macromolecules*, **1988**, 21, 1903.

37. Chung, T.C.; Ramakrishnan, S.; Berluche, E. *Macromolecules*, **1990**, 23, 378.

38. Chung, T.C; Rhubright, D. *Macromolecules*, **1991**, 24, 970.

39. Clark, D.T. and Feast, W.J. *Polymer Surfaces*, Wiley-Interscience: New York, **1978**.

40. Clark, D.T.; Thomas, H.R. *J. Polym. Sci.: Polym. Chem. Ed.*, **1977**, 15, 2843.

41. Clark, D.T.; Wilson, R. *J. Polym. Sci.: Polym. Chem. Ed.*, **1983**, 21, 837.

42. Cohen Stuart, M.A.; Cosgrove, T.; Vincent, B. *Advances in Colloid and Interface Science*, **1986**, 24, 143.

43. Cohen Stuart, M.A.; Fleer, G.J.; Lyklema, J.; Norde, W.; Scheutjens, J.M.H.M *Advances in Colloid and Interface Science*, **1991**, 34, 477.

44. Collins, G.C.S.; Lowe, A.C.; Nicholas, D. *Eur. Polym. J.*, **1973**, 9, 1173.

45. Cosgrove, T.; Finch, N.A.; Webster, J.R.P. *Macromolecules*, **1990**, 23, 3353.

46. Costello, C.A.; McCarthy, T.J. *Macromolecules*, **1987**, 20, 2819.

47. Creton, C.; Brown, H.R.; Deline, V.R. *Macromolecules*, **1994**, 27, 1774.

48. Creton, C.; Brown, H.R.; Shull, K.R. *Macromolecules*, **1994**, 27, 3174.

49. Creton, C.; Kramer, E.J.; Hui, C-Y.; Brown, H.R. *Macromolecules*, **1992**, 25, 3075.

50. Cross, E.M.; McCarthy *Macromolecules*, **1990**, 23, 3916.

51. Dahlgren, M.A.G. *Langmuir*, **1994**, 10, 1580.

52. Danielson, N.D.; Taylor, R.T.; Huth, J.A.; Siergiej, R.W.; Galloway, J.G.; Paperman, J.B. *Ind. Eng. Chem. Prod. Res. Dev.*, **1983**, 22, 303.

53. de Vincenzi, R.D. unpublished work, 1994.

54. Deanin, R.D.; Crugnola, A.M. *Toughness and Brittleness in Plastics*, Advances in Chemistry Series 154, American Chemical Society: Washington, D.C., **1976**.

55. Decher, G.; Hong, J-D. *Makromol. Chem. Macromol. Symp.*, **1991**, 46, 321.

56. Decher, G.; Hong, J-D.; Schmitt, J. *Thin Solid Films*, **1992**, 210/211, 831.

57. Decher, G.; Lvov, Y.; Haas, H.; Mohwald, H. *J. Phys. Chem.*, **1993**, 97, 12835.

58. Decher, G.; Lvov, Y.; Mohwald, H. *Langmuir*, **1993**, 9, 481.

59. Decher, G.; Lvov, Y.; Sukhorukov, G. *Macromolecules*, **1993**, 26, 5396.

60. Decher, G.; Schmitt, J. *Progr. Colloid Polym. Sci.*, **1992**, 89, 160.

61. Decher, G.; Schmitt, J.; Grunewald, T.; Pershan, P.; Kjaer, K.; Losche, M. *Macromolecules*, **1993**, 26, 7058.

62. Definition of Sticky Foot polymes put forth initially by T.J. McCarthy in research discussions and used in this research and the research of Iyengar, D.R., Kolb, B.U., Viviano, K., Franchina, N.F., de Vincenzi, R.D., and Kendall, E.W.

63. Dias, A.J. Ph.D Dissertation, University of Massachusetts, **1986.**

64. Dias, A.J.; McCarthy, T.J. *Macromolecules*, **1985**, 18, 1826.

65. Dias, A.J.; McCarthy, T.J. *Macromolecules*, **1987**, 20, 2068.

66. Dwight, D.W.; Riggs, W.M. *J. Colloid Interface Sci.*, **1974**, 47, 650.

67. Evans, A.G.; Ruhle, M.; Dalgleish, B.J.; Charalambides, P.G. *Mater. Sci. Eng.*, **1990**, A126, 53.

68. Evans, A.G.; Ruhle, M.; Dalgleish, B.J.; Charalambides, P.G. *Metallurgical Transactions A*, **1990**, 21A, 2420.

69. Evers, O.A.; Fleer, G.J.; Scheutjens, J.M.H.M.; Lyklema, J. *J. Colloid Interface Sci.*, **1985**, 111, 446.

70. Evers, O.A.; Scheutjens, J.M.H.M.; Fleer, G.J. *J. Chem. Soc. Faraday Trans.*, **1990**, 86, 1333.

71. Fowkes, F.M. *Contact Angle, Wettability, and Adhesion*, Advances in Chemistry Series 43, American Chemical Society: Washington, D.C., **1964.**

72. Franchina, N.L.; McCarthy, T.J. *Macromolecules*, **1991**, 24, 3045.

73. Gent, A.N.; Kaang, S.Y. *J. Adhesion*, **1987**, 24, 173.

74. Gesser, H.D.; Long, R. *J. Polym. Sci.: Part B*, **1967**, 5, 469.

75. Gledhill, R.A.; Kinloch, A.J. *Polymer Engineering and Science*, **1979**, 19(2), 82.

76. Goldfarb, J.L. Ph.D. Dissertation, University of Massachusetts, **1992**.

77. Goldfarb, J.L.; Farris, R.J., *J. Adhesion*, **1991**, 35, 233.

78. Good, R.J.; Stromberg, R.R. *Surface and Colloid Science*, **1979**, 11, 13.

79. Goodman, I., Ed.: *Developments in Block Copolymers -2*; Elsevier Applied Science Publisher: New York, **1985**.

80. Ha, K.; McClain, S.; Suib, S.L.; Garton, A. *J. Adhesion*, **1991**, 33, 169.

81. Halasa, A.F.; Lohr, D.F.; Hall, J.E. *J. Polymer Sci. Polymer Chem. Ed.*, **1981**, 19, 1375.

82. Hara, K.; Schonhorn, H. *J. Adhesion*, **1970**, 2, 100.

83. Holden, G.; Bishop, E.T.; Legge, N.R. *J. Polymer Sci.: Part C*, **1969**, 26, 37.

84. Holmes-Farley, S.R.; Bain, C.D.; Whitesides, G.M. *Langmuir*, **1988**, 4, 921.

85. Holmes-Farley, S.R.; Reamy, R.H.; McCarthy, T.J.; Deuth, J.; Whitesides, G.M. *Langmuir*, **1985**, 1, 725.

86. Hummel, D.O. *Polymer Spectroscopy*, Verlag Chemie GmbH: Weinheim, **1974**.

87. Huth, J.A.; Danielson, N.D., *Anal. Chem.*, **1982**, 54, 930.

88. Ishizu, K.; Yamada, Y.; Fukutomi, T. *Polymer*, **1990**, 31, 2047.

89. Iyengar, D.R. Ph.D. Dissertation, University of Massachusetts, **1992**.

90. Iyengar, D.R.; McCarthy, T.J. *Macromolecules*, **1990**, 23, 4344.

91. Janarthanan, V.; Stein, R.S.; Garrett, P.D. *J. Polymer Sci.: Part B: Polymer Physics*, **1993**, 31, 1995.

92. Jansta, J.; Dousek, F.P. U.S. Patent #3967018, **1976**.

93. Kaelble, D.H. *J. Adhesion*, **1969**, 1, 102.

94. Kaelble, D.H. *J. Adhesion*, **1992**, 37, 205.

95. Kasemura, T.; Ozawa, S.; Hattori, K. *J. Adhesion*, **1990**, 33, 33.

96. Kato, T. unpublished work, 1994.

97. Kelber, J.A. *Plasma Treatment for Improved Adhesion*, **April 1988**, presented at the Materials Research Society Meeting, Reno, Nevada.

98. Kendall, E.W. Ph.D. Dissertation, University of Massachusetts, **1994**.

99. Kendall, E.W.: McCarthy, T.J. *Polym. Prepr. (Am. Chem. Soc. Div. Polym. Chem.)*, **1992**, 33(2), 158.

100. Kendall, K. *Science*, March **1994**, 263, 1720.

101. Kim, K-S.; Aravas, N. *Int. J. Solids Structures*, **1988**, 24, 417.

102. Kinloch, A.J. *Adhesion and Adhesives Science and Technology*, Chapman and Hall: London, **1987**.

103. Kolb, B.U. Ph.D. Dissertation, University of Massachusetts, **1992**.

104. Kolb, U.B.; Patton, P.A.; McCarthy, T.J. *Macromolecules*, **1990,** 23, 366.

105. Langer, A.W. *Polym Prepr. (Am. Chem. Soc.,Div. Polym. Chem.)*, **1966**, 7(1), 132.

106. Lau, C.C.; Kinloch, A.J.; Williams, J.G. *The Adhesion Society Proceedings of the Sixteenth Annual Meeting*, February **1993**, 96.

107. Lee, H.; Kepley, L.J.; Hong, H-G.; Akhter, S.; Mallouk, T.E. *J. Phys. Chem.*, **1988,** 92, 2597.

108. Lee, K-W.; McCarthy, T.J. *Macromolecules*, **1988**, 21, 2318.

109. Lee, K-W.; McCarthy, T.J., *Macromolecules*, **1987**, 20, 1437.

110. Lee, L-H. *Adhesion Science and Technology*, **1975**, 9A, Plenum Press: New York, 199.

111. Lerchenthal, C.H.; Brenman, M. *Polym. Eng. Sci.*, **1976**, 16, 747.

112. Lerchenthal, C.H.; Brenman, M. *Polym. Eng. Sci.*, **1976**, 16, 760.

113. Lerchenthal, C.H.; Brenman, M.; Yits'Haq, N. *J. Polym. Sci.: Polym. Chem. Ed.*, **1975**, 13, 737.

114. Loukis, M.J.; Aravas, N. *J. Adhesion*, **1991**, 35, 7.

115. March, J., *Advanced Organic Chemistry*, 3rd edition, John Wiley and Sons: New York, **1985**, 287.

116. Marchesi, J.T.; Ha, K.; Garton, A. *J. Adhesion*, **1991**, 36, 55.

117. Marchesi, J.T.; Keith, H.D.; Garton, A. *J. Adhesion*, **1992**, 39, 185.

118. Marques, C.; Joanny, J.F. *Macromolecules*, **1989**, 22, 1454.

119. Marra, J.; Hair, M.L. *J. Phys. Chem.*, **1988**, 92, 6044.

120. McGrath, J.E. *Anionic Polymerization*, American Chemical Society: Washington, DC, **1981**.

121. Messa, T. a Technical Sales Representative with Allied-Signal Inc.

122. Mochel, V.D. *Rubber Chem. Technol.*, **1967**, 40, 1200.

123. Morton, M. *Anionic Polymerization: Principles and Practice*, Academic Press, New York, **1983.**

124. Morton, M.; Fetters, L.J. *J. Rubber Chem. Technol.*, **1975**, 48, 359.

125. Mostovoy, S.; Ripling, E.J. *J. Appl. Polymer Sci.*, **1966**, 10, 1351.

126. Nelso, E.R.; Kilduff, T.J.; Benderly, A.A. *Ind. Eng. Chem.*, **1958**, 50, 329.

127. Nuzzo, R.G.; Allar, D.L. *J. Am. Chem. Soc.*, **1983**, 105, 4481.

128. Oster, G.; Shibata, O. *J. Polym. Sci.*, **1957**, 26, 233.

129. Parfitt, G.D.; Rochester, C.H. editors, *Adsorption From Solution at the Solid/Liquid Interface*, Academic Press, New York, **1983** p.392.

130. Phuvanartnuruks, V. Atomic force microscopy experiments on surface modified PCTFE.

131. Pireaux, J.J.; Bertrand, P.; Bredas, J.L. editors *Polymer-Solid Interfaces*, IOP Publishing Ltd, London, **1992** p. 131.

132. Plueddemann, E.P. *Silane Coupling Agents*, Plenum Press: New York, **1982.**

133. Purvis, R.J.; Back, W.R. U.S. Patent #2789063, **1957**, 3M Corporation.

134. Rasmussen, J.R.; Stedronsky, E.R.; Whitesides, G.M. *J. Am. Chem. Soc.*, **1977**, 99, 4736.

135. Riew, C.K. *Rubber-Toughened Plastics*, Advances in Chemistry Series 222, American Chemical Society: Washington, D.C., **1989**.

136. Riew, C.K.; Gillman, J.K. *Rubber-Modified Thermoset Resins*, Advances in Chemistry Series 208, American Chemical Society: Washington, D.C., **1984**.

137. Riew, C.K.; Kinloch, A.J., Ed.; *Toughened Plastics*, Advances in Chemistry Series 233, American Chemical Society: Washington, D.C., **1993**.

138. Ripling, E.J.; Mostovoy, S. *J. Appl. Polymer Sci.*, **1966**, 10, 1351.

139. Ripling, E.J.; Mostovoy, S.; Corten, H.T. *J. Adhesion*, **1971**, 3, 107.

140. Rossman, K. *J. Polym. Sci.*, **1956**, 19, 141.

141. Rubner, M.F.; Cheung, J.H.; Fou, A.F.; Ferreira, M. *Polym. Prepr. (Am. Chem. Soc., Div. Polym. Chem.)*, **1993**, 34(2), 757.

142. Rubner, M.F.; Fou, A.C.; Ellis, D.; Ferreira, M. *Polymr. Prepr. (Am. Chem. Soc., Div. Polym. Chem.)*, **1994**, 35(1), 221.

143. Scheutjens, J.M.H.M.; Fleer, G.J. *J. Chem. Phys.*, **1980**, 84, 178.

144. Scheutjens, J.M.H.M.; Lyklema, J. *J. Chem. Phys.*, **1979**, 83, 1619.

145. Scheutjens, J.M.H.M; Fleer, G.J. *J. Phys. Chem.* **1979**, 83(12), 1619.

146. Schonhorn, H.; Hansen, R.H. *J. Appl. Polym. Sci.*, **1967**, 11, 1461.

147. Schonhorn, H.; Ryan, F.W. *J. Adhesion*, **1969**, 1, 43.

148. Schonhorn, H.; Ryan, F.W. *J. Polym. Sci.*, **1969**, 7(A2), 105.

149. Schonhorn, H.; Sharpe, L.H. *J. Appl. Polymer Sci.: Part A*, **1965**, 3, 3087.

150. Scott, J.M.; Phillips, D.C. *J. Mater. Sci.*, **1975**, 10, 551.

151. Shoichet, M.S. Ph.D. Dissertation, University of Massachusetts, **1992**.

152. Shoichet, M.S.; McCarthy, T.J. *Macromolecules*, **1991**, 24, 982.

153. Shull, K.R. *J. Chem. Phys.* **1991**, 94(8), 5723.

154. Siperko, L.M.; Thomas, R.R. *J. Adhesion Sci. Technol.*, **1989**, 3, 157.

155. Stockton, W.B.; Rubner, M.F.; *Polymr. Prepr. (Am. Chem. Soc., Div. Polym. Chem.)*, **1994**, 35(1), 319.

156. Stouffer, J.; McCarthy, T.J. *Macromolecules*, **1988**, 21, 1204.

157. Swalen, J.D.; Allara, D.L.; Andrade, E.A.; Chandross, E.A.; Garoff, S.; Israelachvili, J.; McCarthy, T.J.; Murray, R.; Pease, R.F.; Rabolt, J.F.; Wynne, K.J. *Langmuir*, **1987**, 3, 932.

158. Szwarc, M. *Nature*, **1956**, 178, 1168.

159. Szwarc, M; Levy, M.; Milkovich, R. *J. Am. Chem. Soc.*, **1956**, 78, 2656.

160. Thouless, M.D.; Jensen, H.M. *J. Adhesion*, **1992**, 38, 185.

161. Van der Schee, H.A.; Lyklema, J. *J. Phys. Chem.*, **1984**, 88, 6661.

162. Viviano, K. Ph.D. Dissertation, University of Massachusetts, **1994**.

163. Vrtis, J. Ph.D. Dissertation, University of Massachusetts, **1994**.

164. Ward, W.J.; McCarthy, T.J. *Encyclopedia of Polymer Science and Engineering, 2nd ed.; Supplement*, Wiley: New York, **1989**, 674.

165. Weast, R.C. editor, *CRC Handbook of Chemistry and Physics 67th edition*, CRC Press Inc., Boca Raton, **1986**.

166. Whitney, J.M. *J. Reinf. Plastic Comp.*, **1982**, 1, 297.

167. Williams, J.G., *Fracture Mechanics of Polymers*, John Wiley & Sons: New York **1984**.

168. Wu, S. *Polymer Interface and Adhesion*, Marcel Dekker: New York, **1982**.

169. Xiao, F.; Hui, C-Y.; Washiyama, J.; Kramer, E.J. *Macromolecules*, **1994**, 27, 4382.

170. Yamakawa, S. *Macromolecules*, **1979**, 12, 1222.

171. Yamamoto, F.; Yamakawa, S. *J. Polym. Sci.: Polym. Phys. Ed.*, **1979**, 17, 1581.

173. Ziegler, K. *Angew. Chem.*, **1936**, 49, 499.